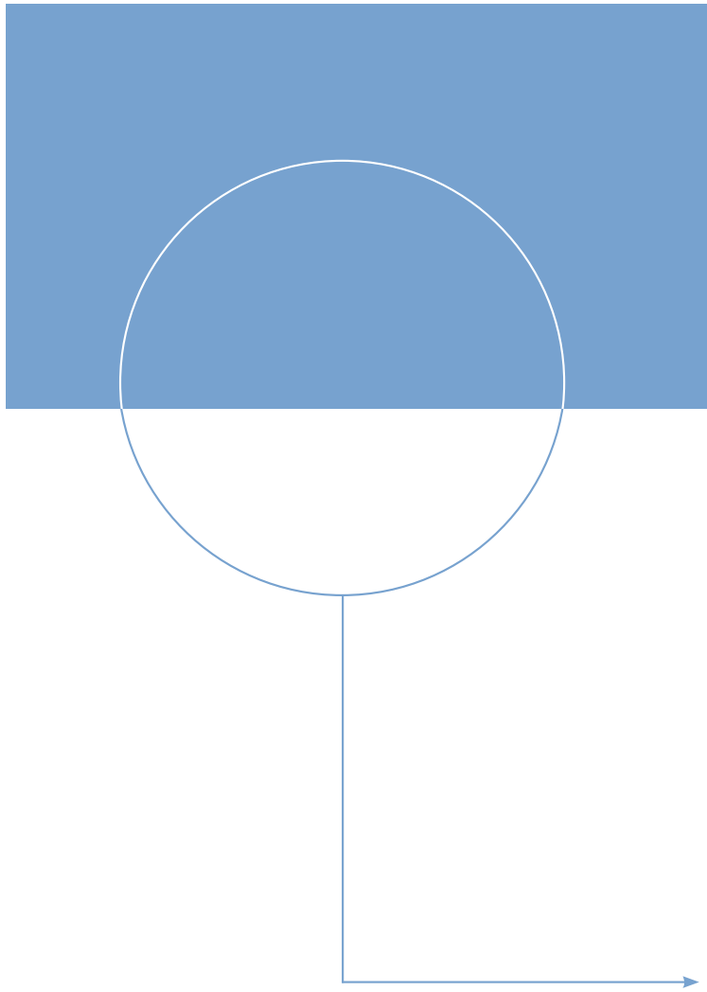

Master's thesis

2020

Tone Dale

NTNU
Norwegian University of
Science and Technology
Faculty of Engineering
Department of Marine Technology

Tone Dale

Development of Simplified Methods for Ship Powering Performance Calculations

July 2020

NTNU
Norwegian University of
Science and Technology

NTNU
Norwegian University of
Science and Technology

NTNU

Norwegian University of
Science and Technology

Development of Simplified Methods for Ship Powering Performance Calculations

Tone Dale

Marine Technology
Submission date: July 2020
Supervisor: Sverre Steen
Co-supervisor: Helene Muri

Norwegian University of Science and Technology
Department of Marine Technology

NTNU Trondheim
Norwegian University of Science and Technology
Department of Marine Technology

MASTER THESIS IN MARINE TECHNOLOGY

SPRING 2020

FOR

Tone Dale

Development of simplified methods for ship powering performance calculations

As part of the KPN research project CLIMMS, NTNU is developing a computational model for the fuel consumption and emissions to air from the world shipping fleet (or subsets of it). The model is using AIS data, combined with a database with ship information (main dimensions, main engine size etc.). Since there is an enormous number of ships, CFD and other complicated models for computing the required propulsion power for the observed speed of each individual ship cannot be used, and experience shows that the commonly used simple empirical models like Hollenbach and Holtrop aren't suitable for all relevant ship types and sizes. Also, the ship data in the database might not contain all the required data for the existing empirical methods for power prediction. However, there are large amounts of in-service data available that might be used to develop improved empirical models.
The project and master thesis will be performed in cooperation with the KPN project CLIMMs. The project will contribute with knowledge and guidance, database access as well as data from ship operation.

The objective of the master thesis is establish and subsequently validate a ship powering performance models suitable for use in the mentioned global fleet emissions calculation. The developed method can be composed of existing methods, or it might partly or wholly be newly developed.

In the thesis the candidate shall present her personal contribution to the resolution of problem within the scope of the thesis work.

Theories and conclusions shall be based on mathematical derivations and/or logic reasoning identifying the various steps in the deduction.

The thesis work shall be based on the current state of knowledge in the field of study. The current state of knowledge shall be established through a thorough literature study, the results of this study shall be written into the thesis. The candidate should utilize the existing possibilities for obtaining relevant literature.

The thesis shall be organized in a rational manner to give a clear exposition of results, assessments, and conclusions. The text should be brief and to the point, with a clear language. Telegraphic language should be avoided.

The thesis shall contain the following elements: A text defining the scope, preface, list of contents, summary, main body of thesis, conclusions with recommendations for further work, list of symbols and acronyms, reference and (optional) appendices. All figures, tables and equations shall be numerated.

NTNU Trondheim
Norwegian University of Science and Technology
Department of Marine Technology

The supervisor may require that the candidate, in an early stage of the work, present a written plan for the completion of the work. The plan shall include a budget for the use of laboratory or other resources that will be charged to the department. Overruns shall be reported to the supervisor.

The original contribution of the candidate and material taken from other sources shall be clearly defined. Work from other sources shall be properly referenced using an acknowledged referencing system.

The thesis shall be submitted electronically (pdf) in Inspera:

- Signed by the candidate
- The text defining the scope (this text) (signed by the supervisor) included

Supervisor : Professor Sverre Steen
Advisors: : Helene Muri
Start : 09.03.2020
Deadline : 31.08.2020

Trondheim, 13.01.2020

Sverre Steen
Supervisor

Preface

This master thesis presents a study of simplified methods for ship powering calculations for the world fleet. The work was completed during the spring/summer of 2020, and serve as the final contribution to my Master of Science degree in Marine Technology.

I would like to thank my supervisor Sverre Steen for giving valuable feedback, and for taking the time to have meaningful discussions throughout the process. Further, I would like to thank my advisor Helene Muri for providing insight to your work at IndEcol and for facilitating access to the MariTEAM model. I am grateful to take part in the research project CLIMMS. Finally, I would like to thank both Prateek Gupta and YoungRong Kim for assisting me in the model development.

Trondheim, July, 2020

Tone Dale

Abstract

International shipping is the main contributor to world trade by carrying more than 80 $\%$ of transported goods. Though emissions per unit of goods transported are lower than any other mode of transport, the fleet is experiencing increasing pressure to reduce global emissions. NTNU has developed a maritime transport emission assessment model (MariTEAM), as part of the research project CLIMMS - Climate mitigation in the maritime sector. MariTEAM is a computational model for the fuel consumption and emissions to air from the world shipping fleet. This thesis contributes by developing and validating a new ship powering performance method suitable for the MariTEAM model.

The current state of knowledge in the field of global fleet-wide power predictions has been reviewed. In line with the literature, various empirical methods are implemented in the model developed in this thesis, which is subdivided into five modules. First, missing input parameters are estimated for the ship. The calm water resistance is calculated, followed by added resistance in wind and waves. Then the propulsive efficiency is determined before the final power is obtained. As a result, the new method can predict the propulsion power in realistic sea-states, for a wide range of ships in the fleet, while requiring few input parameters.

A case study of seven diverse vessels is applied to validate the powering performance of the new model. The validation data include model test reports, sea trial reports and in-service data from voyages. Based on the study, a final new power prediction method is presented. Validation against model test reports and sea trials show that the new model achieves powering predictions with a mean deviation of $\pm$ 3 % and standard deviation of 6% for exact input parameters. When parameter estimates are applied for missing input, deviations are within 10% for the power predictions. Validation against in-service data demonstrates that the powering predictions and the in-service measurements correspond well if the correct loading condition is applied.

Sammendrag

Internasjonal skipsfart er den største bidragsyteren til verdenshandelen, og frakter mer enn 80 $\%$ av transportert gods. Selv om utslippene per enhet som transporteres er lavere enn for noen annen transport, opplever skipsfarten et økende press for å redusere de globale utslippene. Som en del av KPN-forskningsprosjektet CLIMMS, har NTNU utviklet MariTEAM-modellen, en beregningsmodell for drivstofforbruk og utslipp fra verdens skipsflåte. Denne avhandlingen bidrar med å utvikle og validere en ny ytelsesmetode for skip som er egnet for MariTEAM-modellen.

Den nåværende kunnskapen om prediksjon av effektforbruk for skip er gjennomgått. I samsvar med litteraturen er ulike empiriske metoder implementert i modellen, som består av fem overordnede moduler. Først estimeres manglende tekniske parametere for skipet. Deretter beregnes stillevannsmotstanden, etterfulgt av motstandsøkning i vind og bølger. Så bestemmes propulsjonsvirkningsgraden, før det endelige effektforbruket beregnes. Dermed kan den nye metoden estimere effektforbruket i realistiske sjøtilstander og for et bredt spekter av skip i flåten, kun ved hjelp av få parametere.

En casestudie av syv ulike skip er benyttet for å validere prestasjonen til den nye metoden. Valideringsgrunnlaget inkluderer modelltest rapporter, prøvetursdata og in-service data for seilende skip. Valideringen mot stillevannsberegninger viser at den nye metoden kan predikere effektforbruket med gjennomsnittlig avvik på $\pm$ 3 % og med et standardavvik på 6%, hvis eksakte parametere er kjent. Når parameterestimatene anvendes for manglende parametere avviker effektberegningene opp til 10%. Validering av in-service data viser at det målte effektforbruket og det estimerte effektforbruket samsvarer godt hvis korrekt lastkondisjon er brukt.

Table of Contents

List of Tables

List of Figures

List of Equations

Symbols

Hull and Propeller Characteristics

L_{wl}	-	Length of waterline
L_{pp}	-	Length between perpendiculars
L_{os}	-	Length of surface
L_{oa}	-	Length over all
B	-	Ship breadth
T	-	Ship draught
∇	-	Volume displacement
ldt	-	Light displacement tonnage
dwt	-	Deadweight
S	-	Wetted surface area
S_B	-	Wetted base/transom area
S_{app}	-	Wetted surface of appendages
A_{VT}	-	Transverse projected area above the waterline
A_{VL}	-	Longitudinal projected area above the waterline
D	-	Depth from keel to uppermost continuous deck
A_{BT}	-	Transverse cross section area of bulb
C_B	-	Block coefficient
C_M	-	Midship section coefficient
C_P	-	Prismatic coefficient
C_{stern}	-	Stern shape parameter in Holtrop-Mennen
LCB	-	Londitudinal center of buoyancy
V_D	-	Design speed
V_W	-	Reduced speed corrected for added resistance
D_p	-	Propeller diameter
A_E/A_0	-	Propeller expanded ratio
n	-	Propeller rpm

Resistance

C_T	-	Total resistance coefficient
C_R	-	Residuary resistance coefficient
k	-	Form factor
C_F	-	Frictional resistance coefficient
ΔC_F	-	Hull roughness correction
C_{DB}	-	Base drag coefficient
C_{AA}	-	Air resistance coefficient
C_{App}	-	Appendage resistance coefficient
C_A	-	Correlation allowance
V	-	Ship speed
ρ_s	-	Sea water density
ν	-	Sea water kinematic viscosity
R_{tot}	-	Total resistance in wind and waves
R_{wind}	-	Added resistance due to wind
R_{wave}	-	Added resistance due to waves
R_{AWML}	-	Resistance due to induced wave motions
R_{AWRL}	-	Resistance due to wave reflection
F_n	-	Froude number
h	-	Water depth
g	-	Constant of gravity
$H_{1/3}$	-	Significant wave height
ζ_A	-	Wave amplitude

Propulsion

η_D	-	Propulsion efficiency in ideal conditions
η_{tot}	-	Propulsive efficiency in trial conditions
η_0	-	Open-water (propeller) efficiency
η_H	-	Hull efficiency
η_R	-	Relative rotative efficiency
η_M	-	Mechanical losses
η_S	-	Losses in the transmission system
P_D	-	Delivered power at the propeller
t	-	Thrust deduction factor
w	-	Wake fraction
V_A	-	Speed of inflow to the propeller
T	-	Torque
P_S	-	Calm water power requirement
P_{tot}	-	Total power requirement
ξ_P	-	Slope of the linear curve in the load variation test

Abbreviations

GT	=	Gross tonnage
IMO	=	International Maritime Organisation
ITTC	=	International Towing Tank Conference
MCR	=	Maximum continuous rating
SM	=	Sea margin

Chapter 1

Introduction

1.1 Background and Motivation

Shipping is the main contributor to world trade by carrying more than 80 % of transported goods. As of 2018, the world merchant fleet counts about 94,000 vessels of 100 GT and above (UNCTAD, 2018). The main part of the fleet is cargo-carrying ships (dry bulk, tankers, general cargo, container, passenger), followed by non-cargo ships (fishing, research, offshore, and other). The largest ship segments transport cargo over long ranges within a well-defined system of global shipping routes. Figure 1.1 illustrates the fleet-wide CO2 emissions from 2015, related directly to the vessel traffic densities on the sea routes.

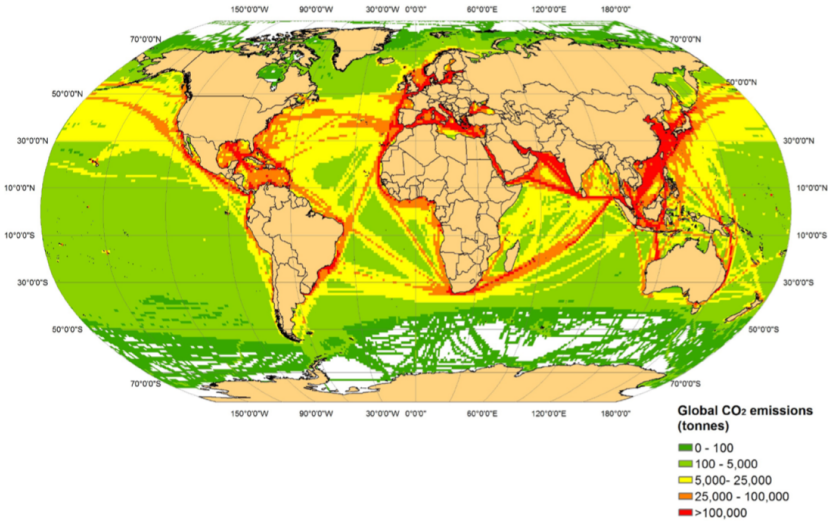

Figure 1.1: Fleet wide CO2 emissions in 2015 from Olmer et al. (2017), International Council on Clean Transport (ICCT, 2017). Data from exactEarth, IHS and ArcGIS.

Merchant ships in international traffic are subject to regulations by the International Maritime Organization of the United Nations (IMO). Despite ships having lower emission intensities per unit mass transported than any other mode of transport (Edenhofer, 2014), it is recognized that the fleet represents a significant reduction potential to contribute to the global efforts of limiting global warming (Hoegh-Guldberg et al., 2019). Although international shipping is excluded from the Paris Agreement, IMO is pursuing the development and implementation of measures to address greenhouse gas (GHG) emissions from the fleet (Olmer et al., 2017). In 2018 they decided that maritime GHG emissions shall be reduced by 50 % (compared to 2008) within 2050. Shipping is experiencing an increasing pressure to decarbonize and reduce emissions to air, on the way to reach the 2-degree target of the Paris Agreement. As of 2020, new emission regulations are applied to the world ship fleet as the limit for sulfur in fuel oil is reduced from 3.5 to 0.5 %.

In order to develop effective strategies for this green transition, IMO member states pursue understanding the

current trends in ship activity and emissions (Hoegh-Guldberg et al., 2019). Identifying the drivers of shipping emissions is decisive in making informed decisions and influencing policymakers. The world shipping fleet emissions can be estimated in terms of fuel consumption, either by top-down or bottom-up (activity-based) approaches. Top-down methods are based on the reported marine fuel sales statistics, and ship-type specific results are not obtained. Bottom-up methods estimate the fuel consumption for each ship based on power produced by the engines. Such power predictions require ship technical and operational data. Due to the enormous number of ships in the fleet, a simplified power prediction method with sufficient accuracy is needed to obtain estimates across the whole fleet and within sub-segments.

Both the third IMO GHG study (Smith et al., 2014) and the 2017 ICCT study on GHG emissions from global shipping, represent bottom-up studies with minor differences in the methodologies. Characteristic for these bottom-up methods is the application of highly simplified empirical methods for the ship powering calculations. Even though empirical bottom-up methods are becoming increasingly accurate with improving AIS data coverage (Olmer et al., 2017), there is a trade-off between the simplified calculations and the accuracy of the results. There exist well established empirical methods like Hollenbach (1998) and Holtrop and Mennen (1982), commonly used for power predictions. The International Towing Tank Conference (ITTC, 2017) is a recognised worldwide association of hydrodynamics research organisations that operate towing tanks or similar model test laboratories. ITTC establishes recommended procedures for powering predictions, including empirical methods. However, several of these methods require many input parameters and may not be suitable for all ship types.

In order to modify the existing methods, there are mainly two approaches found in the literature. A simple method with few parameters is tuned to modern ships, or a detailed method is combined with smart estimates for the required input parameters. Kristensen et al. (2017) studied the simple method of Guldhammer and Harvald (1974) and assessed the accuracy of some of the parameters when applied to various ship types. The study demonstrates a tuning of a historical method to present-day ship segments. Jalkanen et al. (2012) combines several empirical methods in an assessment model of ship traffic exhaust emissions, 'STEAM3'. In this study, the power predictions are based on Hollenbach and demonstrate how many input parameters can be estimated for a traditional method with a higher level of detail. A similar model is 'ShipCLEAN' by Tillig (2020), which combines existing empirical formulas with new developed procedures to predict the ship power performance.

Muri et al. (2019a,b) and Bouman et al. (2016) present global fleetwide emission predictions in the maritime transport emission assessment model (MariTEAM). The model is developed as part of the KPN research project 'CLIMMS' (climate mitigation in the maritime sector), which is an interdisciplinary study connected to SFI Smart Maritime. As a bottom-up model, MariTEAM applies empirical ship power prediction methods for the emission calculations. The model input comprises ship technical data and AIS data combined with hindcast weather data.

1.2 Objective

The main objective of this thesis is to identify, develop, and validate a new ship powering performance method suitable for the MariTEAM model. This includes establishing the current state of knowledge in the field of global fleet-wide power predictions. In line with the literature, various approaches to modifying empirical methods will be assessed. Further, it includes validating the new model with data from model tests, sea trials or in-service measurements for a range of vessel types.

1.3 Outline of Thesis

Chapter 2 presents a review of ship powering theory, in order to establish the most important effects on ship resistance and propulsion. **Chapter 3** identifies existing empirical procedures, which is narrowed down to the most relevant. **Chapter 4** outlines the current power predictions in the MariTEAM model. In addition, relevant ship technical databases are investigated. **Chapter 5** presents the methodology applied in selecting the empirical methods for the new power prediction model. The new method is outlined, and potential improvements to the current MariTEAM model is emphasized. All the empirical methods included in the model are verified,

to ensure that these are implemented correct mathematically. In **Chapter 6**, a case study is conducted for seven vessels. The results are validated against model test reports, sea trial reports and in-service data. In addition, the performance of the new model and the current MariTEAM model is compared. **Chapter 7** discusses the main findings and the performance of the new method. **Chapter 8** presents the final conclusions, before recommendations for further work are given in **Chapter 9**.

During the winter of 2019/2020, the project thesis was conducted as a preliminary study of candidate methods for the ship powering calculations in the MariTEAM model. The study comprised a comprehensive literature review of suitable methods and served as a basis for the current work. However, all relevant findings are included and further elaborated on in this master thesis, which represents a complete and independent assessment.

Chapter 2

Theory of Ship Powering

This chapter outlines the basic theory of ship powering based on ship resistance and total propulsive efficiency. In order to develop a suitable power prediction model, the ship resistance and propulsive efficiency should be determined with the highest possible accuracy. The objective of this chapter is to establish the aspects of ship resistance and propulsive efficiency with significance for ship powering.

2.1 Resistance

As of today, there is a consensus for defining ship resistance in the context of ship hydrodynamics for a calm water sea state. Ships are traditionally optimized for operation in this sea state, although ships travel most of the time in wind, waves, and current. The ideal calm water condition neglects these effects, which is a significant simplification of the real conditions in a seaway. According to Wartsila (2019), when navigating in head-sea, the resistance can increase by 50-100$\%$ of the ship resistance in calm weather. In order to predict the powering performance of ships in a seaway, the added resistance due to wind and waves, and the change of propulsive efficiency must be taken into account. This is further elaborated on in Sections 2.1.2 and 2.2.2.

2.1.1 Calm Water Resistance

The calculation of calm water resistance for a moving ship can be based on two different approaches. Either by considering energy dissipation from the hull or by evaluating the forces acting on the hull. The energy dissipation can be observed in terms of the flow features developing around the hull, as presented in Figure 2.1 by Molland et al. (2017). There is a wave pattern moving with the hull and a wake of turbulent flow extending behind the ship.

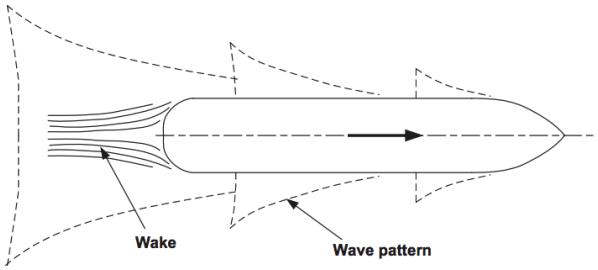

Figure 2.1: Flow features of a moving ship based on Molland et al. (2017)

Based on this method, the governing principle divides the total resistance into viscous resistance and wave-making resistance from the wave pattern generated. It is further assumed that these are independent, which is a practical simplification to illustrate the physical problem (Birk, 2019). Note that until 2017, ITTC applied "Residual resistance" instead of "Wave making resistance" in their recommended procedure.

If the forces acting on the hull is considered, it is differed between pressure resistance, acting normal to the hull and frictional resistance, acting as a shear force on the hull. The viscous ship resistance is defined as the frictional resistance and viscous pressure resistance, corrected for the hull shape and fullness. Ship frictional resistance is calculated as the equivalent resistance of a flat plate with the same Reynolds number, area, and length, moving longitudinally through the water. Due to the ship volume, the velocity along the hull is higher than the ship speed, which increases the viscous resistance relative to a plate (Steen et al., 2016). The viscous pressure resistance is a pressure resistance due to viscous flow effects. It accounts for three-dimensional flow effects such as flow separation due to appendages or in the aft hull shape. In accordance with these definitions, the total resistance can be decomposed as illustrated by Molland et al. (2017) in Figure 2.2

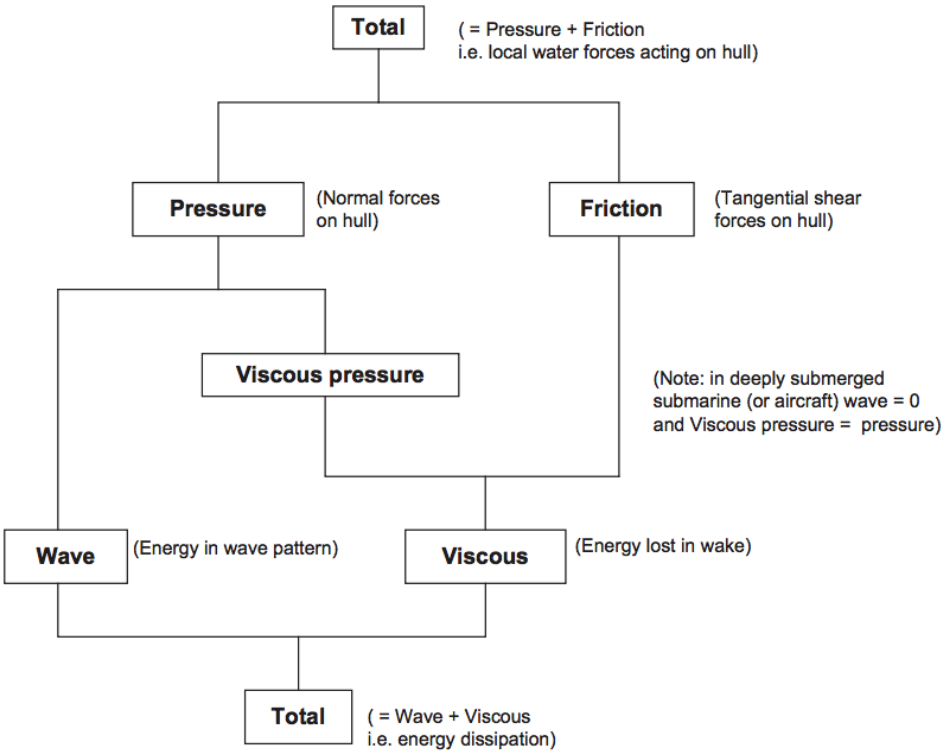

Figure 2.2: Decomposition of ship resistance components based on Molland et al. (2017)

The resistance components are commonly expressed as dimensionless coefficients, as presented in Equation 2.1 for the total resistance coefficient.

$$C_T = \frac{R_T}{0.5 \cdot \rho \cdot S \cdot V^2} \tag{2.1}$$

$R_T\ [N]$ is the total resistance, $\rho\ [kgm^{-3}]$ is the sea water density, $S\ [m^2]$ is the wetted area, and V is the ship speed $[ms^{-1}]$.

MARINTEK restistance decomposition

Under the main assumption of resistance being divided into wave making (or residual) and viscous resistance, there are several ways of decomposing the total resistance into smaller components. These include air resistance, base drag, roughness effects, and more. In the current work, it is chosen to apply a decomposition suggested by MARINTEK (2020), given in Equation 2.2.

$$C_T = C_R + (1+k)\left(C_F + \Delta C_F\right) + C_{DB} + C_{AA} + C_{App} + C_A \tag{2.2}$$

where the dimensionless coefficients are:

C_T - Total resistance
C_R - Residuary resistance
k - Form factor
C_F - Frictional resistance
ΔC_F - Hull roughness correction
C_{DB} - Base drag
C_{AA} - Air resistance
C_{App} - Appendage resistance
C_A - Correlation allowance

MARINTEK applies a modification of the ITTC'78 procedure following Equation 2.3 (ITTC, 2017). In ITTC'78, the base drag coefficient C_{DB} is not included, and the hull roughness correction ΔC_F may include correlation allowance. Further, the viscous resistance is defined differently in the two methods. As seen in Equation 2.2, MARINTEK includes the roughness correction in the viscous resistance term.

$$C_T = (1+k)C_F + \Delta C_F + C_A + C_R + C_{AA} \tag{2.3}$$

The theory of the various ship resistance components will be briefly elaborated on in the following, based on the basic division into components as outlined by MARINTEK. The respective calculation methods are presented in Section 2.3.

Residuary resistance

Froude first defined the term residuary resistance in the 1860s as the remaining resistance when the friction is subtracted from the total. Today the method is refined, and it is common to subtract all other non-Froude scaled resistance components, in accordance with Equation 2.2. It is difficult to determine the residuary resistance accurately, but the main contributions are from wave resistance and viscous pressure resistance. The viscous pressure resistance represents the smaller contribution and is mainly due to flow separation behind the hull. As presented previously, the ship generates a typical wave system that contributes to the wave resistance. The interaction between the hull and the wave system is complex to evaluate but depends strongly on the local shape (Schneekluth and Bertram, 1998). The wave resistance dominates the total resistance for a fast, slender ship. According to Wartsila (2019), the residual resistance typically accounts for the following amount of total resistance:

- 40-60$\%$ for high-speed ships (such as container ships and passenger ships)
- 10-25$\%$ for low-speed ships (such as bulk carriers and tankers)

It is therefore deemed important to predict the residual resistance with high accuracy.

Form factor

The calculation of frictional resistance assumes a flat plate, and the form factor is introduced to account for the hull's shape and fullness. Form factors commonly express the relation between the viscous resistance C_V and the frictional resistance, as presented in Equation 2.4. The value of the form factor can both refer to k and $(1+k)$ (Steen et al., 2016). It is also important to note that the value of the form factor is related to the friction line applied to find the frictional resistance C_F.

$$C_V = (1+k)\left(C_F + \Delta C_F\right) \tag{2.4}$$

Several friction lines exist and the ITTC'57 correlation line is among the widely used methods. The frictional coefficient is expressed empirically as a function of the dimensionless Reynolds number R_n, as presented in Equation 2.5

$$C_F = \frac{0.075}{\left(log(R_n) - 2\right)^2} \tag{2.5}$$

A correction for form effect is included in the ITTC'57 formula and initially it was applied without an additional form factor. However, today it is common practice to consider the ITTC'57 as a flat plate friction line and add a form factor.

A number of empirical formulas to determine the form factor exist, including MARINTEK's formula and Holtrop's formula. Since the formulas are determined by fitting a curve to scatter plots, results can range from upper to lower estimates, i.e., include varying resistance contributions. According to Steen (2011) it is convenient to apply a form factor which includes the viscous pressure if model tests are unavailable. The Holtrop formula includes viscous pressure effects and is therefore considered relevant to evaluate in selecting the form factor method. The selection of form factor for the power prediction model is presented in Section 5.1.

Frictional resistance

The frictional resistance of a full scale ship is computed as the resistance of a flat plate with the same speed, area, and length, corrected for the increased frictional resistance due to hull roughness $(C_F + \Delta C_F)$. The hull roughness is a function of coating type, fouling, fractures in the coating, and rust and damage from mechanical devices. Fouling is the marine growth on the hull and can develop faster than other roughness contributions. As fouling is a living organism, it depends on temperature, light, salinity, and a number of parameters, which makes it challenging to make a reliable estimate of the increased resistance. The roughness is measured in μm and increases over time. Typical roughness values are presented in the following. It is important to note that the values are dependent on the frequency of docking and cleaning or recoating the hull.
Based on Steen et al. (2016):

- Newbuild vessel: $100 - 150\mu m$
- Yearly growth rate due to rust and paint detoriation: $20\mu m$
- 10-15 year old vessel: $300\mu m$

Based on Townsin and Byrne (1980):

- Newbuild vessel: $80 - 120\mu m$
- Yearly growth rate due to rust and paint detoriation:
  $10\mu m$ for high-performance coating and cathodic protection
  $75 - 150\mu m$ for resinous coatings and no cathodic protection

The total frictional resistance depends on the size of the wetted area of the ship, Reynolds number, and roughness. However, above a certain Reynolds number, the roughness contribution dominates, and the frictional resistance is no longer dependent on the Reynolds number (Steen et al., 2016). Wartsila (2019) estimate the frictional resistance to represent $70 - 90\%$ of the total resistance for low-speed ships and up to 40% for high-speed ships.

According to Townsin and Kwon (1983), the deterioration from a good newbuilding hull surface $(100\mu m)$ to a typical in-service value $(220\mu m)$ can result in the same added resistance as from wind and waves. Another significant effect is the growth of roughness and fouling on the propeller, which can significantly reduce the power performance of the ship further. It is therefore considered important to include the effects of roughness in the fleetwide calculations. MARINTEK (2020) suggests the following roughness correction formula:

$$\Delta C_F = \left[110 \cdot (H \cdot V)^{0.21} - 403\right] \cdot C_F^2 \tag{2.6}$$

where $H\ [\mu m]$ is the roughness. Other empirical formulas exist, such as Equation 2.7 according to Townsin and Mosaad (1985), recommended by ITTC (2017).

$$\Delta C_F = 0.044 \left[\left(\frac{H \cdot 10^{-6}}{L_{WL}} \right)^{1/3} - 10 \cdot R_n^{-1/3} \right] + 0.000125 \tag{2.7}$$

where $L_{WL}\ [m]$ is the ship waterline length. The roughness correction applied in the model is presented in Section 5.1.

Base drag

Most ships have a partly submerged transom stern, which causes a separated flow at the transom. The separation creates the base drag force, which can be represented dimensionless in accordance with Steen et al. (2016) as Equation 2.8.

$$C_{DB} = \frac{D_B}{\frac{1}{2}\rho V^2 S} = 0.029\sqrt{\frac{(S_B/S)^3}{C_F}} \tag{2.8}$$

where S $[m]$ is the wetted surface area, excluding that of the transom, and S_B is the base/transom/frontal area. The formula is based on a body shaped like a projectile in infinite fluid and is valid for ships as long as the speed is sufficiently low for the transom stern to be wetted. Base drag effects are important for ships with low Froude numbers and large transoms.

Air resistance

The ship structure above the waterline (superstructure) is subject to air resistance, which depends on the superstructure size, shape, and ship speed. The air resistance coefficient C_{AA} can be calculated according to the ITTC'78 procedure presented in Equation 2.9 by Birk (2019).

$$C_{AA} = C_{DA}\frac{\rho_{\text{air}} \cdot A_{VT}}{\rho \cdot S} \tag{2.9}$$

where C_{DA} is the air drag coefficient, commonly determined by wind tunnel test data or by empirical estimates. A_{VT} is the transverse projected area above the waterline. Note that air resistance refers to a ship traveling in still air, hence it does not account for wind. The resistance contribution is not significant for slow ships.

Appendage resistance

Typical ship appendages like rudders, bilge keels, stabilizer fins, shaft brackets, and more, add to the ship resistance. The resistance contribution is mainly frictional, although bluff or poorly aligned appendages may cause flow separation. Molland et al. (2017) estimate the main appendages (rudder and bilge keel) resistance to be 2-5$\%$ relative to the hull naked resistance of single-screw ships and it is predicted to be higher for twin screw ships. Several empirical formulas to predict appendage resistance exist and these typically require detailed characteristics of the appendages. Fortunately, most merchant ships only have a few appendages and the difficulties in estimating effects of appendages are only significant for some unconventional ships (Bertram, 2012). The error of neglecting this contribution is therefore considered relatively small.

Correlation factor

When resistance is calculated based on model tests, an empirical correlation factor C_A is applied in the scaling process. The factor depends on the model test and scaling method. It accounts for deviations between the predicted resistance from the model test, and the calculated full-scale resistance from power measurements. Some of the empirical resistance prediction methods are regression-based from model tank tests and include correlation factors.

Shallow water correction

Correction of the ship performance can be made due to the effects of shallow water. Shallow water can increase the frictional resistance and the wave resistance for the ship (Schneekluth and Bertram, 1998). A significant increase occurs at a depth h near the critical depth Froude number $F_{nh} = V/\sqrt{gh} = 1$. It is difficult to calculate the increase if the effect is strong, but simple corrections can be made for a weak influence e.g. as suggested by Lackenby (1963).

2.1.2 Added Resistance due to Wind and Waves

The calculation of added resistance due to wind and waves is needed to predict the powering performance of a ship in a seaway. Wind resistance is enforced on the superstructure, while wave resistance is generated by wave-induced ship motions and wave reflection of the hull. The contributions add to the calm water resistance from Equation 2.2 to predict the real conditions in a seaway. Equation 2.10 illustrates the summation as suggested by ITTC (2018). In the current work, R_{tot} defines the total ship resistance, including weather effects, and R_T defines the total calm water resistance.

$$R_{\mathrm{tot}} = R_{\mathrm{T}} + R_{\mathrm{wind}} + R_{\mathrm{wave}} \tag{2.10}$$

R_{tot} - Total resistance in wind and waves
R_T - Total calm water resistance
R_{wind} - Added resistance due to wind
R_{wave} - Added resistance due to waves

Added wave resistance

The added wave resistance can be further subdivided as Equation 2.11, composed of mean resistance due to wave reflection R_{AWRL} and mean resistance due to induced wave motions R_{AWML}.

$$R_{\mathrm{wave}} = R_{\mathrm{AWRL}} + R_{\mathrm{AWML}} \tag{2.11}$$

The predictions of added resistance from a specific region or route depend on seastate and weather data. Regarding ship characteristics, the added wave resistance is generally more dependent on ship size than the ship shape (Schneekluth and Bertram, 1998). For ships with a large length L relative to the wavelength λ, wave reflection dominates the wave resistance. This is typically the case for ships in head waves if the sea state is mild, and the wave height is restricted (ISO Technical Committee, 2015). If the ship's length is short relative to the wavelength, wave-induced motions are significant and must be considered. Faltinsen et al. (1980) presents a relation between typical wavelengths and added resistance for ships in regular head sea waves in Figure 2.3.

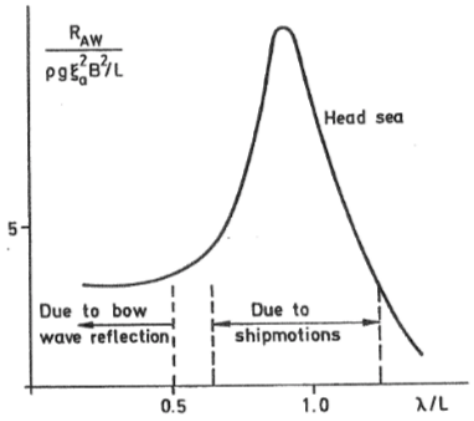

Figure 2.3: Typical wavelength dependence of added resistance R_{wave} in regular head sea waves. ζ_a is the wave amplitude, B is the beam of the ship. (Faltinsen et al., 1980)

The illustrated relation considers regular waves, a simplified representation of the irregular sea that the ship meets. In order to calculate the mean wave resistance in irregular seas, it is common to simulate the irregular sea as a number of regular wave components and summarise the wave loads from each component by linear theory. The sea state can be evaluated in terms of a wave energy spectrum $S(w)$ as a function of circular frequency w.

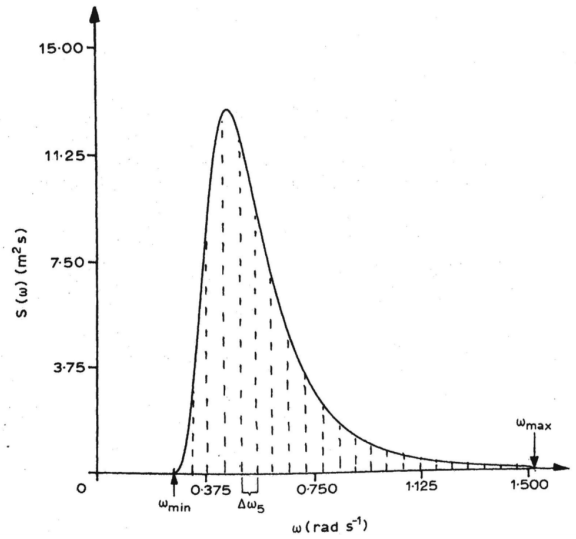

Figure 2.4: Example of ISSC-spectrum with $H_{1/3} = 8m$ and $T = 10s$, from Faltinsen (1993). (The energy is distributed into the energy of $N = 10$ regular wave components)

The modified Pierson-Moskowitz (ISSC) spectrum in Figure 2.4 by Faltinsen (1993) demonstrate a widely-used model, recommended by the ITTC for fully-developed seas. It is characterised by two sea state parameters, the significant wave height $H_{1/3}$, and wave period T. Several empirical methods to predict wave resistance exist and are further elaborated on in Section 3.2.

Added resistance in wind

The wind resistance enforced on the superstructure depends on the projected area above the waterline, wind direction, and velocity. The resistance increase is significant for ships like container ships and ferries, with large areas above the waterline. Wind resistance coefficients depend on ship type, shape, and geometry, as well as the relative wind direction. Equation 2.12 presents the resistance increase according to ITTC (2014).

$$R_{\mathrm{wind}} = \frac{1}{2}\rho_{\mathrm{A}} V_{\mathrm{WR}}^2 C_{\mathrm{X}}\left(\psi_{\mathrm{WR}}\right) A_{VT} - 0.5\rho_{\mathrm{A}} \cdot C_{\mathrm{X}}(0) \cdot A_{\mathrm{VT}} \cdot V_{\mathrm{G}}^2 \tag{2.12}$$

ρ_A - Mass density of air
V_{WR} - Relative wind speed
C_X - Wind resistance drag coefficient
ψ_{WR} - Relative wind direction
A_{VT} - Transverse cross-sectional area above waterline
V_G - Ship speed over ground

The wind resistance drag coefficients are derived from wind tunnel tests or may be determined by empirical data sets. As values for wind velocity and direction vary with time, mean values over specific periods are commonly applied in calculations. Calculation procedures are presented in Section 3.2.

Sea margin

In the design stages of a ship, it is common practice to account for the speed loss due to wind and waves by using a sea margin of 15 $\%$ on the power (SFI, 2016). However, this margin often accounts for other service condition effects as well (like roughness). Current standard procedures can calculate effects of wind to still air conditions with confidence, however it is difficult to make corrections for waves with a high level of accuracy (Townsin and Kwon, 1983). Despite this, there exist several computational and empirical methods, which will be presented in Section 3.2.

2.2 Propulsion

The propulsive efficiency η_D must be determined in order to calculate the necessary machinery power of the ship. It expresses the relationship between the effective power and the power developed by the propeller P_D in ideal conditions. Since the propulsion system and the ship hull interacts, the flow field changes. The propeller inflow is influenced by the hull upstream, and the presence of the propulsion system itself changes the aft hull flow. By taking the effect of these interactions into account, the propulsive efficiency can be determined in accordance with Equation 2.13 (Schneekluth and Bertram, 1998).

$$\eta_D = \eta_0 \cdot \eta_H \cdot \eta_R = \frac{R_T \cdot V}{P_D} \tag{2.13}$$

η_0 - Open-water (propeller) efficiency
η_H - Hull efficiency
η_R - Relative rotative efficiency
P_D - Delivered power at the propeller
R_T - Total calm water resistance
V - Ship speed

2.2.1 Propulsive Efficiency in Ideal Conditions

The propulsive efficiency coefficients are commonly evaluated in ideal calm water conditions. However, it is well known that the propulsive efficiency changes in a seaway and the amount of change depends on the added resistance. The following sections establish the efficiency components in ideal conditions, and the effect of load variation in a seaway is outlined in Section 2.2.2.

Propeller efficiency

The propeller efficiency η_0 evaluates the propeller's performance in open water, i.e., without the influence of the hull. It is often determined by model tests but can be estimated empirically based on propeller series data or by the use of different numerical methods. According to Steen et al. (2016), the propeller efficiency for conventional propellers in design condition is typically in the range of 0.6-0.8.

Hull efficiency

The hull efficiency η_H is defined by Equation 2.14

$$\eta_H = \frac{1-t}{1-w} \tag{2.14}$$

w is the effective mean wake fraction, accounting for the speed reduction from the ship speed V to the inflow to the propeller V_A. It is defined as

$$w = 1 - V_A/V \tag{2.15}$$

The thrust deduction factor t accounts for the increased resistance on the hull introduced by the working propeller. The resistance is mainly due to the propeller accelerating the water inflow, and the increased speed results in reduced propeller efficiency. The thrust factor is defined as

$$t = 1 - R_T/T \tag{2.16}$$

where R_T is the total resistance and T is the propeller thrust. Both the thrust factor and the wake fraction are often determined by model tests, but can be found by empirical methods. The hull efficiency for single screw ships are usually larger than 1.0, and typically in the range of 1.05-1.1 (Birk, 2019).

Relative rotative efficiency

The relative rotative efficiency η_R accounts for the variable propeller blade loads due to the non-homogenous wakefield inflow. It is normally in a narrow range of 0.97-1.03 (Steen et al., 2016).

2.2.2 Load Variation Correction

The propulsive efficiency changes due to load variations introduced by the added resistance in a seaway. Increased load on the propeller due to wind and waves usually decreases the efficiency. According to Valanto and Hong (2017), the propulsive efficiency losses are strongly connected to the decreasing open-water efficiency η_0, under increased propeller loading in waves. The propeller efficiency is reduced as a result of the changed propulsion point. Methods to predict the change in the propeller efficiency are presented in Section 3.3.4.

The changes in hull interaction factors such as wake and thrust deduction are less known effects (SFI, 2016). According to Tillig (2020), the changes in thrust factor, wake fraction, and relative rotative efficiency are small and it may be reasonable to neglect these effects.

The final corrected propulsive efficiency is denoted as η_{tot} in the current work, and is defined by Equation 2.17.

$$\eta_{tot} = \eta_{0,corrected} \cdot \eta_H \cdot \eta_R = \frac{(R_T + R_{wave} + R_{wind}) \cdot V}{P_D} \tag{2.17}$$

2.2.3 Total Delivered Power

When the total resistance and the propulsive efficiency is determined, the final power requirement can be calculated. The total delivered brake power P_B must overcome mechanical losses, losses in the transmission system due to shafts and bearings, and is finally determined by Equation 2.18.

$$P_B = \frac{P_D}{\eta_G \cdot \eta_S} = \frac{R_{tot} \cdot V}{\eta_G \cdot \eta_S \cdot \eta_{tot}} \tag{2.18}$$

η_G - Gear box losses
η_S - Losses in the transmission system

By knowing the propulsive efficiency and losses in mechanical and transmission systems, and by calculating the ship resistance at a certain speed V, the required power can be found. According to Schneekluth and Bertram (1998), the shaft efficiency η_S is typically 0.98-0.985. If the system is fitted with gears, η_G is usually larger or equal to 0.95 (Birk, 2019).

2.3 Ship Powering Methods

The ship powering evaluation methods range from traditional model tests to advanced numerical (CFD) methods. Generally, these methods are applied at a design stage in the absence of a prototype to test at full scale. Model tests are well established and considered to be a reliable performance prediction method at a design stage. Numerical analyses, i.e., CFD simulations, are of increasing significance, but are time-consuming and not as reliable as model tests unless the user has significant experience. Therefore, model tests and CFD simulations are not considered relevant to develop simplified prediction methods and are not further studied in the current work.

In order to compute the required power for the observed speed of each ship in the world fleet, empirical methods represent the most suitable approach. Historically, many systematic ship model tests and propeller series have been conducted. The empirical regression methods available are results of regression analyses of data from these model tests and full-scale ship trials. Most estimates are simple but have limited accuracy and application area. Despite a limited accuracy of $\pm 10\%$, the empirical regression methods are generally the method of choice in early design stages (Birk, 2019).

Some of the old regression-based empirical methods can be re-visited and modified to apply to fleet-wide calculations of ships in service. For some of the methods having general applicability, there is a considerable variation in the level of detail, i.e., the required number of input parameters for the calculations. This applies to both resistance estimates and propulsive efficiency predictions. A review of the relevant empirical prediction procedures will be presented in the next chapter.

Chapter 3

Empirical Prediction Methods

This chapter presents the relevant existing ship powering performance prediction methods. As discussed in Section 2.3 it is focused on computationally simple models with a wide application area, while requiring limited input. Methods to predict resistance, propulsion and the change of performance due to wind and waves are included. A comparison of these methods is presented in Section 5.1. Some parts of this chapter are based on a comprehensive literature study from the project thesis (Dale, 2020), although outlined in a more concise version in the following.

3.1 Empirical Resistance Procedures

A wide range of empirical resistance methods are identified, and systematic series and regression analysis are amongst the main approaches to empirically predict ship power requirements. The relevance of the well-known procedures is reviewed in the following. The empirical methods with limited applicable areas are listed in Table 3.1.

Table 3.1: Empirical resistance procedures with limited applicable area

Method	Applicable area	Author and publication
Ayre	Cargo ships	Remmers and Kempf (1949)
Taggart	Tugboats	Taggart (1954)
Taylor-Gertler	Slender cargo ships and warships	Gertler (1954)
Series-60	Cargo ships	Todd (1957)
BSRA	Cargo ships	Moor et al. (1961)
Helm	Small ships	Helm (1964)
Danckwardt	Cargo ships and trawlers	Danckwardt (1969)
Oortmessen	Small ships	Van Oortmerssen (1971)
Lap-Keller	Cargo and passenger ships	Lap (1954) and Auf'm Keller (1973)
NPL	Small ships	Bailey (1976)
Digernes formula	Fishing vessels	Digernes (1982)
HSVA	Catamarans	Fritsch and Bertram (2002), Bertram (2012)

According to Bertram (2012), all the systematic series and most of the regression-based methods in Table 3.1 are out of date, and several inaccurately predict the ship resistance. The reason may be the evolution of the hull form. Therefore, these are disregarded as suitable methods in the current work. However, some more 'modern' empirical methods with general applicability are widely used today, and these are presented in the following.

3.1.1 Guldhammer-Harvald

The procedure by Guldhammer and Harvald (1974) in its latest form, including update of procedure by Andersen and Guldhammer (1986) and by Kristensen et al. (2017).

Published: 1965, 1974, 1986 (update of procedure), 2012 (update of procedure)

Area of application: Universal, tankers, single and twin screw vessels

Basis for procedure: Extensive analysis of well-known published model tests such as Lap (1954), Gertler (1954), Todd (1957), Moor et al. (1961)

Output: Total calm-water resistance R_T, thrust factor t, wake fraction w

Key calculations:

$$C_T = C_R + C_F + C_A + C_{AA} \tag{3.1}$$

Where the residual resistance coefficient C_R is $f(F_n$ or $V/\sqrt{L}, L/\nabla^{1/3}, C_P)$. C_F is found by the ITTC'57 line and no form factor is applied. The hull-propeller interaction parameters are based on values given in diagrams in Harvald (1992). Kristensen et al. (2017) presents regression formulas for the diagrams that may be used for the calculations, including a bulb correction and corrections for t and w.

Input: As defined in accordance with Birk (2019)

Table 3.2: Required and optional input parameters for the Guldhammer-Harvald method

Required parameters	Symbol
Length between perpendiculars	L_{pp}
Length in waterline	L_{wl}
Length over wetted surface	L_{os}
Max. molded beam in waterline	B
Molded draft	T
Volumetric displacement	$\bigtriangledown$
Block coefficient	C_B
Prismatic coefficient	C_P
Area of ship and cargo above waterline	A_{VT}
Propeller diameter	D_p
Optional parameters	
Longitudinal center of buoyancy	LCB
Transverse cross section area of bulb	A_{BT}
Wetted surface	S
Wetted surface of appendages	S_{app}
Form factors, fore and aft body	F_F, F_A

Permissible range: As defined in accordance with Birk (2019)

Table 3.3: Recommended range for speed and main dimensions in Guldhammer-Harvald

Parameter	Symbol	Unit	Range
Froude number	F_n	$-$	≤ 0.33
Block coefficient	C_B	$-$	$[0.55, 0.85]$
Length-beam ratio	L/B	$-$	$[5.0, 8.0]$
Length-displacement ratio	$L/\sqrt[3]{\bigtriangledown}$	$-$	$[4.0, 6.0]$

Remarks:

- The resistance for ships with small L/B is underestimated (Schneekluth and Bertram, 1998).

References:
Guldhammer and Harvald (1974), Andersen and Guldhammer (1986), Schneekluth and Bertram (1998), Birk (2019).

3.1.2 Holtrop-Mennen

Resistance procedure by Holtrop (1984), often referred to as Holtrop'84.

Published: 1977, 1978, 1982, 1984, 1988 (Update of procedure not applied in the current work)

Area of application: Universal, wide range of ship types

Basis for procedure: Regression analysis of database of the Dutch model basin MARIN

Output: Total calm-water resistance R_T, w, t and power prediction

Key calculations: ITTC'78 resistance procedure applied including form factor

$$R_T = (1+k)R_F + R_W + R_A + R_{APP} + R_{AA} + R_B + R_{DB} \tag{3.2}$$

R_B is resistance due to bulbous bow near the water surface. Coefficients for computing the form factor (1+k) and the wave resistance R_W is added to Appendix C. A viscous resistance coefficient C_V is introduced for the hull-propeller interaction parameters w, t and η_H:

$$C_V = \frac{(1+k)R_F + R_{APP} + R_A}{\frac{1}{2}\rho V^2 \left(S + \sum_i S_{APP_i}\right)} \tag{3.3}$$

Input: As defined in accordance with Birk (2019)

Table 3.4: Required and optional input parameters for Holtrop-Mennen's method

Required parameters	Symbol
Length in waterline	L_{wl}
Max. molded beam in waterline	B
Molded mean draft, typically $T = \frac{1}{2}(T_A + T_F)$	T
Molded draft at aft and forward perpendicular	T_A, T_F
Volumetric displacement	∇
Block coefficient	C_B
Prismatic coefficient	C_P
Midship section coefficient (or $C_M = C_B/C_P$)	C_M
Waterplane area coefficient	C_{WP}
Longitudinal center of buoyancy	LCB
Area of ship and cargo above waterline	A_V
Area of immersed transom	A_T
Area of bulbous bow	A_{BT}
Height of center of A_{BT}	h_B
Stern shape factor	C_{stern}
Propeller diameter	D_p
Optional parameters	
Wetted surface	S
Wetted surface of appendages	S_{app}
Half angle of waterline entrances	i_E
Diameter of bow thruster tunnel	d_{TH}

Permissible range: As defined in accordance with Birk (2019)

Table 3.5: Recommended range for speed and main dimensions in Holtrop-Mennen

Parameter	Symbol	Unit	Range
Froude number	F_n	$-$	≤ 0.45
Prismatic coefficient	C_P	$-$	$[0.55, 0.85]$
Length-beam ratio	L/B	$-$	$[3.9, 9.5]$

Remarks:

- Bulbous bow and transom stern taken into account.
- According to Steen (2020), the bulb correction in Holtrop-Mennen is generally not applied.
- Covers a wide range of ships but require many parameters.

References: Holtrop (1977, 1984), Holtrop and Mennen (1982), Schneekluth and Bertram (1998), Birk (2019), Bertram (2012), Steen (2020)

3.1.3 Hollenbach

Resistance and power prediction procedure by Hollenbach (1998). The estimation of residuary resistance is emphasized in the following.

Published: 1997, 1998

Area of application: Universal, modern cargo ships, single and twin screw ships

Basis for procedure: Analysis of database of Vienna ship model basin

Output: Total calm-water resistance R_T, w, t and power prediction

Key calculations:
Mean, minimum and maximum total resistance coefficients:

$$\begin{aligned} C_{T,mean} &= C_{R,mean} + C_F + C_A + C_{APP} + C_{AA} \\ C_{T,min} &= C_{R,min} + C_F + C_A + C_{APP} + C_{AA} \\ C_{T,max} &= h_1 C_{R,mean} \end{aligned} \tag{3.4}$$

The residuary resistance is based on (BT) instead of wetted surface S. The method does not include a form factor k. According to Steen et al. (2016) the calculation can be improved by introducing a form factor as follows:

$$C_T = (C_F + \Delta C_F) \cdot (1 + k) + C_R + C_A + C_{APP} + C_{AA} \tag{3.5}$$

where the residual coefficient is a function of ship model frictional coefficient C_{Fm} as $f\,(R_n, F_n)$:

$$C_R = C_{\text{R,Hollenbach}} \cdot \frac{B \cdot T}{S} - k \cdot C_{Fm} \tag{3.6}$$

Coefficients of $C_{\text{R,Hollenbach}}$ is added to Appendix A. The added frictional resistance is also included as discussed in Section 2.1. The resistance estimate is combined with open water tests and corrected for the hull-propeller interaction by:

η_R - relative rotative efficiency
t - thrust deduction fraction
w - wake fraction

Input: As defined in accordance with Birk (2019)

Table 3.6: Required and optional input parameters for Hollenbach's method

Required parameters	Symbol
Length between perpendiculars	L_{pp}
Length in waterline	L_{wl}
Length over wetted surface	L_{os}
Molded beam	B
Molded draft at aft and forward perpendicular	T_A, T_F
Volumetric displacement	∇
Propeller diameter	D_p
Block coefficient	C_B
Area of ship and cargo above waterline	A_V
No. of appendages (rudders, shaft brackets, bossings, thrusters)	$N_{appendages}$
Optional parameters	
Wetted surface	S
Wetted surface of appendages	S_{app}
Diameter of bow thruster tunnel	d_{TH}

Permissible range: As defined in accordance with Birk (2019) for a single screw vessel on design draught

Table 3.7: Recommended range for main dimensions in Hollenbach
(*) Extended range for mean resistance calculation by Birk (2019)

Parameter	Symbol	Unit	Range
Block coefficient	C_B	$-$	$[0.49, 0.83]^*$
Length-beam ratio	L_{pp}/B	$-$	$[4.71, 7.11]$
Beam-draught ratio	B/T	$-$	$[1.99, 4.00]$
Propeller diameter-draught ratio	D_p/T_A	$-$	$[0.43, 0.84]$
Length-displacement ratio	$L_{pp}/\sqrt[3]{\nabla}$	$-$	$[4.49, 6.01]$

Remarks:

- Resistance estimated for trial conditions and for a ship without propulsor.
- Based on a relatively modern database.

References:
Hollenbach (1998), Schneekluth and Bertram (1998), Bertram (2012), Birk (2019)

3.2 Added Resistance due to Wind and Waves

Several empirical methods to predict added resistance due to wind and waves are identified in this section. The methods vary in level of detail and applicable range and will be compared in Section 5.1.

ITTC (2014) recommends four different methods to predict added wave resistance. Two of the methods require tank tests and are not relevant for fleet calculations. However, the other two are empirical and are also recommended in ISO 15016 standard by ISO Technical Committee (2015). The respective empirical methods for added wave resistance predictions are developed by MARIN (2006). These are presented in the following based on the recommended procedures in the ISO 15016 standard. If limited heave and pitch motions can be assumed, STAWAVE-1 is applicable, otherwise, STAWAVE-2 is recommended.

In cases where wind tunnel tests are unavailable, ITTC (2014) recommends two empirical methods for predicting added wind resistance. The methods are developed by MARIN (2006) and Fujiwara et al. (2017) and presented in the following. In addition, the method by Blendermann (1995) is included. The study is based on extensive wind tunnel tests and is widely applied in the literature.

3.2.1 STAWAVE-1

A simplified method to estimate the added resistance in waves for modern ships when limited input data is available. Developed by MARIN (2006) and recommended in ISO 15016.

Published: 2006 (MARIN), 2015 (ISO 15016)

Area of application: Universal, present-day ships, limited to low-to-mild sea states (defined under 'Remarks')

Basis for procedure: Model tests in MARIN's Depressurised Wave Basin (DWB)

Output: Mean wave resistance in long crested irregular waves, approximated by the mean wave reflection resistance

Key calculations: Equation 3.7 estimates the mean wave resistance R_{AWL}, in long crested irregular waves:

$$R_{\text{wave}} \approx R_{\text{AWL}} = \frac{1}{16}\rho_{\text{S}} g H_{1/3}^2 B \sqrt{\frac{B}{L_{BWL}}} \tag{3.7}$$

Input: As defined in Table 3.8

Table 3.8: Required input parameters for STAWAVE-1

Required parameters	Symbol
Significant wave height	$H_{1/3}$
Ship breadth	B
Length between perpendiculars	L_{PP}
Distance of the bow to 95 $\%$ maximum breadth on the waterline	L_{BWL}

Where L_{BWL} is defined according to Figure 3.1 from ISO 15016.

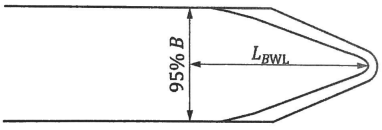

Figure 3.1: Definition of L_{BWL} in STAWAVE-1 (ISO Technical Committee, 2015)

Remarks: Method limited to sea states where the following can be assumed:

- Low to mild sea states with restricted wave heights $(H_{1/3} \leq 2.25\sqrt{L_{\text{PP}}/100})$
- Waves from ahead $[0$ to $\pm 45\,(^\circ)]$
  - $\Rightarrow$ Limited heave and pitch motions
  - $\Rightarrow$ Wave reflection dominates the added wave resistance
  - $\Rightarrow$ Wave induced ship motions can be neglected

References: MARIN (2006), ISO Technical Committee (2015)

3.2.2 STAWAVE-2

An empirical correction method developed by MARIN (2006). The method applies a frequency response function for ships with heave and pitch, and covers both wave reflection and induced motion effects.

Published: 2006 (MARIN), 2015 (ISO 15016)

Area of application: Universal, present-day ships, within the defined range defined in Table 3.10

Basis for procedure: Model tests in MARIN's Depressurised Wave Basin (DWB)

Output: Mean wave resistance in long crested irregular waves

Key calculations: Equation 3.8 estimates the mean wave resistance in long crested irregular waves:

$$R_{wave} = 2\int_0^\infty \frac{R_{\mathrm{AWL}}\left(\omega; V_{\mathrm{S}}\right)}{\zeta_{\mathrm{A}}^2} S_\eta(\omega) d\omega \tag{3.8}$$

The mean resistance increase in regular waves R_{AWL} is

$$R_{\mathrm{AWL}} = R_{\mathrm{AWML}} + R_{\mathrm{AWRL}} \tag{3.9}$$

where the motion induced resistance component is

$$R_{\mathrm{AWML}} = 4\rho_{\mathrm{S}} g \zeta_{\mathrm{A}}^2 \frac{B^2}{L_{\mathrm{PP}}} \overline{r_{\mathrm{aw}}}(\omega) \tag{3.10}$$

and the wave reflection component is

$$R_{\mathrm{AWRL}} = \frac{1}{2}\rho_{\mathrm{S}} g \zeta_{\mathrm{A}}^2 B \alpha_1(\omega) \tag{3.11}$$

$\overline{r_{\mathrm{aw}}}(\omega)$ is the empirical transfer function as $f(F_n, L_{pp}, k_{yy}, g, C_B)$. The entire calculation is lengthy and therefore not outlined further here.

Input: As defined in Table 3.9

Table 3.9: Required input parameters for STAWAVE-2

Required parameters	Symbol
Ship speed	V
Ship breadth	B
Length between perpendiculars	L_{PP}
Draught at midships	T
Block coefficient	C_B
Radius of gyration in lateral direction	k_{yy}
Significant wave height	$H_{1/3}$
Wave amplitude	ζ_A
Wave number	k
Modified Bessel function of first kind of order 1	I_1
Modified Bessel function of second kind of order 1	K_1
Frequency spectrum (ISSC for wind waves)	S_η

Permissible Range: As defined in Table 3.10

Table 3.10: Permissible range for STAWAVE-2

Parameter	Symbol	Unit	Range
Wave heading direction	β	deg [°]	$[0, \pm 45]$
Length	L_{pp}	m	$[75, 350]$
Block coefficient	C_B	$-$	$[0.50, 0.90]$
Length-beam ratio	L_{pp}/B	$-$	$[4.0, 9.0]$
Beam-draught ratio	B/T	$-$	$[2.2, 5.5]$
Froude number	Fn	$-$	$[0.10, 0.30]$

Remarks:

- Wave spectrum defined without forward speed.
- Pierson-Moskowitz spectrum recommended for fully developed sea.
- JONSWAP spectrum recommended for young developing sea states.

References: MARIN (2006), ISO Technical Committee (2015)

3.2.3 STA-JIP wind

An empirical method to predict wind resistance by MARIN (2006), and recommended in ISO 15016. The method presents wind resistance coefficients for a range of common present-day ship types.

Published: 2006 (MARIN), 2015 (ISO 15016)

Area of application: Common present-day ship types, including tankers, LNG carriers, container ships, car carriers, ferry/cruise ships and general cargo ships

Basis for procedure: Systematic wind tunnel experiments and CFD simulations conducted by MARIN (2006), Witherby & Co (1985) for OCIMF, and Blendermann (1995)

Output: Wind resistance R_{wind}

Key calculations: Equation 3.12 estimates the wind resistance, based on tabulated values for the wind resistance coefficient $C_X\left(\psi_{\mathrm{WR}}\right)$

$$R_{\mathrm{wind}} = 0.5\rho_{\mathrm{A}} \cdot C_{\mathrm{X}}\left(\psi_{\mathrm{WR}}\right) \cdot A_{\mathrm{VT}} \cdot V_{\mathrm{WR}}^2 - 0.5\rho_{\mathrm{A}} \cdot C_{\mathrm{X}}(0) \cdot A_{\mathrm{VT}} \cdot V_{\mathrm{G}}^2 \tag{3.12}$$

Input: As defined in Table 3.11

Table 3.11: Required input parameters for STAJIP wind

Required parameters	Symbol
Air density	ρ_A
Wind resistance coefficient	C_X
Relative wind direction at the reference height	ψ_{WR}
Transverse projected area above waterline	A_{VT}
Relative wind velocity at reference height	V_{WR}
Ship speed over ground	V_G

Remarks:

- Wind resistance coefficients are applicable to tankers, LNG carriers, container ships, car carriers, ferry/cruise ships and general cargo ships.
- Procedure is not applicable to tugs, offshore supply vessels, fishing vessels and fast craft.

References: MARIN (2006), ISO Technical Committee (2015)

3.2.4 Fujiwara

A method to predict wind resistance coefficients by Fujiwara (2005), and recommended in ISO 15016. The method is extended by Fujiwara et al. (2017) to include regression formulas to estimate geometric parameters of the ship superstructure.

Published: 2005, 2017 (extension)

Area of application: Universal, wide range of ship types

Basis for procedure: Wind tunnel test data and regression formulas

Output: Wind resistance coefficient C_X (ψ_{WR})

Key calculations: C_X as function of the relative wind direction, regression coefficients, and a number of geometrical properties listed in Table 3.12, and illustrated in Figure 3.2 from Fujiwara et al. (2017)

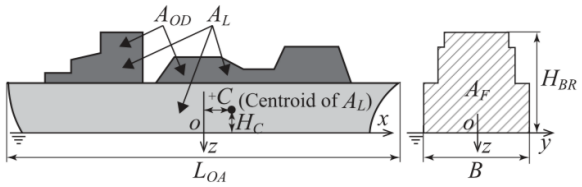

Figure 3.2: Definition of structural parameters in Fujiwara et al. (2017)

Input: As defined in Table 3.12

Table 3.12: Required input parameters for Fujiwara wind resistance coefficients

Required parameters	Symbol
Relative wind direction at the reference height	ψ_{WR}
Length overall	L_{oa}
Breadth	B
Transverse projected area above waterline	A_{VT}
Lateral projected area above waterline	A_{VL}
Lateral projected area above upper deck	A_{OD}
Distance from midship section to centre of A_{VL}	C_{MC}
Height of top of superstructure	H_{BR}
Height from waterline to centre of A_{VL}	H_C
Smoothing range (normally 10 degrees)	μ

Remarks:

- The method require a high level of detail for superstructure parameters.

References: Fujiwara (2005), Fujiwara et al. (2017), ISO Technical Committee (2015)

3.2.5 Blendermann

Blendermann (1986, 1994, 1995, 2004) presents an extensive study of wind loads on ships. The method is extended in later studies to include various wind load coefficients. Here, the method is outlined with regards to the longitudinal resistance.

Published: 1986, 1994, 1995, 2004

Area of application: Universal, wide range of ship types

Basis for procedure: Wind tunnel test data and regression formulas

Output: Wind resistance coefficient C_X (ψ_{WR}), for both lateral and longitudinal resistance, cross-force and rolling-moment

Key calculations: Tabulated values for the wind resistance coefficient C_X (ψ_{WR}) as function of the relative wind direction at the reference height ψ_{WR}. Table 3.13 presents the longitudinal wind resistance coefficients for head wind (Blendermann, 1994). The complete set of coefficients are tabulated and added to Appendix E.

Table 3.13

Type of Vessel	C_X ($\psi_{\mathrm{WR}} = 0$)
Car carrier	0.55
Cargo vessel, loaded/container on deck	0.65/0.55
Container ship, loaded	0.55
Drilling vessel	0.60
Ferry	0.45
Fishing vessel	0.70
LNG tanker	0.60
Offshore supply vessel	0.55
Passenger liner	0.40
Research vessel	0.55
Speed boat	0.55
Tanker loaded/ballast	0.90/0.75
Tender	0.55

Input:
Ship type and relative wind direction

References:
Blendermann (1986, 1994, 1995, 2004)

3.2.6 Townsin & Kwon

Townsin and Kwon (1983) presents a study on estimating the influence of weather on ship performance. An extension to the method by Kwon (2008) presents a formula to estimate the speed loss due to added resistance in wind and waves. Here, the method is outlined in the newest version with the extension. Lu et al. (2015) presents a modification of Kwon, but the new coefficients are not published and therefore not further studied here.

Published: 1983, 1993, 2008 (Extension by Kwon)

Area of application: All weather directions are applicable, as head sea and head wind is modified by direction factors in the procedure

Basis for procedure: Analysis of a wide range of ships having Series 60 forms

Output: The reduced speed in weather due to increased resistance in wind and waves expressed as added resistance

Key calculations:

$$\left(\frac{\triangle V}{V}\right) \cdot 100\% = C_\beta C_U C_{Form} \tag{3.13}$$

Where:
C_β is the direction angle coefficient as $f(BN)$, measured with respect to the ship bow
C_U is the speed reduction coefficient as $f(C_B, F_n)$
C_{form} is the ship form coefficient as $f(\mathrm{shiptype}, BN, \nabla)$

Let x be the reduction factor:

$$x = \left(\frac{\triangle V}{V}\right) = \frac{C_\beta C_U C_{Form}}{100\%} \tag{3.14}$$

The ship brake power P_B is computed as follows, where η_{tot} is a function of $(V + \triangle V)$.

$$
\begin{aligned}
P_B &= \frac{R_T \cdot (V + \triangle V)}{\eta_{tot}} \\
&= \frac{R_T \cdot (V + x \cdot V)}{\eta_{tot}} \\
&= \frac{V \cdot (R_T + x \cdot R_T)}{\eta_{tot}} \\
&= \frac{V \cdot (R_T + R_{added})}{\eta_{tot}}
\end{aligned}
\tag{3.15}
$$

R_T is the calm water resistance and the final added resistance is computed as $R_{added} = x \cdot R_T$. The method originally expresses the reduced speed as $V_W = V - \triangle V$. However, if a ship speed of V is observed for a ship, the calculated added resistance must include $V + \triangle V$.

Input: As defined in Table 3.14

Table 3.14: Required input parameters for the Kwon method

Required parameters	Symbol
Ship speed	V
Beaufort number	BN
Length in waterline	L_{WL}
Block coefficient	C_B
Volumetric displacement	∇
Mean wave and wind direction relative to ship	β

Remarks:

- Wind-generated waves are assumed.
- Not possible to differ between increased resistance due to waves and increased resistance due to wind.
- In the current work, BN is computed based on the official Beaufort Wind Scale.

References:
Townsin and Kwon (1983, 1993), Kwon (2008).

3.3 Propulsion Prediction Methods

Empirical procedures to determine the propulsive efficiency range from simple empirical estimates to more detailed propeller design procedures. Primarily three different approaches to determine the propulsive efficiency are suggested and will be outlined in the following.

The first approach is to determine each propulsive efficiency term, i.e., $\eta_D = \eta_0 \eta_H \eta_R$. This implies finding the open water efficiency, which require an estimated propeller design. Relevant propeller series to determine the required parameters are outlined in Subsection 3.3.1.

The second approach is to apply simple empirical formulas requiring limited input for the propulsive efficiency η_D directly. Several methods are found in the literature and presented in Section 3.3.2. Section 3.3.3 presents the third suggested approach, which is to apply the sea-margin to find the propulsive efficiency.

As the empirical prediction methods mainly are valid for calm water conditions, corrections for the load variations in waves must be applied. Relevant correction methods are presented in Section 3.3.4.

3.3.1 Propulsive Efficiencies

Methods to determine each propulsive efficiency term are identified in the following.

Open water efficiency

A wide range of propeller series are identified and outlined briefly in the following, as presented in Birk (2019). The relevance of the series is reviewed, and those with limited applicable areas are listed in Table 3.15.

Table 3.15: Propeller series with limited applicable area

Method	Applicable area	Author and publication
Gawn series	High speed and naval vessels	Gawn (1953)
KCA (Gawn-Burrill) series	High speed and naval vessels	Gawn and Burrill (1957)
Newton-Rader series	Small high speed vessels	Newton and Rader (1961)
DTMB skewed series	Not applicable for propeller design	Boswell (1971)
KA-series	Ducted propellers only	Oosterveld (1970)
Tillig new propeller series	Conventional ships	Tillig (2020)

According to Birk (2019), all the listed propeller series listed in Table 3.15 have limited applicability, and some are out of date. Therefore, these are not further considered in the current work. In addition to the listed propeller series, some series for controllable pitch propellers exist. These also have limited applicability. However, the Wageningen B-series (Oosterveld and van Oossanen, 1975) covers a wide range of principal propeller characteristics and has a wide area of applicability. The series represents the most 'modern' and extensive procedure. Tillig (2017) suggests the Wageningen-B series is outdated and presents a new propeller series, developed to account for present propeller designs. However, Kristensen et al. (2017) presents a simplified method to obtain quick estimates with the Wageningen-B series based on limited input, and it is therefore selected for further investigation.

Wageningen B-series

The Wageningen B-Series (Troost, 1951) also referred to as Troost series in the litterature, is the most extensive propeller series developed (Birk, 2019). There is a wide data range in terms of combinations of number of blades Z, expanded area ratio A_E/A_0 and pitch-diameter ratio P/D_p. Applying the series require a number of estimated parameters, which is a challenge when the propeller design is unavailable. However, Kristensen et al. (2017) present a simplified version of applying the method which is outlined in the following.

Approximated values from Wageningen B-series

Breslin and Andersen (1994) present curves for approximated values for η_0 from the Wageningen B-series, denoted as $\eta_{0,Wag}$. The efficiency is defined as a function of the thrust load bearing coefficienct C_{Th} as presented in Equation 3.16

$$\mathrm{C_{Th}} = \frac{8}{\pi} \cdot \frac{\mathrm{R_T}}{(1-\mathrm{t}) \cdot \rho \cdot (\mathrm{V_A} \cdot \mathrm{D_p})^2} \tag{3.16}$$

Here, the coefficient is independent of the rate of revolutions. R_T is the ship resistance and $V_A = (1-w) \cdot V$ is the inflow velocity to the propeller. Kristensen et al. (2017) present a relation between the ideal propeller efficiency and the approximated values $\eta_{0,Wag}$ to expand the range for the approximated Wageningen method. The efficiency can then be estimated as follows, as long as $f\left(C_{Th}\right)$ is not lower than 0.69:

$$\eta_0 = \eta_{0,Wag} = \frac{2}{1+\sqrt{C_{Th}+1}} \cdot f\left(C_{Th}\right) \tag{3.17}$$

where

$$f\left(C_{Th}\right) = 0.81 - 0.014 \cdot C_{Th} \tag{3.18}$$

Hull efficiency

In order to determine the hull efficiency, the thrust deduction factor and the wake factor must be found, as Equation 3.19 presents.

$$\eta_H = \frac{1-t}{1-w} \tag{3.19}$$

The wake and thrust factor are significantly influenced by the shape of the ship, specifically the aft hull. Therefore, prediction methods are usually a function of the block coefficient C_B or the prismatic coefficient C_P. Other influencing factors regarding the propeller are often not considered. Several empirical estimates with few input parameters for t and w exist. It is only considered relevant to elaborate on those with general applicability. As identified in Section 3.1, all the calm water resistance methods include predictions of thrust and wake factors. These are considered to have general applicability and are briefly outlined below.

Guldhammer-Harvald:

Harvald (1992) presents estimates for t and w as outlined by Kristensen et al. (2017), according to Equation 3.20

$$\begin{aligned} w &= w_1\left(\tfrac{B}{L}, C_B\right) + w_2\left(\text{form}, C_B\right) + w_3\left(\tfrac{D_\text{p}}{L}\right) \\ t &= t_1\left(\tfrac{B}{L}, C_B\right) + t_2(\text{form}) + t_3\left(\tfrac{D_\text{p}}{L}\right) \end{aligned} \tag{3.20}$$

where w_2 and t_2 is equal to zero for the common N-shaped hull form, and D_P is the propeller diameter. The parameters of Equation 3.20 can be approximated in accordance with diagrams from Harvald (1992). Kristensen et al. (2017) present approximated values from these diagrams by regression formulas. The calculation is lengthy and therefore added to Appendix B.

Holtrop-Mennen:

Equation 3.21 and 3.22 by Holtrop (1977) represent general formulas for single-screw ships.

$$t = 0.001979 \cdot \frac{L}{B\left(1-C_P\right)} + 1.0585 \cdot \frac{B}{L} - 0.00524 - 0.1418 \cdot \frac{D_P^2}{B \cdot T} \tag{3.21}$$

$$w = c_9 c_{20} C_V \frac{L_{WL}}{T_A}\left[0.050776 + 0.93405\frac{c_{11} C_V}{1-C_{P1}}\right] + 0.27915 c_{20}\sqrt{\frac{B}{L_{WL}\left(1-C_{P1}\right)}} + c_{19} c_{20} \tag{3.22}$$

The coefficients of Equation 3.22 are tabulated values from Birk (2019), added to Appendix C.

Hollenbach:

Hollenbach (1998) estimates t, w, and η_H, somewhat differently from Guldhammer-Harvald and Holtrop-Mennen. Here, the procedure is outlined according to Birk (2019) for a single screw vessel on design draught. The thrust deduction factor is assumed to be constant, $t = 0.190$. The wake fraction and hull efficiency is determined based on the model scale hull efficiency in Equation 3.23.

$$\eta_{HM} = 0.948 C_B^{0.3977}\left(\frac{R_{T\text{mean}}}{R_T}\right)^{-0.58}\left(\frac{B}{T}\right)^{0.1727}\left(\frac{D_P^2}{BT}\right)^{-0.1334} \tag{3.23}$$

R_T is the calm water resistance, while R_{Tmean} is the mean calm water resistance in Hollenbach. Then, the model scale wake fraction is computed according to Equation 3.24

$$w_{TM} = 1 - \frac{1-t}{\eta_{HM}} \tag{3.24}$$

Finally the full scale wake fraction is determined by Equation 3.25, according to the ITTC'78 Performance Prediction Method

$$w = w_{TS} = (t + 0.04) + (w_{TM} - (t + 0.04)) \left[\frac{C_{FS} + C_A}{C_{FM}} \right] \tag{3.25}$$

C_{FS} and C_{FM} are the frictional resistance coefficients for full scale, and model scale, respectively. When w is calculated, η_H is finally determined.

Relative rotative efficiency

As outlined in the theory section, the relative rotative efficiency is influenced by several effects, which makes it difficult to estimate with few input parameters. However, Holtrop (1977) presents Equation 3.26 for single-screw ships:

$$\eta_R = 0.9922 - 0.05908 \cdot A_E/A_0 + 0.07424 \cdot (C_P - 0.0225 \cdot \mathrm{LCB}) \tag{3.26}$$

where

A_E/A_0 - Propeller expanded blade area ratio (EAR)
C_P - Prismatic hull coefficient
LCB - Longitudinal centre of buoyancy

The relative rotative efficiency is often close to 1.00 and Alte and Baur (1986) recommend using η_R = 1.00 for single-screw ships as a simple estimate.

3.3.2 Empirical Formulas for the Propulsive Efficiency

There are some complete empirical procedures developed to estimate the propulsive efficiency. Several of these are only applicable for specific ship types and belong to the methods in Table 3.1. The identified methods are presented in Table 3.16.

Table 3.16: Empirical Propulsive Efficiency Prediction formulas

Estimation Formula	Applicable area	Reference
$\eta_D = 0.836 - 0.000165 \cdot n \cdot \nabla^{1/6}$	Cargo ships and trawlers	Danckwardt (1969)
$\eta_D = 0.885 - 0.00012 \cdot n \cdot \sqrt{L_{pp}}$	Cargo and passenger ships	Auf'm Keller (1973)
$\eta_\mathrm{D} = 0.84 - \frac{n\sqrt{L_{pp}}}{10000}$	General applicability	Emersons formula (Watson, 1998)

Here, n is the propeller rpm. According to Watson (1998), Emersons formula is derived for low propeller rpm although extended to modern propeller design. These ranges define the applicable areas and are illustrated in Figure 3.3 below. QPC refers to the quasi-propulsive constant i.e. the propulsive efficiency η_D.

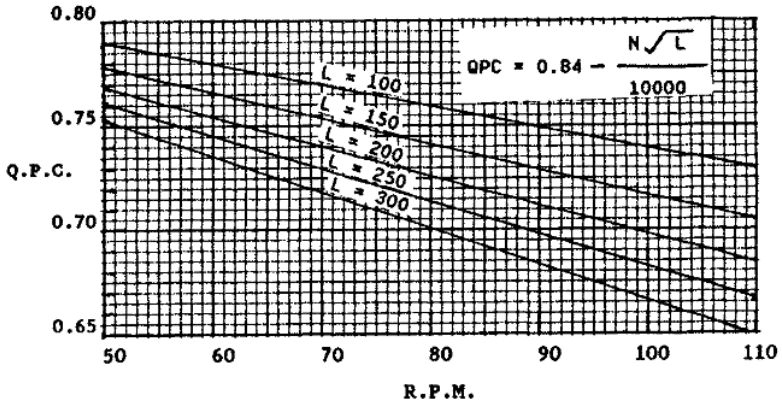

Figure 3.3: Applicable ranges for Emersons formula, inclduing the extension by Watson (1998)

3.3.3 Prediction Based on Sea-Margin

The following method represents a simple way to estimate the propulsive efficiency in ideal conditions, which can be tuned to fit the fleet better. In ship design, it is common practice to account for wind and waves by using a sea-margin (SM) on the power, which is typically set to 15% (SFI, 2016). Further, ships operate on a nominal continuous rating (NCR), which is typically 85 % of the max continuous rating (MCR). Sea-web provides installed power on the ship, which can be combined with these margins to find the required power in ideal conditions (i.e., assuming that the 15% sea-margin is applied) as presented in Equation 3.27.

$$P_s \approx \underbrace{(100 - 15\%)}_{SM} \cdot \underbrace{85\%}_{MCR} \cdot P_{installed} \tag{3.27}$$

By calculating the related calm-water resistance for a ship with speed V, the final ideal propulsive efficiency can be estimated by modifying Equation 2.18 for required calm-water power as presented in the Theory Section, to Equation 3.28

$$\eta_D \approx \frac{R_T \cdot V}{P_s \cdot \eta_S} \tag{3.28}$$

The ship speed can be taken as the service speed provided by Sea-web, and losses in the transmission system η_S must be estimated.

3.3.4 Load Variation Correction

The former methods outlined in this section are mainly valid for calm water conditions and must be corrected for the load variations on the propeller in a seaway. Three correction procedures are presented in the following.

ISO 15016 correction

A procedure to correct for the change of propulsive efficiency due to added resistance is recommended in the ISO 15016 standard (ISO Technical Committee, 2015). The method is based on a load variation test and as presented in Equation 3.29, the efficiency is varying linearly with the increased resistance.

$$\frac{\eta_{\mathrm{tot}}}{\eta_{\mathrm{D}}} = \xi_P \frac{\Delta R}{R_{\mathrm{T}}} + 1 \tag{3.29}$$

η_{tot} - Efficiency in trial conditions
η_{D} - Efficiency in ideal conditions
ΔR - Added resistance in weather
R_T - Calm water resistance
ξ_P - Slope of the linear curve in the load variation test

The expression for the power correction is presented in Equation 3.30:

$$\begin{aligned} P_{\text{tot}} &= P_{\text{S}} + \Delta P \\ \Delta P &= \frac{\Delta RV}{\eta_{\text{tot}}} + P_{\text{D}} \left(1 - \frac{\eta_{\text{tot}}}{\eta_{\text{D}}}\right) \end{aligned} \tag{3.30}$$

ΔP - Increased power required due to efficiency loss
P_{tot} - Delivered power in trial conditions
P_S - Delivered power in ideal conditions

Here, ξ_P is the unknown parameter that must be estimated. $\xi_P = 0$ represent zero correction for changed efficiency, which is a significant simplification of real conditions. In the ISO 15016 standard test, ξ_P remains at [0.25,0.24,0.25] for the speed increase of [14.0,15.0,16.0] knots. It may be reasonable to assume a constant value of $\xi_P = 0.25$ at this stage.

Modified Wageningen B-series

The approximated Wageningen method by Kristensen et al. (2017) may be modified to include the added resistance in a seaway. Equation 3.31 calculates the thrust loading coefficient due to calm water resistance and the added resistance due to wind and waves.

$$\mathrm{C_{Th}} = \frac{8}{\pi} \cdot \frac{(\mathrm{R_T} + \mathrm{R_{added}})}{(1 - \mathrm{t}) \cdot \rho \cdot (\mathrm{V_A} \cdot \mathrm{D_p})^2} \tag{3.31}$$

By including the added resistance, C_{Th} is corrected and a corrected propeller efficiency is determined $\eta_{0,corrected}$.

Propulsive efficiency by Lindstad et al. (2011, 2013, 2014)

Lindstad et al. (2011, 2013, 2014) present the propulsive efficiency as η_{tot} according to Equation 3.32. The ideal efficiency η_D is corrected for speed reductions and waves in the seastate.

$$\eta_{tot} = \min \left(\eta_D \left(j + k \cdot \sqrt{\frac{V}{V_d}} \right), \eta_D \left(1 - r \cdot H_{\frac{1}{3}}\right) \right) \tag{3.32}$$

Here, V_d is the design speed. The relation is determined based on the work by Minsaas (2006) and empirical investigations of propulsion efficiencies by the authors. η_D is typically in the range of $0.6 - 0.7$ (Lindstad et al., 2011). The first term corrects the propulsion efficiency for voluntarily reduced speeds below the design speed. j and k are empirical constants related by $j + k = 1$. These are determined based on empirical analysis, and determine the rate of reduced efficiency for reduced speed. The second term determines the correction for waves based on the significant wave height of the sea state. r is the factor determining the rate of reduction and must be found empirically.

3.4 Complete Power Prediction Models

As mentioned in the introduction, new models have been developed for ship powering prediction estimates with the common objective of fleet-wide emission calculations. Therefore, the models differ from the previously evaluated empirical methods commonly used in preliminary ship design. Amongst other things, the new models combine existing empirical methods with new research. An overview of the relevant models is given in the following.

3.4.1 ShipCLEAN by Tillig et al.

ShipCLEAN by Tillig et al. (2018) is a power prediction method composed of existing empirical formulas and new developed procedures. The method is applicable to conventional ships. Tillig (2020) presents four approaches for predicting the power, based on stages of available information. This section outlines ShipCLEAN

according to stage 1, requiring only main dimensions as input.

The calm water resistance coefficient is decomposed as Equation 3.33

$$C_T = C_F + C_R \tag{3.33}$$

where the residual resistance is evaluated according to Hollenbach and the updated Guldhammer-Harvald method by Kristensen et al. (2017). The valid ranges are checked for both methods and the resistance is calculated as the mean of the valid methods. For Hollenbach, the mean resistance estimate for a ship on ballast-draught is applied.

Added resistance due to waves are determined by the average of STAWAVE-2 and a method by Liu and Papanikolaou (2016). The added wind resistance is predicted by Blendermann (1995).

The propulsive efficiency is computed according to Equation 3.34

$$\eta_D = \eta_H \cdot \eta_0 \tag{3.34}$$

where a new propeller series is developed to determine the propeller efficiency. The hull efficiency is calculated according to the author's own estimate, as function of the block coefficient:

$$\eta_H = 1.05 + 0.2\,(C_B - 0.4)$$

The average of five empirical methods is applied to determine the wake fraction then the thrust factor is estimated by:

$$1 - t = \eta_H\,(1 - w)$$

A study on load variations on the propeller due to waves is presented. The author suggests to correct the propeller efficiency, and presents negligible variations in thrust and wake factors.

The study presents several estimates for hull and propulsion parameters. Two new hull series for slender ships and ships with higher blockage coefficients are developed and applied to find the wetted surface area.

3.4.2 A Power Prediction model by Kristensen et al.

The power prediction method suggested by Kristensen et al. (2017) is composed of existing empirical formulas and regression estimates for the input parameters. The resistance calculations are based on the original ITTC 1957 method, decomposed as follows:

$$C_T = C_F + C_A + C_{AA} + C_R = \frac{R_T}{\frac{1}{2}\rho \cdot S \cdot V^2} \tag{3.35}$$

The frictional resistance is estimated by the ITTC'57 friction line and the wave making resistance is determined by Harvald 1983 method. Effects of wind and waves are included in the service allowance ranging from 20-30$\%$. The study presents a new method to make the bulbous bow correction, as well as new estimates for thrust factor and wake fraction. In the analysis it is assumed that the bulbous bow is a function of the same parameters as Harvalds C_R estimate, i.e. $f(L/\nabla^{1/3}, C_P, F_n)$. A separate analysis is also conducted for the value of the wetted surface area. The calculation is based on Mumford's formula:

$$S = 1.025 \cdot L_{PP} \cdot (C_B \cdot B + 1.7 \cdot T) = 1.025 \cdot \left(\frac{\nabla}{T} + 1.7 \cdot L_{PP} \cdot T\right) \tag{3.36}$$

In the study, a regression analysis is conducted for 129 modern ships of different types and sizes, to tune the constants of the equation above to fit the main ship types more accurately. The propulsive efficiency is determined by Wageningen B-series and estimation of propeller characteristics to compute the required input:

$$\eta_{tot} = \eta_H \cdot \eta_0 \cdot \eta_R \cdot \eta_S \tag{3.37}$$

A regression analysis is conducted to modify the Harvald formulas for wake fraction and thrust deduction to modern ships. There is not made any corrections for change in propulsive efficiency due to added resistance. The final power P_{tot} is then determined by:

$$P_E = R_T \cdot V \cdot \left(1 + \frac{\text{service allowance in } \%}{100}\right) \tag{3.38}$$

$$P_{tot} = \frac{P_E}{\eta_{tot}} \tag{3.39}$$

3.4.3 STEAM 3 by Jalkanen et al.

STEAM3 by Johansson et al. (2017) and Jalkanen et al. (2012), is a ship traffic emission assessment model, extended from previous versions (STEAM and STEAM2). The model is similar to the MariTEAM model although the power calculations are evaluated differently. The calm-water resistance is evaluated by Hollenbach and the ITTC friction line, and added weather resistance is calculated according to Kwon (2008).

$$P_{tot} \approx \frac{1}{\eta_D} \cdot (R_F + R_R)\, V_W \tag{3.40}$$

The propulsive efficiency is determined by Emersons formula for quasi propulsive constant η_D, as function of propeller rate of revolutions n, and ship length between perpendiculars L_{pp}:

$$\eta_{\mathrm{D}} = 0.84 - \frac{n\sqrt{L_{pp}}}{10000}$$

The study is based on a database including about 30,000 ships with propeller characteristics. For the ships with unknown propeller diameter, this is estimated by a regression analysis on fraction of draught distances. With regards to simplifications, there is not applied a correction for the change in propulsive efficiency due to weather or any roughness corrections to the frictional resistance.

3.4.4 A Power Prediction model by Lindstad et al.

Lindstad et al. (2014) presents an empirical power prediction method according to Equation 3.41.

$$P_{tot} = \frac{P_s + P_w + P_a}{\eta_{tot}} + P_{aux} \tag{3.41}$$

η_{tot} is the propulsive efficiency, including corrections for voluntarily speed reductions, and modified to include effects of waves in the seastate:

$$\eta_{tot} = \min\left(\eta_D\left(j + k \cdot \sqrt{\frac{v}{V_d}}\right), \eta_D\left(1 - r \cdot H_{\frac{1}{3}}\right)\right)$$

P_s is the calm water power requirement, computed as function of the total resistance coefficient C_T:

$$P_s = \frac{\rho \cdot C_T \cdot S \cdot v^3}{2}$$

P_w is the added power required due to increased resistance in wind and waves, calculated similar to the STAWAVE-1 procedure in ISO 15016:

$$P_s = \frac{1}{2}\frac{c_{aw} \cdot \rho \cdot g \cdot \left(H_{1/3}/2\right)^2 \cdot B^2}{L}(v + u)$$

The required power due to wind P_a is evaluated as the ITTC added resistance due to wind procedure:

$$P_a = \frac{C_{DA} \cdot \rho_a \cdot A_{VT} \cdot (v + u_a)^2}{2} v$$

3.5 Methods to Estimate Input Parameters

Even though empirical methods requiring limited input are emphasized in the current work, some input parameters must be estimated. This section outlines the parameters considered most important to estimate, and identifies suitable methods for the calculations. Some of the formulas are rough estimates for preliminary design, and some are new regression estimates, such as the formulas by Kristensen et al. (2017).

3.5.1 Hull Parameters

Table 3.17 presents various hull parameter estimates. The parameters include the waterline length L_{WL}, midsection coefficient C_M, waterplane coefficient C_{WP}, and wetted surface area S, which are all important for the resistance calculations. The applicability of the estimates for the new power prediction model are evaluated further in Section 5.1.4.

Table 3.17: Estimation formulas for hull parameters

Estimation Formula	Applicable area	Reference
$L_{WL} = 1.02L_{PP}$	Tanker/Bulk	Kristensen et al. (2017)
$L_{WL} = 1.01L_{PP}$	Container	Kristensen et al. (2017)
$L_{WL} = 1.01L_{PP}$	Ro-Ro	Kristensen et al. (2017)
$C_M = 0.93 + 0.08C_B$	General	Schneekluth and Bertram (1998)
$C_M = 0.80 + 0.21C_B$	Large ships	Molland (2011)
$C_M = 0.78 + 0.21C_B$	Small ships	Molland (2011)
$C_{WP} = 0.67C_B + 0.32$	General	Molland (2011)
$C_{WP} = 0.763(C_P + 0.34)$	Tanker/Bulk/Cargo	Bertram and Wobig (1999)
$C_{WP} = 3.226(C_P - 0.36)$	Container	Bertram and Wobig (1999)
$C_{WP} = (1 + 2C_B)/3$	General	Papanikolaou (2014)
$S = 0.99 \cdot \left(\frac{\nabla}{T} + 1.9 \cdot L_{WL} \cdot T\right)$	Tanker/Bulk	Kristensen et al. (2017)
$S = 0.995 \cdot \left(\frac{\nabla}{T} + 1.9 \cdot L_{WL} \cdot T\right)$	Container	Kristensen et al. (2017)
$S = 0.87 \cdot \left(\frac{\nabla}{T} + 2.7 \cdot L_{WL} \cdot T\right) \cdot (1.2 - 0.34 \cdot C_{BW})$	Ro-Ro	Kristensen et al. (2017)
$S = 1.025 \cdot \left(\frac{\nabla}{T} + 1.7 \cdot L_{PP} \cdot T\right)$	General	Mumfords formula

Estimates to determine the superstructure dimensions are presented in Table 3.18. The superstructure parameters are important for calculating the air and wind resistance. It is generally difficult to obtain accurate estimates applicable to all ship types. A_{VT} and A_{VL} is the projected area in the transverse and longitudinal direction, respectively. B_s is the calculation breadth, h_s is the calculation height and L_s is the calculation length for the superstructure geometry.

Table 3.18: Estimation formulas for superstructure dimensions

Estimation Formula	Applicable area	Reference
$A_{VT} = B_s \cdot (D - T + h_s)$	Tanker/Bulk	Kristensen et al. (2017)
$A_{VL} = L_{OA} \cdot (D - T) + L_s \cdot h_s$	Conventional ships	Tillig et al. (2018)
$D = 0.087 \cdot L_{PP}$	General	Bertram and Wobig (1999)
$h_s = 3 \cdot (\text{no. of decks}) + 2\,[m]$	Tanker/Bulk	Kristensen et al. (2017)
$h_s = [11 - 20.6]\,[m]$	Feeder	Kristensen et al. (2017)
$h_s = 24.2\,[m]$	Panamax	Kristensen et al. (2017)
$h_s = [24.2 - 26.8]\,[m]$	Post Panamax	Kristensen et al. (2017)
$h_s = 24 + 2\,[m]$	PCTC $(L_{pp} > 100\,m)$	Tillig (2020)
$h_s = 15 + 2\,[m]$	Conventional ships $(L_{pp} > 100\,m)$	Tillig (2020)
$h_s = 12 + 2\,[m]$	Conventional ships $(L_{pp} \leq 100\,m)$	Tillig (2020)
$B_s = 30\,[m]$	Tanker/Bulk $(B > 30\,m)$	Tillig (2020)
$L_s = L_{PP}/2\,[m]$	Ro-Ro	Tillig (2020)
$L_s = L_{PP}\,[m]$	Cruise/Container/PCTC	Tillig (2020)
$L_s = L_{PP}/7\,[m]$	Conventional ships $(L_{PP} \leq 30\,m)$	Tillig (2020)

3.5.2 Propulsion Parameters

Table 3.19 presents estimates for the propeller diameter D_p. It should be noted that the estimates by Kristensen et al. (2017) are based on regression analysis of modern ships, and the estimates by MAN (2018) are rough rule-of-thumb estimates.

Table 3.19: Estimation formulas for propeller dimensions

Estimation Formula	Applicable area	Reference
$D_p = 0.396 \cdot T_{max} + 1.30$	Tanker/Bulk	Kristensen et al. (2017)
$D_p = 0.623 \cdot T_{max} - 0.16$	Container	Kristensen et al. (2017)
$D_p = 0.713 \cdot T_{max} - 0.08$	Ro-Ro	Kristensen et al. (2017)
$D_p = 0.65 \cdot T_{max}$	Tanker/Bulk	MAN (2018)
$D_p = 0.75 \cdot T_{max}$	Container	MAN (2018)
$D_p = 0.85 \cdot T_{max}$	Volume ships, high speed	MAN (2018)

Chapter 4

The MariTEAM Model

This chapter presents the MariTEAM model, developed by IndEcol at NTNU, an interdisciplinary research program specialising in environmental sustainability analysis (IndEcol, 2019). The MariTEAM model calculates fuel consumption and emissions across ship types, various fuels, engines, weather states, and trade routes. A bottom-up approach is applied to generate results from individual ships to across the fleet. As illustrated in Figure 4.1, the model can combine ship technology modules, including fuel type, installed engine power, speed profile, and route, to generate fleet-level assessments, i.e, fleet-wide emission calculations. The objective of the chapter is to assess the current model's data streams and power prediction calculations. Some parts of the assessment are based on a comprehensive study from the project thesis (Dale, 2020).

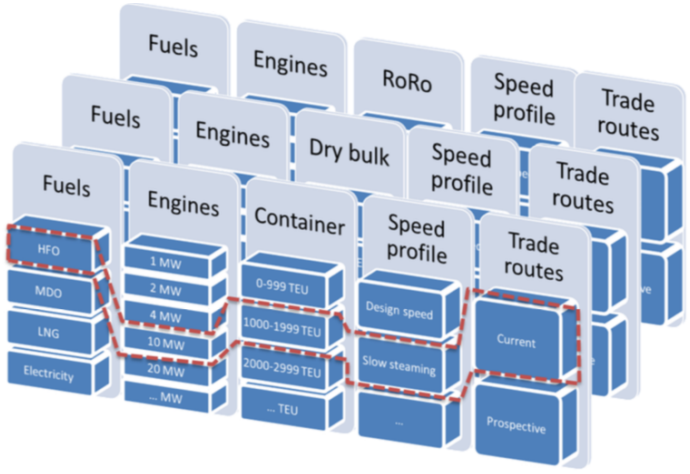

Figure 4.1: Modules in the MariTEAM model - From ship to fleet by Bouman et al. (2016)

4.1 Data Input

This section outlines the relevant databases for the fleet-wide power predictions in the MariTEAM model. The objective is to identify suitable databases and assess the typical data quality. It is expected that inaccurate data represent the main challenge for data quality, i.e., data containing misspellings, wrong numbers, missing information, or blank fields.

The input data sources to the MariTEAM model are composed of ship AIS data, technical ship data, and weather data combined with restricted emission area (ECA) data. As illustrated in the model flowchart in Figure 4.2, the current model input is ship technicals from Sea-web, speed and location of the vessel from AIS, and data describing wind and waves from the European Centre for Medium-Range Weather Forecasts (ECMWF). These data streams are parsed and stored before high-performance computing (HPC) is applied to complete the ship tracks and assign wind and wave conditions to each ship along its track. The flowchart illustrate the data streams relevant for the power prediction calculation which is further outlined in Section 4.2.

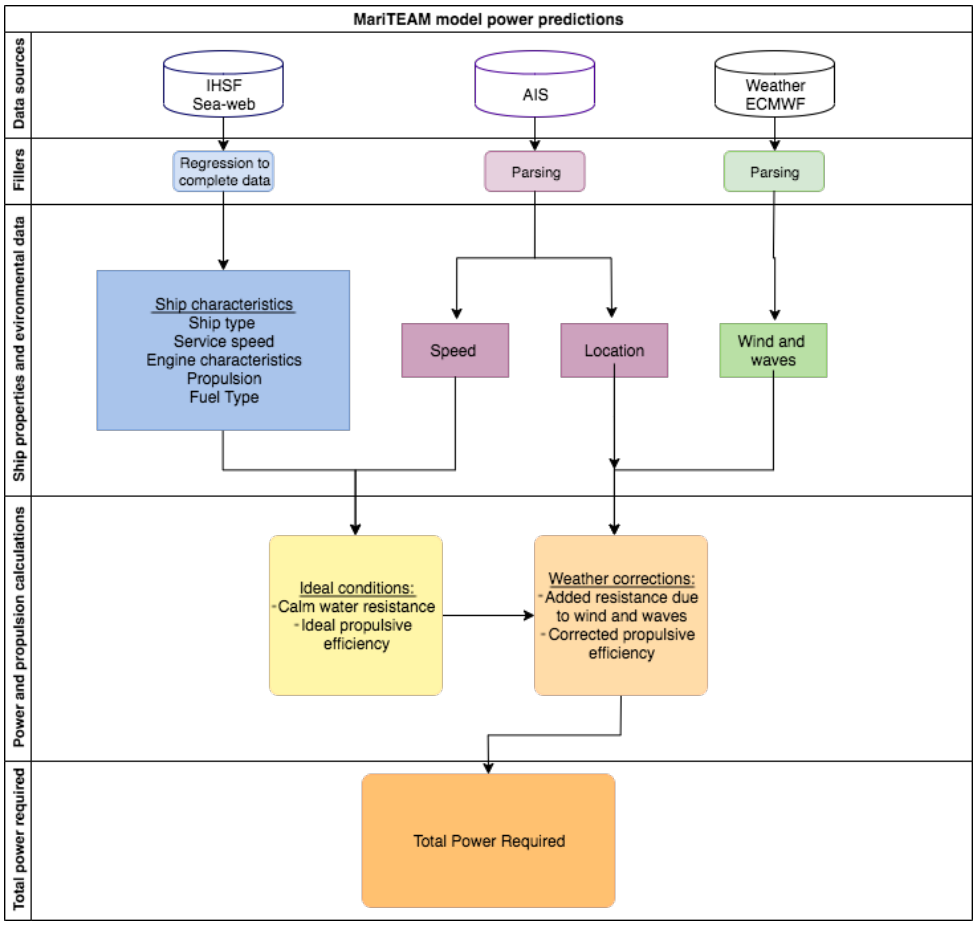

Figure 4.2: Flowchart of the MariTEAM power prediction model

As most of the input data analysed in the current work are from Sea-web, this database is outlined in detail. However, other relevant databases are also briefly assessed.

4.1.1 Sea-web

The IHS Maritime & Trade' Fairplay database Sea-web™, is the largest commercial maritime ship database, containing technical and operational data on over 200,000 ships (IHS, 2020). According to IMO, Sea-web is the official database, and is considered to represent the entire world fleet. Figure 4.3 presents the distribution of ship types in the fleet in terms of the number of ships (blue), and dwt (grey). As can be seen, general cargo ships represent the largest segment in terms of the number of ships, and dry bulk carriers represent the primary carrier of dwt.

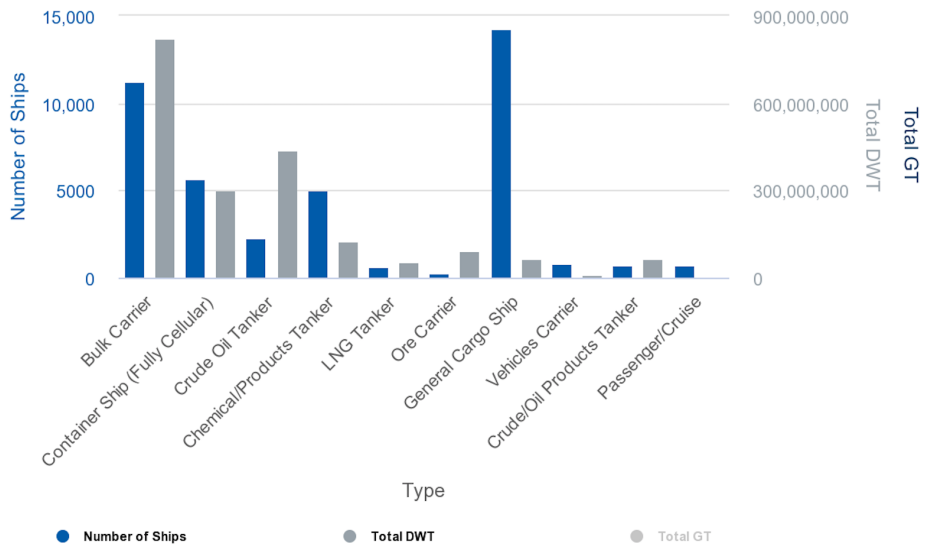

Figure 4.3: Distribution of ship types in the merchant fleet by IHS (2020)

In Sea-web, there are 214 different fields to describe the technical, formal, and operational properties of each ship. A complete list is added to Appendix D. Among the available fields, a selection of 16 parameters is considered relevant for the power performance calculations based on the review of empirical methods. These are presented in Table 4.1 below, and most of these are currently included in the MariTEAM model. The respective definition of each parameter in Sea-web is also included.

Table 4.1: Relevant Sea-web parameters for the power performance predictions

Parameter	Symbol	Sea-web definition
Breadth	B	Moulded breadth, otherwise extreme breadth
Deadweight	dwt	The load corresponding to maximum summer draught
Depth	D	From the lowest point on the keel to uppermost continuous deck
Draught	T	Maximum draught at the summer load load line
Engine Stroke Type	-	2 stroke or 4 stroke
Engine rpm	N	Revolutions per minute
IMO number	-	Unique number, remains constant during the life of the ship
Lightship weight	ldt	Light displacement tonnage
Length overall	L_{OA}	The length overall
Length between perpendiculars	L_{PP}	The length between perpendiculars
Main engine installed power	-	Power output of main engines
MMSI number	-	Identification number for VHF radio communication
Number of decks	-	Number of non-continuous decks
Service Speed	V_d	Speed maintained under normal load and weather conditions
Ship Type	-	Specified by a main category and sub-categories
TEU	TEU	(20 Foot Equivalent Unit) Capacity

Data quality

The MariTEAM model presents a fleet size analysis based on the 2018 Sea-web data, including about 74,000 ships representing the main fleet segments. First, the data is filtered, outliers are removed, and values are estimated for missing entries. Outliers are identified as faulty data typically with wrong dimensions or odd values relative to the trend of its segment. As of Sea-web 2018 data, the MariTEAM model identified 18 ships

with deviating characteristics. Individual analyses were conducted for the respective ships by checking the values against Marine Traffic. This way, some of the deviations were corrected.

Statistics of the coverage of each of the fields of interest are also obtained. The ship displacement (LDT) is the parameter with the most missing entries among the key physical properties. Of the about 74,000 ships analysed, 1 $\%$ is missing the lightship displacement (ldt) value. Of the remaining fields, auxiliary engine stroke type has the poorest coverage with 74 $\%$ missing entries, i.e., more missing entries than present. Methods for filling in missing data are presented in Section 4.1.3.

4.1.2 Additional Databases

Additional databases have been reviewed with regards to suitability for the MariTEAM model power predictions. The data from Sea-web may be combined with other ship data sources to achieve improved coverage of the required calculation parameters. Both Sea/Net by Clarksons (2020) and Lloyds list intelligence by (Lloyd's, 2020) offer similar resources to Sea-web. However, subscriptions for the databases have not been available in the current work. For future work, the databases should be further investigated.

EU Fuel consumption reporting

According to the EU-council (2019), a new regulation for reporting fuel consumption is implemented, partly to align the rules with the IMO global data collection system (DCS) for ship fuel consumption. As of 2019, shipping companies of the EU member states are obliged to follow the EU MRV (monitoring, reporting, verification) and the IMO DCS system. This includes monitoring fuel consumption, CO2 emissions, and energy efficiency from ships undergoing voyages and in port. The first reports are to be submitted in 2019 for EU MRV and 2020 for IMO DCS. The data from these reportings may be utilised in power prediction calculations or for validation purposes. A suggestion for future work is to investigate the reports when released.

4.1.3 Methods to Fill In Missing Data

Methods to fill in missing entries from the ship technical database are outlined in the following. First, an overview of the current filling process in the MariTEAM model is presented. Second, a review of additional methods are described.

Current filling procedures

In the MariTEAM model, regression rules are established and programmed for each input parameter within each ship segment. E.g., if the ship segment is 'container' and the response variable that represents the missing entry is 'ldt', then the regression rule selects 'GT' as the first predictor variable. A second predictor variable is also defined, which gives the second-best fit for the 'ldt' response data. This example can be illustrated by the study on container ships in the MariTEAM model by Ringvold (2017). In the master thesis study, Ringvold compares potential predictor parameters to estimate 'ldt'. Figure 4.4 presents the response variable 'ldt' plotted against six different potential predictor variables.

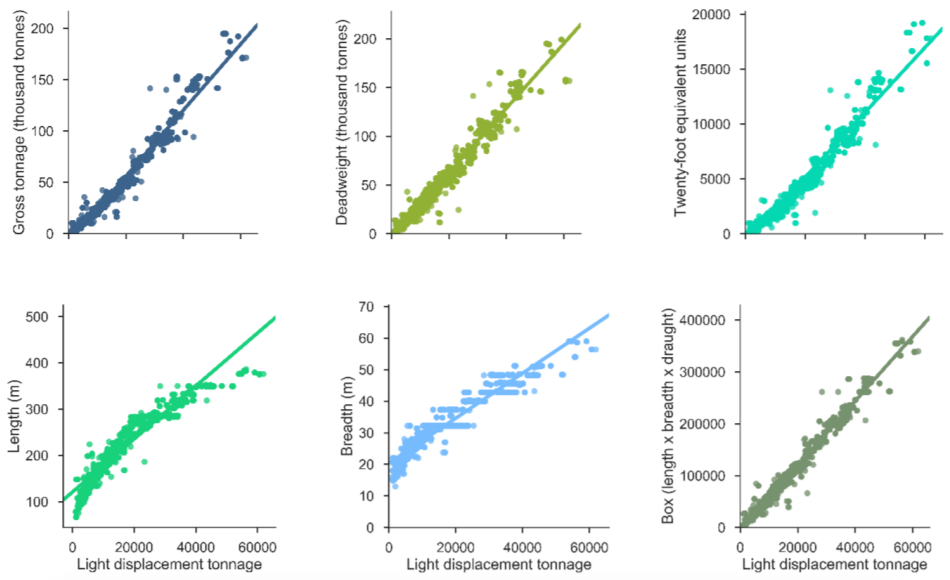

Figure 4.4: Scatter plot of ldt against potential predictor parameters by Ringvold (2017)

All the parameters follow this regression pattern except 'Main engine stroke' and 'Main engine rpm'. 'Main engine rpm' is assigned a regression rule based on whether it is 2-stroke or 4-stroke. 'Main engine rpm' must be either 2- or 4-stroke and is therefore assigned a value based on whether the predictor is above or below a specific delimiter value.

4.1.4 AIS Data

AIS is a vessel tracking system, introduced by the IMO International Convention of Safety of Life at Sea (SOLAS) in 2000 IMO (2020). The system is required to identify ships, improve the safety and efficiency of navigation, and maritime environmental protection. AIS data is both global and historical. In the present work, the AIS data is supplied by Kystverket. The following data is generally transmitted from a ship by the AIS system:

- **IMO and MMSI number**
- Name
- Type
- **Position**
- **Heading**
- **Speed**
- Size (dimensions)
- Draught
- Weight

The highlighted data are input to the power prediction procedure in the MariTEAM model. The IMO and MMSI number identifies the ship and connect the Sea-web data. Generally, the ship AIS system transmits MMSI, position, speed, and heading angle every 2 to 10 seconds depending on the ship speed, and every 3 minutes if the ship is anchored. The remaining data is usually transmitted every 6 minutes. AIS data is transmitted by VHF radio signals, which typically have an average range of about 20-30 miles (30-50 km) (MarineTraffic, 2018). When the data is received, it may be partially incomplete or incorrectly formatted. Therefore, the process of parsing and cleaning the data is vital for data quality.

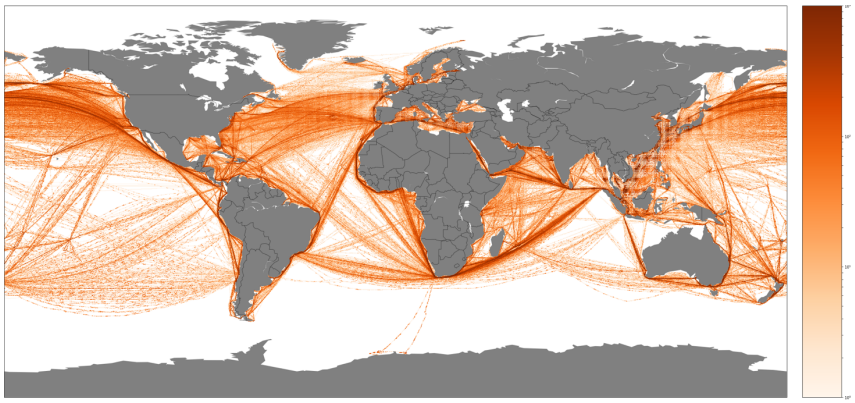

Figure 4.5: The MariTEAM AIS data track completer (Containerships, 2017). Figure courtesy of Radek Lonka, IndEcol, NTNU.

In the MariTEAM model, the AIS data is initially parsed and filtered such that outliers are removed. Then the post-processing of filling in missing data points is run on high-performance computers. This ship track completer fills any gaps by interpolating between AIS location data. Figure 4.5 illustrate the completed AIS data for container ships in 2017. There is a trade-off between computational time and accuracy of the predicted route for the track completer. Port calls provide data about the ship arrival and departure from ports, which is applied to help generating the most likely ship route.

ITU List V

ITU is the UN specialized agency for information and communication technologies (ITU, 2018). The ITU list V is a list of ship stations and maritime mobile service identity assignments (MMSI numbers). It contains all ships designated with an MMSI number, which is an internationally standardized number for the vessel. It identifies the ship and is programmed into the AIS and VHF systems onboard. Therefore, the MMSI is considered the key parameter connecting ship data from Sea-web and AIS. Since the MMSI number is missing for some Sea-web entries, ITU list V can be used to fill in the missing numbers. According to the MariTEAM model, about 20$\%$ of the MMSI numbers are missing in Sea-web and filled in from ITU list V.

4.1.5 Weather Data

The weather data in the MariTEAM model include historical wave and wind data acquired by the ECMWF (2014) reanalysis dataset ERA-Interim. ERA-Interim supplies hindcast weather data, continuosly updated in real time. The data variables for waves and wind are included in Table 4.2

Table 4.2: ECMWF Weather Data Variables

Variable	Temporal resolution
Significant wave height of combined wind waves and swell $[m]$	6 hours
Mean wave period $[s]$	6 hours
Mean wave direction	6 hours
Northward wind speed (10 m above sea surface) $[m/s]$	3 hours
Eastward wind speed (10 m above sea surface) $[m/s]$	3 hours

The weather data is combined with the AIS data of the ship to obtain the relative direction angle and velocity between ship and weather components.

4.2 Power Prediction Procedure

The MariTEAM model applies empirical methods to develop ship power profiles. Since the methods require parameters which are not usually available from commercial ship technical databases, some simplifications and assumptions are made and elaborated on in the following.

4.2.1 Calm Water Resistance

The total calm water resistance is estimated by Equation 4.1

$$R_T = R_F + R_R \tag{4.1}$$

where R_F is the frictional resistance and R_R is the residual resistance as defined in Section 2.1. The frictional resistance is determined according to the ITTC'57 friction line:

$$R_F = C_F \frac{\rho}{2} V^2 S \tag{4.2}$$

where

$$C_F = \frac{0.075}{(log(R_n) - 2)^2} \tag{4.3}$$

And the wetted area S is defined by the Mumford formula:

$$S = 1.7 \cdot L \cdot T + \frac{\nabla}{T} \tag{4.4}$$

The residual resistance is evaluted according to Hollenbach (1998), assuming the 'minimum resistance' hull form. The related residual resistance coefficient is then:

$$C_R = C_{R,Standard} \cdot \left(\frac{T}{B}\right)^{a1} \cdot \left(\frac{B}{L}\right)^{a2} \cdot \left(\frac{L_{os}}{L_{lwl}}\right)^{a3} \cdot \left(\frac{L_{lwl}}{L}\right)^{a4} \tag{4.5}$$

where $C_{R,Standard}$ is determined by the Froude number and a number of tabulated coefficients which can be found in Appendix A. The total resistance is evaluated without including a form factor and without accounting for roughness effects. It is further assumed that the resistance from air and from moving in shallow water are small relative to the total resistance and is neglected in the resistance calculations.

4.2.2 Added Resistance in Wind and Waves

The added resistance effects from weather is accounted for by adjusting the speed in accordance with the method(s) presented by Townsin and Kwon (1983) and the Kwon (2008) extension. The weather data input is from ERA-Interim, including significant wave height of combined wind waves and swell, and magnitude of 10 m wind speed.

$$\begin{gathered} \left(\frac{\triangle V}{V}\right) \cdot 100\% = C_\beta C_U C_{Form}, \\ V_W = V - \triangle V \end{gathered} \tag{4.6}$$

4.2.3 Propulsive Efficiency

K is the propulsive efficiency defined by Lindstad et al. (2011).

$$K = \frac{1}{\eta_{tot}} \cdot \frac{1}{\eta\left(j + k\sqrt{V/V_d}\right)} \tag{4.7}$$

The propulsion efficiency factor K is a function of the vessel speed V and η gives the efficiency at the design speed V_d. η is typically in the range of $0.6 - 0.7$. The MariTEAM model applies the following constant values $\eta = 0.65, j = 0.8, k = 0.2$.

4.2.4 Total Power

The total brake power is finally determined by:

$$P_B = \frac{1}{\eta_{tot}} \cdot (R_F + R_R)\, V_W \tag{4.8}$$

where V_W is the speed over ground corrected for added resistance due to wind and waves according to Townsin and Kwon (1983); Kwon (2008). If the vessel is a containership that exclusively carries refrigerated containers (a reefer), additional power required is calculated and added to the total without accounting for propulsion efficiency.

4.2.5 Assumptions

This section elaborates on the simplifications and unique assumptions made in the power calculations.

Resistance contributions

The calm water resistance is calculated as the sum of frictional and residual contributions. Other contributions such as form factor, roughness, air resistance, shallow water, base drag (etc.) are considered small relative to these and therefore neglected.

Hollenbach

The residual resistance is evaluated assuming the 'minimum resistance' hull form as defined by Hollenbach. The range of validity for this assumption in terms of ship characteristics are presented below in Figure 4.6. In Section 5.1 the range is checked against ship data to investigate the validity.

	Single-screw	*Twin-screw*
$F_{n,\min},\ C_B \leq 0.6$	0.17	0.15
$F_{n,\min},\ C_B > 0.6$	$0.17 + 0.2 \cdot (0.6 - C_B)$	0.14
$F_{n,\max}$	$0.614 - 0.717 \cdot C_B + 0.261 \cdot C_B^2$	$0.952 - 1.406 \cdot C_B + 0.643 \cdot C_B^2$

Figure 4.6: Range of validity for minimum resistance in Hollenbach's method by Schneekluth and Bertram (1998)

Propulsive efficiency

The propulsive efficiency is evaluated as suggested by Lindstad et al. (2011). In addition to the calm water propulsive efficiency, the formula includes changes in propulsive efficiency due to voluntarily speed reduction. However, effects of added resistance due to wind and waves are not accounted for in the calculations. This can be included by the extended formula by Lindstad et al. (2014) or the ITTC method recommended in the ISO 15016 standard.

Chapter 5

New Performance Prediction Method

This chapter presents a new performance prediction method, composed of the most suitable empirical procedures identified in Chapter 3. The objective of the new method is to improve the power prediction procedure for the current MariTEAM model. In order to achieve a suitable method for fleetwide calculations, calculation procedures with general applicability is emphasized. The selected calculation procedures applied to the new model will be described in detail in the following.

5.1 Selection of Methods

In Chapter 3, a wide range of methods are identified, and the following section narrows the selection down to the most applicable. Several criteria are considered important in the selection of calculation methods for resistance and propulsion factors. An ideal method applies to a wide range of ship types, provides highly accurate results, and requires limited input. Further, it should be computationally simple to program. These requirements serve as the basis for selecting the calculations methods for the new program.

5.1.1 Calm Water Resistance

The literature review of empirical resistance methods presented in Chapter 3 identifies three methods with general applicability; Guldhammer-Harvald, Holtrop-Mennen, and Hollenbach. All methods present regression-based formulas based on extensive analysis of model tests and are widely applied today.

The applicability of each method is defined in terms of dimensionless ship characteristics. Guldhammer-Harvald and Hollenbach include more limitations than Holtrop-Mennen. However, all three are expected to apply for conventional merchant ships. An assessment of the fleet-wide applicability is conducted for the current MariTEAM database, including 73,000 ships. Each ship in the fleet is checked against the requirement of each method, and Figure 5.1.1 presents the percentage of ships in the fleet valid to analyse.

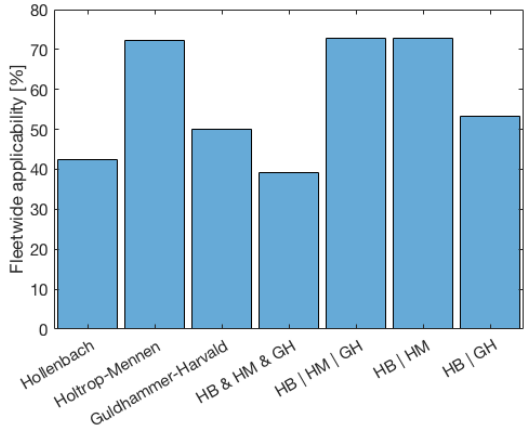

Table 5.1: Number of ships in the fleet [%] passing the requirement of each method, all three methods, one of the three methods, or either Hollenbach or Holtrop-Mennen.

Method	Applicability [%]
Hollenbach	42.2 %
Holtrop-Mennen	72.2 %
Guldhammer-Harvald	50.2%
HB & HM & GH	39.2 %
HB | HM | GH	72.8 %
HB | HM	72.8 %
HB | GH	53.4 %

As seen in Figure 5.1.1, Holtrop-Mennen covers the broadest range of the fleet by 72.2 $\%$. The combination of applying either Holtrop-Mennen or Hollenbach gives the most extensive coverage of 72.8 %. Only half of the fleet can be analysed if either Hollenbach or Guldhammer-Harvald is applied alone. Therefore, it is considered relevant to include more than one of the methods in the new model.

Hollenbach's Ph.D. thesis presents a comparison of the accuracy of the three methods when applied to a wide range of ships (Hollenbach, 1997). Figure 5.1 from Steen et al. (2016) presents the results in terms of mean deviation and standard deviation of each method. All methods provide the most accurate results for single-screw vessels on design draught, and the variability increases on ballast draught. Overall, Hollenbach gives lower standard deviation relative to the others.

	single-screw design draft		single- screw ballast draft		twin-screw design draft	
	Mean	standard deviation	Mean	standard deviation	mean	standard deviation
Holtrop-Mennen	- 0.5 %	12.8 %	6.3 %	16.1 %	5.8 %	18.4 %
Guldhammer	0.8 %	11.0 %	10.5 %	17.9 %	11.2 %	19.2 %
Lap-Keller	- 0.5 %	12.9 %	27.9 %	32.9 %	14 %	23.4 %
Series-60	- 1.0 %	11.6 %	37.3 %	42.7 %	15.2 %	23.3 %
Hollenbach	- 1.0 %	9.4 %	- 0.2 %	11.2 %	3.5 %	13.3 %

Figure 5.1: Comparison of mean and standard deviation of the total resistance predicted by Holtrop-Mennen, Guldhammer-Harvald and Hollenbach by Hollenbach (1997), retrieved from Steen et al. (2016)

The accuracy of the methods is expected to be dependent on the ship type analysed, since the methods are regression-based on model tests. As the oldest method, Guldhammer-Harvald is based on the oldest hull forms (model tests conducted before 1961) and may be expected to provide the least accurate results. However, the method has been revisited by Kristensen et al. (2017) and is updated for modern tankers, bulk carriers, and container ships. The update includes a bulb correction, and according to Schneekluth and Bertram (1998), modern bulbs may decrease the resistance up to 15-20 %. With this correction, Guldhammer-Harvald is considered relevant to include in the new method.

In terms of required input, Guldhammer-Harvald represents the simplest method. Both Holtrop-Mennen and Hollenbach require a considerable number of input parameters unavailable from Sea-web, which must be estimated by other methods. The accuracy of the methods is expected to decrease with the number of estimated input parameters. However, both Tillig (2020) and Kristensen et al. (2017) present several modern parameter estimation formulas that may be applied. Regarding computational simplicity, there are negligible differences between the three methods. Guldhammer-Harvald is based on diagrams of length-displacement ratios, which Kristensen et al. (2017) presents regression formulas for.

The three methods' assessment can be summarised in terms of the main criteria; applicability, accuracy, and required input. Holtrop-Mennen provides the broadest applicable range, which makes it relevant to include. Based on Hollenbach's study, Holtrop-Mennen and Hollenbach appear to be more accurate than the original Guldhammer-Harvald. According to Birk (2019), Hollenbachs' study indicate that the method is the most reliable of the three. Both Hollenbach and Holtrop-Mennen are therefore suitable for the new model. However, since Guldhammer-Harvald is updated by Kristensen et al. (2017) to fit modern ships, it is considered relevant to include as well. Without any other clear indication of which method is best, all three are included for further analyses and a mean estimate of the three methods is computed. Whether the final power prediction benefit from applying the mean of all three methods will be assessed in Chapter 6 Results and Validation, and further discussed in Chapter 7.

Total resistance decomposition

In Chapter 2, the resistance components are reviewed according to MARINTEK's procedure. The most important resistance contributions are the residuary resistance and the viscous (frictional) resistance. Further, the roughness correction is expected to be significant, and air resistance may be significant for fast ships. In addition, the correlation coefficient depends on the selected method; Hollenbach, Holtrop-Mennen, or

Guldhammer-Harvald. Therefore, these components are included in the new model, decomposing the total resistance coefficient as presented in Equation 5.1

$$C_T = C_R + (1+k)\left(C_F + \Delta C_F\right) + C_{AA} + C_A \tag{5.1}$$

Following this decomposition, resistance contributions from base drag and appendages are neglected. These contributions require detailed input parameters for the transom and appendages which are not available from Sea-web. The simplification is not expected to be significant for the results. Further, shallow-water effects are not considered.

The calculation of total calm water resistance follows this decomposition for Hollenbach, Holtrop-Mennen, and Guldhammer-Harvald. The frictional resistance is computed by the ITTC'57 correlation line:

$$C_F = \frac{0.075}{\left(log(R_n) - 2\right)^2} \tag{5.2}$$

The air resistance is calculated according to the ITTC'78 procedure:

$$C_{AA} = C_{DA}\frac{\rho_{\text{air}} \cdot A_{VT}}{\rho \cdot S} \tag{5.3}$$

where C_{AA} is defined by Table 5.2 for container ships, tankers and bulk carriers as suggested by Kristensen et al. (2017). For other ships, the air drag coefficient C_{DA} is determined by Blendermann (1994) according to Table 3.13 or set to the default value of 0.8 as recommended by Birk (2019). The transverse projected area above the waterline A_{VT} is estimated by parameter estimates, further outlined in Section 5.1.4.

Table 5.2: Air resistance coefficient values for container ships, tankers and bulk carriers as recommended by Kristensen et al. (2017)

Ship type	$C_{AA}\cdot$ 1000 [-]
Container ships	0.28$\cdot TEU^{-0.126}$
Small tanker/bulk	0.07
Handysize tanker/bulk	0.07
Handymax tanker/bulk	0.07
Panamax tanker/bulk	0.05
Aframax tanker/bulk	0.05
Suezmax tanker/bulk	0.05
VLCC	0.04

The residual resistance, roughness correction, form factor and correlation allowance are defined somewhat differently in each method, and the following sections outline the details.

Hollenbach

The total resistance and the hull-propeller interaction parameters in Hollenbach are computed for single-screw vessels on design draught. This is a simplification, as parts of the fleet comprise twin-screw vessels and vessels on ballast draught. It is assumed to be a reasonable simplification at this stage, but methods to correct the varying loading conditions are discussed in Section 7.

In the new model, both the minimum and the mean resistance estimate by Hollenbach is included. The mean resistance prediction $R_{T,mean}$ is considered most relevant and is included in the averaged prediction in the new model together with Holtrop-Mennen and Guldhammer-Harvald. However, the current MariTEAM model applies the minimum resistance estimate $R_{T,min}$, and it is therefore included for comparison and further investigation in the case study. The total resistance coefficient is calculated as follows (for both the mean and the minimum estimate):

$$C_T = \left(C_F + \Delta C_F\right) \cdot (1+k) + C_R + C_A + C_{AA} \tag{5.4}$$

where $C_A = 0.06 \cdot 10^3$ (Birk, 2019). The residuary resistance is based on (BT) instead of wetted surface S. The method is modified by including a form factor k according to MARINTEK (2020), adjusted for slender ships according to Steen et al. (2016):

$$k = k_0 + k_1 = 0.6 \cdot \Phi + 75 \cdot \Phi^3 \tag{5.5}$$

where

$$\Phi = \frac{C_B}{L_{WL}} \cdot \sqrt{B \cdot (T_A + T_F)} \tag{5.6}$$

The residual coefficient is further modified as a function of ship model frictional coefficient C_{FM}:

$$C_R = C_{\text{R,Hollenbach}} \cdot \frac{B \cdot T}{S} - k \cdot C_{FM} \tag{5.7}$$

$C_{\text{R,Hollenbach}}$ is determined based on tabulated coefficients depending on the mean or minimum resistance estimate. The coefficients are added to Appendix A. Further, the roughness correction ΔC_F is calculated according to MARINTEK (2020), for $H = 150$ $[\mu m]$:

$$\Delta C_F = \left[110 \cdot (H \cdot V)^{0.21} - 403\right] \cdot C_F^2 \tag{5.8}$$

The hull-propeller interaction parameters comprise the thrust factor and the wake fraction. In Hollenbach, the thrust factor for single screw ships on design druaght is a fixed value $t = 0.190$. The wake fraction is determined by the hull efficiency at model scale η_{HM} according to Equation 5.9

$$\eta_{HM} = 0.948 C_B^{0.3977} \left(\frac{R_{T\,\text{mean}}}{R_T}\right)^{-0.58} \left(\frac{B}{T}\right)^{0.1727} \left(\frac{D_P^2}{BT}\right)^{-0.1334} \tag{5.9}$$

where R_T is either $R_{T,mean}$ or $R_{T,min}$. Further, the model scale wake fraction is determined as Equation 5.10

$$w_{TM} = 1 - \frac{1 - t}{\eta_{HM}} \tag{5.10}$$

Finally the full scale wake fraction is determined by Equation 5.11

$$w = (t + 0.04) + (w_{TM} - (t + 0.04)) \left[\frac{C_F + C_A}{C_{FM}}\right] \tag{5.11}$$

The hull efficiency is then computed according to Equation 5.12

$$\eta_H = \frac{1 - t}{1 - w} \tag{5.12}$$

When all parameters are computed, the Froude number limitation is applied. In Hollenbach, the valid Froude number range depend on coefficients and C_B.

Holtrop-Mennen

The total resistance and the hull-propeller interaction parameters in Holtrop-Mennen are computed according to Holtrop'84 for single-screw vessels. Equation 5.13 presents the total resistance:

$$R_T = (1 + k)R_F + R_W + R_A + R_{AA} \tag{5.13}$$

The calculation of the resistance components are lengthy and include a number of coefficients, these are therefore added to Appendix C. Only the key calculations are outlined here. The wave resistance R_W is a function of Froude number, subdivided into three sections according to Equation 5.14 (Birk, 2019)

$$R_W(Fn) = \begin{cases} c_1 c_2 c_5 \rho g V \exp\left[m_1 Fn^d + m_4 \cos\left(\lambda Fn^{-2}\right)\right] & \text{if } Fn \leq 0.4 \\ \text{Interpolation} & \text{if } 0.4 < Fn \leq 0.55 \\ c_{17} c_2 c_5 \rho g V \exp\left[m_3 Fn^d + m_4 \cos\left(\lambda Fn^{-2}\right)\right] & \text{if } Fn > 0.55 \end{cases} \tag{5.14}$$

where the coefficients are found in Appendix C. c_2 depend on the height of centre of bulb area h_B, which is assumed to be $0.6T_F$ based on Birk (2019). The form factor k is computed according to Holtrop's own formula, also added to Appendix C. R_A includes the effect of hull roughness equal to $H = 150$ $[\mu m]$ and is computed by Equation 5.15

$$R_A = \frac{1}{2}\rho V^2 \left(C_A + \Delta C_A\right) \left[S + \sum S_{APP}\right] \tag{5.15}$$

where S_{APP} is neglected in the current work. As discussed in Section 3.1.2, the bulb correction is also neglected. A viscous resistance coefficient C_V is introduced for the hull-propeller interaction parameters w, t, and η_H:

$$C_V = \frac{(1+k)R_F + R_{APP} + R_A}{\frac{1}{2}\rho V^2 \left(S + \sum_i S_{APP_i}\right)} \tag{5.16}$$

The equations for w, t, and η_H are previously presented in Section 3.3.1. When all parameters are computed, the Froude number limitation is applied. In Holtrop-Mennen, the valid Froude number range is [0,0.45].

Guldhammer-Harvald

The total resistance and the hull-propeller interaction parameters are computed according to the updated Guldhammer-Harvald procedure by Kristensen et al. (2017). Equation 5.17 presents the total resistance coefficient, where the correlation factor C_A includes the effects of roughness of the ship hull.

$$C_T = C_R + C_F + C_A + C_{AA} \tag{5.17}$$

The residuary resistance C_R is determined according to diagrams by Guldhammer-Harvald and corrected for B/T ratio, hull form and bulb. A correction for LCB not being placed amidships is neglected in the current work. Equation 5.18 outlines the calculation of C_R, where the coefficients of $\mathrm{C_{R,\ Diagram}}$ is added to Appendix B.

$$\mathrm{C}_R = \mathrm{C_{R,\ Diagram}} + \Delta C_{\mathrm{R,B/T}\neq 2.5} + \Delta \mathrm{C_{R,LCB}} + \Delta C_{\mathrm{R,\ form}} + \Delta C_{\mathrm{R,\ bulb}} \tag{5.18}$$

where

$$\Delta C_{\mathrm{R,B/T}\neq 2.5} = 0.16 \cdot \left(\frac{B}{T} - 2.5\right) \cdot 10^{-3} \tag{5.19}$$

if $B/T \neq 2.5$. And the hull form correction is applied for ships with aft or fore body with extremely U or V form:

$$\begin{array}{l} \Delta C_{\mathrm{R,\ form}}: \\ \begin{array}{lll} \text{Fore body} & \text{Extreme } U: -0.1 \cdot 10^{-3} & \text{Extreme } V: +0.1 \cdot 10^{3} \\ \text{After body} & \text{Extreme } U: +0.1 \cdot 10^{-3} & \text{Extreme } V: -0.1 \cdot 10^{-3} \end{array} \end{array} \tag{5.20}$$

In the current work, it is assumed that modern tankers/bulk carriers with large C_B (> 0.85) have U-shaped fore body, and fast container ships ($V_d > 20$knots) have V-shaped entrances. Equation 5.21 and 5.22 present the bulb correction formula for tankers/bulk carriers and container ships, respectively:

$$\Delta C_{R,\ \mathrm{bulb}} = \max(-0.4; -0.1 - 1.6 \cdot \mathrm{Fn}) \tag{5.21}$$

$$\Delta C_{R,\ \mathrm{bulb}} = (250 \cdot Fn - 90) \cdot \frac{C_{R\ \text{Harvald no bulbous bow}}}{100} \tag{5.22}$$

The hull-propeller interaction parameters t, w, and η_H are computed as presented in Section 3.3.1. A common N-shaped hull form is assumed for the calculations in the current work. When all parameters are computed, the Froude number limitation is applied. In Guldhammer-Harvald, the valid Froude number range is [0,0.33].

5.1.2 Added Resistance in Wind and Waves

Chapter 3 identifies a range of empirical methods to predict the added resistance in wind and waves. Table 5.3 summarises the the identification and highlights the selected methods for the new model.

Table 5.3: Selected methods to predict the increased resistance in wind and waves

Method	Added resistance parameter	Reference
STAWAVE-1	**Wave resistance**	**MARIN (2006)**
STAWAVE-2	**Wave resistance**	**MARIN (2006)**
STA-JIP wind	**Wind resistance**	**MARIN (2006)**
Fujiwara	Wind resistance	Fujiwara et al. (2017)
Blendermann	**Wind resistance**	**Blendermann (1994)**
Townsin & Kwon	**Wave and wind resistance**	**Townsin and Kwon (1983), Kwon (2008)**

The current MariTEAM model applies Townsin & Kwon for the resistance increase in wind and waves. The method is widely applicable but does not differ between wave resistance and wind resistance. In order to obtain a more accurate prediction, methods to predict wave resistance and wind resistance independently are added to the new model. The selected methods are ellaborated on in the following. Townsin & Kwon is also included to compare the performance of the various methods.

Wave resistance methods

Both the STAWAVE methods estimate the added resistance in waves for modern ships when limited input data is available. The methods are recommended in ISO 15016 and are generally applicable to all ship types. However, STA-1 is limited to mild sea states and returns zero resistance in the new model if the wave height is above a required limit. STA-2 is therefore included to increase the applicability in higher sea states. In a study of 10 ships, MARIN (2006) presents a comparison between STA-1, STA-2, and other existing methods to predict added resistance in waves. The computed results are compared to model test measurements and indicate that both STAWAVE methods provide a more reliable prediction of added resistance in bow wave trial conditions, relative to the other methods. Figure 5.2 illustrate the results for a 174 m tanker on various loading conditions.

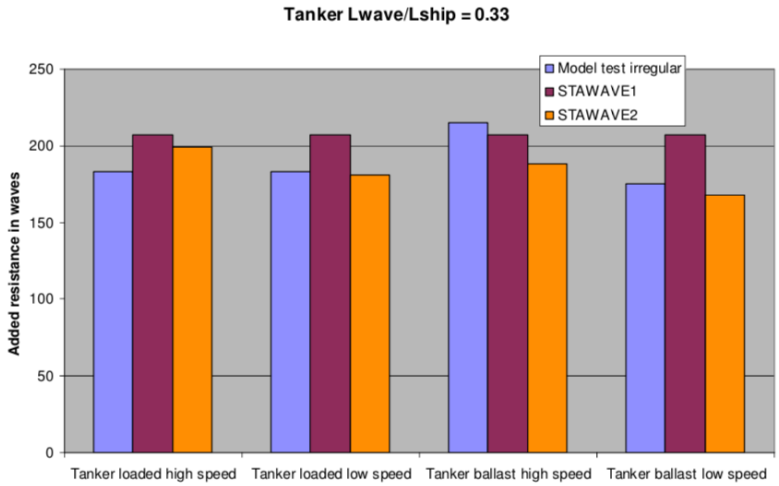

Figure 5.2: Comparison of the STAWAVE methods and irregular wave model tests for a 174 m tanker (MARIN, 2006)

A limitation of STA-1 is the required input parameter L_{BWL}, defining the distance of the bow to 95 % of the maximum breadth on the waterline, as illustrated in Figure 5.3. The length depends on the fore hull shape and is difficult to estimate based on the limited input available from Sea-web. In the current work, comparison ships with known L_{BWL} are applied to express the length as a fraction of L_{PP} for the case study. A suggestion for

further work is to develop a parameter estimate based on typical hull forms within the ship types, and this is further discussed in Chapter 9.

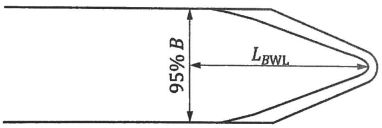

Figure 5.3: Definition of L_{BWL} in STAWAVE-1 (ISO Technical Committee, 2015)

STA-2 depends on a defined wave spectrum, and MARIN (2006) recommends applying Pierson-Moskowitz for fully developed seas or JONSWAP for young developing seas. The most suitable spectrum depends on the vessel route and will vary within the fleet-wide calculations. For coastal waters, JONSWAP is commonly applied. In the current work, it is assumed that the majority of ships travel in deep sea with a fully developed sea state and Pierson-Moskowitz is applied.

Wind resistance methods

ISO 15016 recommends two empirical methods to predict wind resistance; STA-JIP wind and Fujiwara. Both methods are therefore expected to provide reliable predictions within the applicable ship types. While STA-JIP wind only requires A_{VT} as input, Fujiwara require a high level of detail for superstructure parameters. Although Fujiwara et al. (2017) presents regression formulas to estimate the required geometric parameters, the number of estimated parameters is expected to reduce the accuracy of the results. As presented in Figure 5.4, the two methods apply to five segments each, and it is therefore deemed sufficient only to include one. As the most straightforward method, STA-JIP is selected. STA-JIP suggests a method to calculate the relative wind velocity vector, which is neglected in the current work since the parameter is estimated by hindcast weather data. By including Blendermann (1994), the applicable range of ship types is significantly increased. Blendermann's method is widely applied in the literature and is expected to provide reliable predictions for the wind resistance coefficients. The current work includes coefficients for the ship types added to Appendix E. It is assumed that the wind resistance for tankers also apply to bulk carriers.

Table 5.4: Comparison of the applicable area for the wind resistance methods

Ship type	Blendermann	STAJIP-wind	Fujiwara
Bulk carrier			x
Car carrier	x		
Cargo vessel	x	x	
Container ship	x	x	x
Drilling vessel	x		
Ferry	x		
Fishing vessel	x		
LNG tanker	x	x	x
Offshore supply vessel	x		
Passenger liner	x	x	x
Research vessel	x		
Speed boat	x		
Tanker loaded/ballast	x	x	x
Tender	x		

5.1.3 Propulsion Factors

Section 3.3 presents various approaches to determine the propulsion factors and these are narrowed down to the selected procedure in the following. Propeller information is missing in Sea-web. Therefore, the option of

applying a method requiring a significant amount of input parameters is unachievable. Without any other information, single screw vessels are considered, following the same assumption as for the resistance calculations.

The current MariTEAM model applies a simple empirical formula by Lindstad et al. (2011) to calculate the propulsive efficiency. The procedure requires several estimated parameters, such as the propulsive efficiency in calm water, and empirical constants. In the current work, accurate estimates for these parameters are not identified, and the method is therefore not implemented. Other existing formulas for η_D are presented in Section 3.3.2 and are deemed too simple for the calculations. Further, a prediction based on sea-margin is assessed and provides a quick estimate of η_D. However, it does not capture load variations on the propeller due to increased resistance in weather, and therefore not considered suitable for the new model.

A suggested approach is to determine each propulsive efficiency term, i.e., $\eta_D = \eta_0 \eta_H \eta_R$. This implies finding the open water efficiency, which requires an estimated propeller design. Kristensen et al. (2017) present an updated and approximated procedure to apply the Wageningen B-series when only the propeller diameter is known. A number of parameter estimates for the propeller diameter are identified in Section 3.5.2, enabling to apply this procedure in the new model. Assuming the calm water resistance methods are valid, the hull efficiency is determined by these. This procedure is further suitable for the calculations as it accounts for the varying load on the propeller. Equations 5.23-5.26 present the calculation:

$$\eta_0 = \frac{2}{1 + \sqrt{C_{Th} + 1}} \cdot f\left(C_{Th}\right) \tag{5.23}$$

where

$$f\left(C_{Th}\right) = 0.81 - 0.014 \cdot C_{Th} \tag{5.24}$$

and the thrust load bearing coefficient C_{Th} is computed for the total resistance, including added resistance:

$$\mathrm{C_{Th}} = \frac{8}{\pi} \cdot \frac{\mathrm{R_{tot}}}{(1 - \mathrm{t}) \cdot \rho \cdot \left((1 - w) V \cdot \mathrm{D_p}\right)^2} \tag{5.25}$$

where w and t are determined by Guldhammer-Harvald, Holtrop-Mennen or Hollenbach. The hull efficiency is then determined:

$$\eta_H = \frac{1 - t}{1 - w} \tag{5.26}$$

It is further assumed a constant rotative efficiency $\eta_R = 1.0$ and a constant value of losses in the transmission system $\eta_S = 0.98$. Effects of gearbox are therefore neglected.

5.1.4 Input Parameter Estimates

Sea-web provides a limited number of ship characteristics, and empirical formulas and regression estimate the missing required hull and propulsion input parameters. Based on the selected methods for the new model, a set of estimated input parameters is selected. The selection comprises modern estimates when available, ship-type specific estimates, and some assumptions. Propeller diameter estimates are selected based on the maximum draught, as this is the draught available in Sea-Web. Assumptions include equal trim fore and aft, no submerged transom and neglected wetted surface of appendages. The significance of these simplifications is further discussed in Chapter 7. Tables 5.5 - 5.7 present the estimation formulas for hull dimensions and propeller dimensions.

Table 5.5: Estimation formulas for superstructure dimensions

Estimation Formula	Applied to	Reference
$A_{VT} = B \cdot (D - T + h_s)$	General	Assumption
$h_s = 3 \cdot (\text{no. of decks}) + 2\,[m]$	General	Assumption
$h_s = [11 - 20.6]\,[m]$	Feeder	Kristensen et al. (2017)
$h_s = 24.2\,[m]$	Panamax	Kristensen et al. (2017)
$h_s = [24.2 - 26.8]\,[m]$	Post Panamax	Kristensen et al. (2017)

Table 5.6: Estimation formulas for hull dimensions

Estimation Formula	Applied to	Reference
$L_{WL} = 1.01 L_{PP}$	Container	Kristensen et al. (2017)
$L_{WL} = 1.01 L_{PP}$	Single screw Ro-Ro	Kristensen et al. (2017)
$L_{WL} = 1.02 L_{PP}$	Other	Assumption
$T_F = T$	General	Assumption
$T_A = T$	General	Assumption
$\bigtriangledown = \frac{(ldt+dwt)10^3}{\rho}$	General	Universal
$C_B = \frac{\nabla}{L_{pp} \cdot B \cdot T}$	General	Universal
$S = 0.99 \cdot \left(\frac{\nabla}{T} + 1.9 \cdot L_{WL} \cdot T\right)$	Tanker/Bulk	Kristensen et al. (2017)
$S = 0.995 \cdot \left(\frac{\nabla}{T} + 1.9 \cdot L_{WL} \cdot T\right)$	Container	Kristensen et al. (2017)
$S = 0.87 \cdot \left(\frac{\nabla}{T} + 2.7 \cdot L_{WL} \cdot T\right) \cdot (1.2 - 0.34 \cdot C_{BW})$	Single screw Ro-Ro	Kristensen et al. (2017)
$S = 1.025 \cdot \left(\frac{\nabla}{T} + 1.7 \cdot L_{PP} \cdot T\right)$	Other (general)	Mumfords formula
$S_{app} = 0$	General	Assumption
$S_B = 0$	General	Assumption
$C_M = 0.93 + 0.08 C_B$	General	Schneekluth and Bertram (1998)
$C_P = C_B / C_M$	General	Universal
$C_{WP} = 0.763(C_P + 0.34)$	Tanker/Bulk/Cargo	Bertram and Wobig (1999)
$C_{WP} = 3.226(C_P - 0.36)$	Container	Bertram and Wobig (1999)
$C_{WP} = (1 + 2C_B)/3$	Other (general)	Papanikolaou (2014)

Table 5.7: Estimation formulas for propeller dimensions

Estimation Formula	Applied to	Reference
$D_p = 0.396 \cdot T_{max} + 1.30$	Tanker/Bulk	Kristensen et al. (2017)
$D_p = 0.623 \cdot T_{max} - 0.16$	Container	Kristensen et al. (2017)
$D_p = 0.713 \cdot T_{max} - 0.08$	Ro-Ro	Kristensen et al. (2017)
$D_p = 0.5 \cdot ((0.396 \cdot T_{max} + 1.30) + (0.623 \cdot T_{max} - 0.16))$	Cargo	Assumption
$D_p = 0.70 \cdot T_{max}$	Other	Assumption
$n_p = 1$ (no. of propellers)	General	Assumption

5.1.5 Potential Improvements to the Current MariTEAM model

Table 5.8 summarises the potential improvements to the current MariTEAM model. First, a filter to identify the valid methods for a specific ship is implemented in all parts of the calculation. Both the calm water resistance methods and most of the added resistance methods apply to vessels with dimensions within a limited range. Further, the calm water resistance is determined by three methods, extending the applicable range for the current model. Two additional methods are implemented for the added resistance in both wind and waves, which is expected to provide more accurate results. Finally, the propulsive efficiency is determined by an extensive propeller series, which is expected to provide a more reliable prediction than the current empirical formula.

Table 5.8: Potential Improvements to the Current MariTEAM model

Calculation part	Current model	New model
Filter for identifying valid methods	No filter	Filter for all methods
Calm water resistance	One method	Three methods (and mean)
Added resistance in wind and waves	One method combining wind and waves	Two additional methods for wind Two additional methods for waves
Propulsive efficiency	One empirical method	Applying the most extensive propeller series as of today

5.1.6 Limitations

This section outlines the main limitations in the new model. The significance of these are further discussed in Chapter 7.

Calm water resistance

- Neglected resistance contributions: Shallow water, wetted transom and appendages
- Single screw ships on design loading is assumed
- Sea-web only provides maximum draught on summer load line
- Even with three methods, 30% of the fleet is not valid to analyse
- The modified Guldhammer-Harvald bulb-correction is only updated for tankers/bulk carriers and container ships

Added resistance in wind and waves

- Both STAWAVE methods are only valid for head sea $[0°, \pm 45°]$
- STA-1 input parameter L_{BWL} is estimated by comparison ships
- STA-2 wave spectrum assumes fully developed sea
- Wind resistance accuracy depend on the estimated transverse superstructure area

Propulsive efficiency

- Single screw ships is assumed
- Propulsion factors strongly depend on the estimated propeller diameter
- Rough assumption of constant values for $\eta_R = 1.0$ and $\eta_S = 0.98$
- Direct drive assumed and gearbox losses are neglected

5.2 Program Structure

This section is dedicated to explaining how the new model is implemented in MATLAB and the function of each calculation part. The code is added to Appendix F. Figure 5.4 illustrate the overall structure of the program, composed of five main modules. First, missing input parameters are estimated. Then the calm water resistance is calculated, followed by the added resistance in wind and waves. The propulsive efficiency is calculated as a function of the total resistance before the final brake power requirement is computed. The details of each of the five modules are elaborated on in the following.

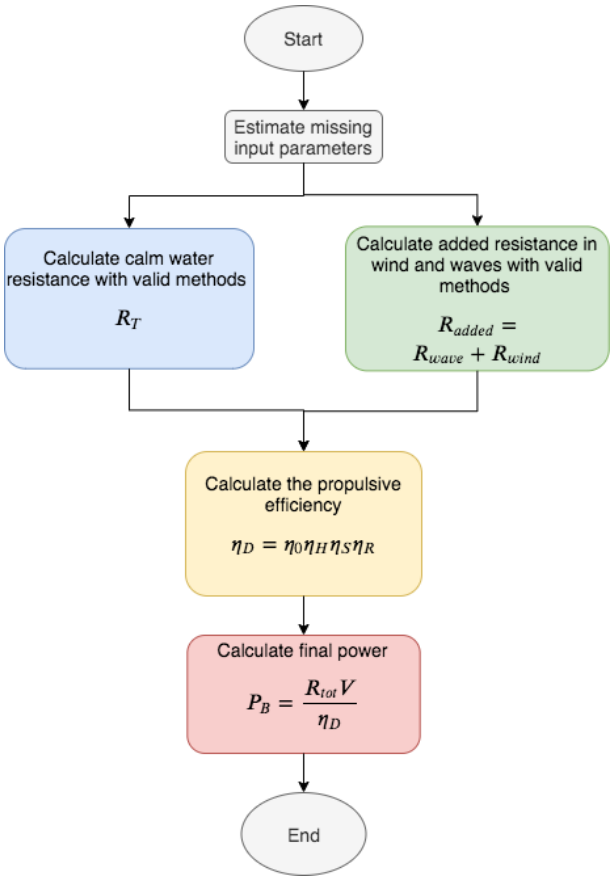

Figure 5.4: Conceptual flowchart of the new program

5.2.1 Modules

The details of the five main modules are listed below, and a flowchart, including all functions, are presented in Section 5.2.2. Note that HB, HM, and GH are abbreviations of Hollenbach, Holtrop-Mennen and Guldhammer-Harvald, respectively.

Module 1: Estimate missing input

- Estimate missing hull parameters in accordance with Table 5.6
- Estimate propeller diameter based in accordance with Table 5.7

Module 2: Calm water resistance

- Check requirements and determine valid calm water methods (HB, HM or GH)
- Compute the resistance, thrust factor, and wake fraction for all valid methods
- Compute mean values from valid methods: R_T, t, w

Module 3: Added resistance in wind and waves

- Check requirements and determine valid added resistance methods
- Compute the added resistance for all valid methods
- Compute mean values from valid methods: $R_{added} = R_{wave} + R_{wind}$
- Compute total resistance:
  $R_{tot} = R_T + R_{added}$

Module 4: Propulsive efficiency

- Compute propulsive efficiency for total resistance: η_D

Module 5: Final power and plot

- Compute the final brake power: P_B

5.2.2 Flowchart

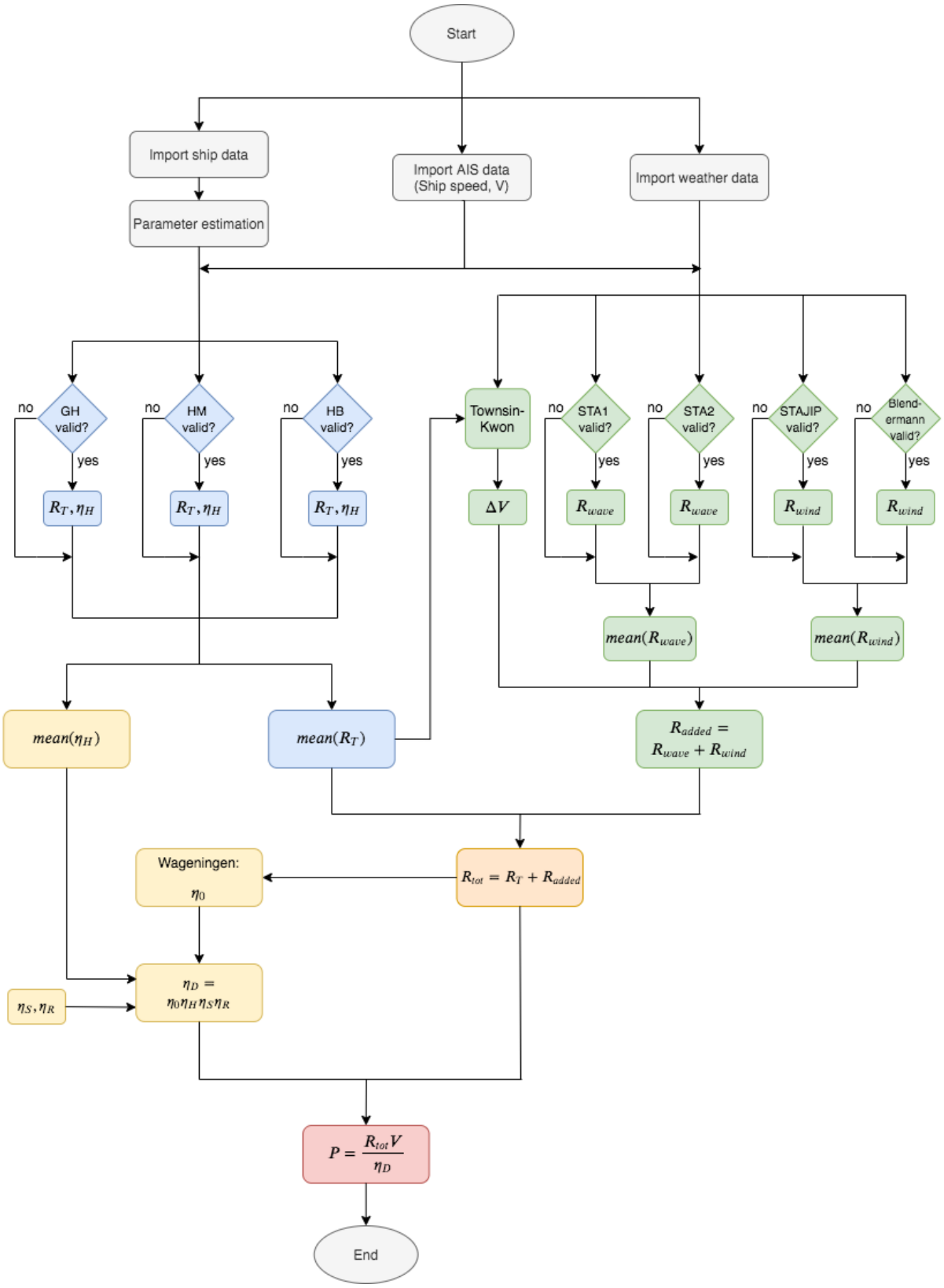

Figure 5.5: Flowchart of the new power prediction method

5.2.3 Coordinate Systems

The direction of wind and waves is defined relative to the ship reference frame. A coordinate system is defined in the program as follows.

Wave direction

The relative wave angle is defined within [0°,±180°], where 0° is head sea and ±180° is following sea. It is equally defined for port and starboard side, see Figure 5.6.

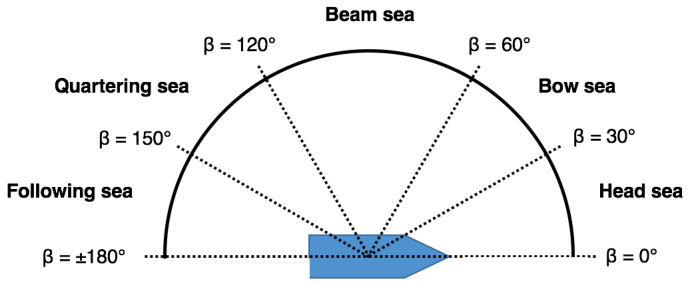

Figure 5.6: Relative wave angle in the ship reference frame

Wind direction

The relative wind angle is defined within [0°,360°], where 0° and 360°is head wind, and 180° is following wind. Figure 5.7 illustrates the system.

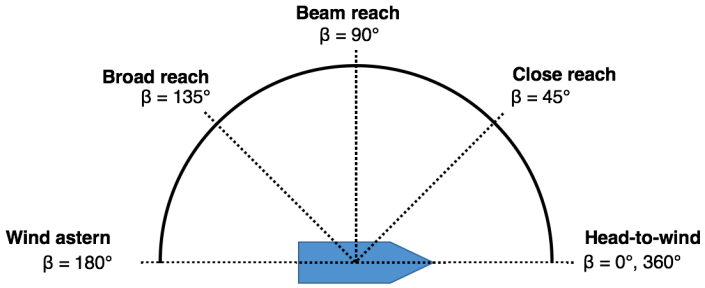

Figure 5.7: Relative wind angle in the ship reference frame

5.3 Verification of Methods

An important part of obtaining reliable power predictions is to ensure the methods and calculation procedures are implemented correctly in the MATLAB program. This may be verified by reproducing the results to independent calculations. As most of the procedures are well known, several calculation examples exist in the literature. This section briefly outlines the applied verification process for the program.

An example presented in Birk (2019) is applied to verify the calm water resistance methods, i.e. Hollenbach, Holtrop-Mennen and Guldhammer-Harvald. The example presents the power prediction of a 1000 TEU container ship for all three methods. The container ship parameters are given as input to the MATLAB program in order to reproduce the results from the example. As Birk (2019) applies Hollenbach and Holtrop-Mennen as originally presented by the respective authors, these versions are also selected for the comparisons. The program successfully reproduces the results with a deviation of 0-2% for the three different methods. The deviations are assumed to be a result of the parameter estimates. This indicates the methods are implemented correctly. However, as presented in Chapter 3, some suggested modifications to Hollenbach and Holtrop-Mennen are implemented in the program. In order to investigate the reliability of these improvements,

a validation process with ship trial data must be conducted.

For the verification of STA-1 and STA-2 a report by MARIN (2006) is applied. The report presents estimates for the added resistance in waves calculated by the respective methods for several ships. A 180 m product tanker is selected for reproducing the results in MATLAB. It gives a deviation of less than 1% for the two methods. A calculation example in the ISO 15016 standard is applied for STA-JIP wind which gives a deviation of 3%. The latter deviation is assumed to be due to the simplification of the relative wind velocity vector, as discussed in Section 5.1.2.

No example calculations with sufficient level of details are found for the Townsin-Kwon method or the simplified Wageningen B-series method by the author. However, the methods are computationally simple, and it is therefore considered reasonable to verify the procedures with hand calculations. The product tanker from Marin report is applied for Townsin & Kwon, and a model test report is applied for Wageningen B. The hand calculations correspond to the program computations with 0 $\%$ deviation in both cases.

Chapter 6

Results and Validation

The goal of this chapter is to assess how well the new model predicts the ship power and whether the results are improved from the current MariTEAM model. This include evaluating the performance of each method implemented in the model as well as the parameter estimates. In order to investigate the performance, a case study is conducted for seven ships of different type and size. The accuracy of the parameter estimates are computed, and the predicted power for each ship is compared to the actual ship power at sea or from model tests. Power predictions are performed both for the new model and the current MariTEAM model to compare the results. The following section outlines the case study and the corresponding validation process.

6.1 Case Study

The objective of the case study is to test the new method on a range of ships and assess the performance. Since the method is developed for fleet-wide calculations, seven vessels of various type and size are included in the case study. Ideally, the case data should be representative of the whole fleet and include more than seven ships. However, the selected cases comprise validation data which is crucial in the power prediction performance assessment. The case vessel data is further outlined in the following.

6.2 Case Vessel Data

The case vessel data comprise detailed hull characteristics, model test reports, sea trial reports and in-service data. Since Sea-web only provides displacement and draught on maximum load line, Sea-web data is included for two of the ships to investigate the effect of varying loading conditions on the power prediction performance. Table 6.1 gives an overview of the data available for each case vessel. The validation process is described in detail in Section 6.4

Table 6.1: Overview of case vessel data in the case study

Case	Ship type	Model test data (design load)	Sea trial data (heavy ballast)	Sea-web data (maximum load)	In-service data (in-service load)
1	Cargo ship	x		x	x
2	Container (13,000 TEU)		x	x	x
3	Vehicles carrier	x			
4	Wellboat	x			
5	Chemical tanker	x			
6	Container (3,500 TEU)	x			
7	Bulk carrier		x		

Model test reports include detailed information on ship resistance and propeller performance for various loading conditions and large speed ranges. All the available model test reports in this case study present full-scale powering predictions for calm water conditions. The data is therefore applied to validate the predicted power,

resistance, and propulsion factors in calm water.

Sea trial reports typically contain fewer details about hull and propeller performance, relative to model test reports. The two available reports in this case study comprise the power measured on heavy ballast loading over a small speed range. Further, the power is corrected for environmental effects and presented for calm water conditions. The reports are applied to validate the calm water power prediction for the two cases. However, the data is scarce, and the ballast loading condition deviates from the design loading assumed in the new method.

In addition to the calm water data available, two of the cases also comprise one month of in-service data. The measured in-service power is valuable for validating the power prediction in a seaway, including the performance in weather. The measured power is related to the ship's position in time and space, and for a given speed. The ship route is then applied to connect hindcast weather data and identifies the weather state for the ship. This is further described in the following section.

6.3 Weather Data

In-service measurements of voyage data are available for the cargo ship (Case 1) and the 13,000 TEU container ship (Case 2). The respective routes are plotted in Figures 6.1a and 6.1b.

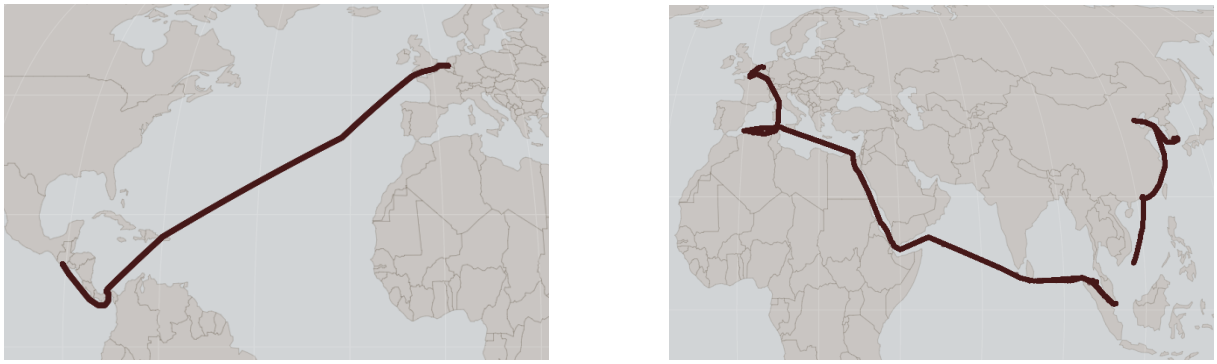

(a) Case 1: Cargo ship

(b) Case 2: Container ship (13,000 TEU)

Figure 6.1: In-service routes for the recorded voyage data

Before the in-service measurements are analysed, the datasets are cleaned, and outliers are removed. The in-service data for Case 1 and Case 2 are processed by Gupta et al. (2019) and Kim (2020), respectively. This processing includes removing transient conditions and connecting hindcast weather data to the voyage. As presented in Section 4.1.5, the temporal solution of wave and wind parameters from ECMWF (2014) are respectively 6 hours and 3 hours. The parameters are therefore interpolated in time to fit the in-service measurements. For in-shore areas the environmental parameters are typically zero and these parts of the route are neglected in the validation analysis. Finally, the weather data for wind and waves are transformed into the ship reference frame. Table 6.2 outlines the weather data available for Case 1 and Case 2.

Table 6.2: In-service weather data variables

Parameter	Symbol	Unit
Significant wave height	H_s	$[m]$
Mean wave period	T_w	$[s]$
Relative mean wave direction	β_{wave}	$[^\circ]$
True wind speed	U	$[m/s]$
Relative wind speed	U_{rel}	$[m/s]$
Relative wind direction	β_{wind}	$[^\circ]$

In addition to the measured power, the in-service data comprise the actual fore and aft draught of the ship. For Case 1, the actual displacement is also obtained by Gupta et al. (2019), using a 3D model of the ship.

6.4 Validation Methods

The validation process consists of two parts. The first part is validating the calm water power requirements without including the effects of wind and waves. This is done by comparing the calculations to model test results or sea-trial measurements. The second part of the validation is to include the effects of wind and waves and compare the power predictions to in-service data. Both parts are conducted both with the new model and with the current MariTEAM model to compare the performance. Results for the new model is presented first in Sections 6.5 - 6.7, followed by a comparison to the current MariTEAM model in Section 6.8.

6.5 Validation of Calm-Water Power Prediction

The calm water power prediction is computed as the mean of the valid methods (Guldhammer-Harvald, Holtrop-Mennen or Hollenbach). Results for all three methods are, however, included in the validation analysis. In cases where only one method is applicable, the mean is still calculated for all methods and added to the results. The objective of this is to assess how well the calm water resistance methods and the propulsion method perform. Mean and standard deviations are computed for the predicted power in each case.

As presented previously, the new method applies a number of parameter estimates for missing input parameters in Sea-web. These parameters are, however, known for the seven validation cases. The calm water validation is therefore first conducted for a complete set of exact input parameters, without utilising the parameter estimates. This way, the implemented methods are evaluated without any influence of error from the parameter estimates. Then, the computations are performed, including the estimated parameters to assess the performance of the parameter estimates. Mean and standard deviations are computed for these calculations as well, although presented in Section 6.8 together with the current MariTEAM model.

6.5.1 Case 1: Cargo Ship

Case 1 is a cargo ship with main particulars as listed in Table 6.3. The validation data comprise full-scale power predictions at design draught from a model test report. Calculated results are presented in the following, both with the complete set of exact input parameters, and when the parameter estimates are included.

Table 6.3: Main particulars of Case 1: Cargo ship at design draught

Parameter	Symbol	Value	Unit
Length between perpendiculars	L_{pp}	194.00	$[m]$
Breadth	B	32.26	$[m]$
Draught	T	12.00	$[m]$
Volume displacement	$\bigtriangledown$	59,691.00	$[m^3]$
Block coefficient	C_B	0.795	$[-]$
Propeller diameter	D_P	7.00	$[m]$
No. of blades	Z	4	$[-]$
No. of propellers	-	1	$[-]$

Exact input parameters

Figure 6.2 presents the delivered power P_D, computed by each calm water method and by the model test. All calm water methods are applicable in this case, and the Hollenbach minimum estimate is plotted as a stapled line as it is not included in the calculated mean.

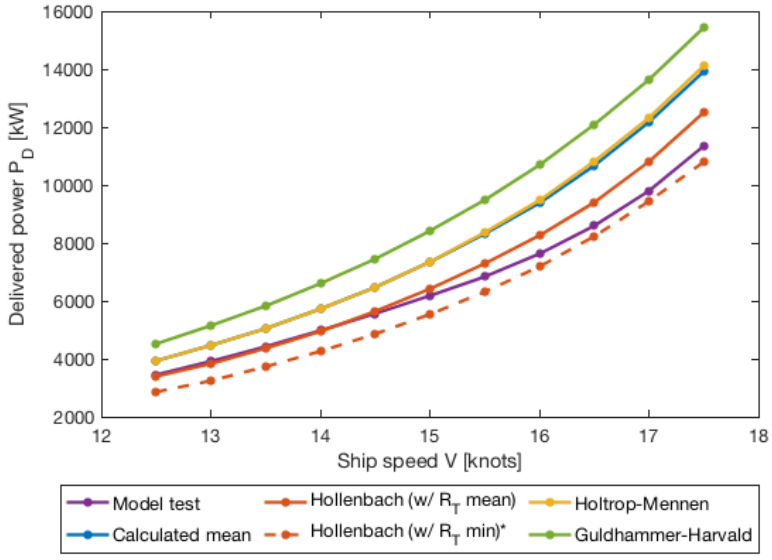

Figure 6.2: Validation of power prediction for Case 1 with design loading and exact input parameters. Model test results and calculated results.

Table 6.4 presents the deviation between the calculated results and the model test, expressed in terms of the mean deviation plus the standard deviation. Hollenbach's mean estimate is the most accurate in this case, with a mean deviation of 4% and standard deviation of 5%. While all methods overestimate the power, Hollenbach's minimum estimate underestimates the power by 10% on average. Guldhammer-Harvald significantly overpredicts the power, on average by 36%. A reason for this may be that cargo ships are not included in the modernised Guldhammer-Harvald by Kristensen et al. (2017), so the calculations are computed without the bulb correction. Similarly, for Holtrop-Mennen, a bulb correction is not included in the method, as discussed in Section 3.1.2.

Table 6.4: Deviation between calculated power and model test power for Case 1 (exact input parameters)

Method	Mean deviation	Std. deviation	Applicable
Hollenbach (w/ mean resistance)	4%	5%	yes
Holtrop-Mennen	19%	5%	yes
Guldhammer-Harvald	36%	4%	yes
Calculated mean	19%	5%	yes
Hollenbach (w/ minimum resistance)*	-10%	5%	yes
* Not included in the calculated mean			

Estimated input parameters

Figure 6.3 presents the computed results including the parameter estimates. Compared to the results with exact input, there is little difference in the predicted power. It is slightly lower for all the computed cases, although the trend is the same.

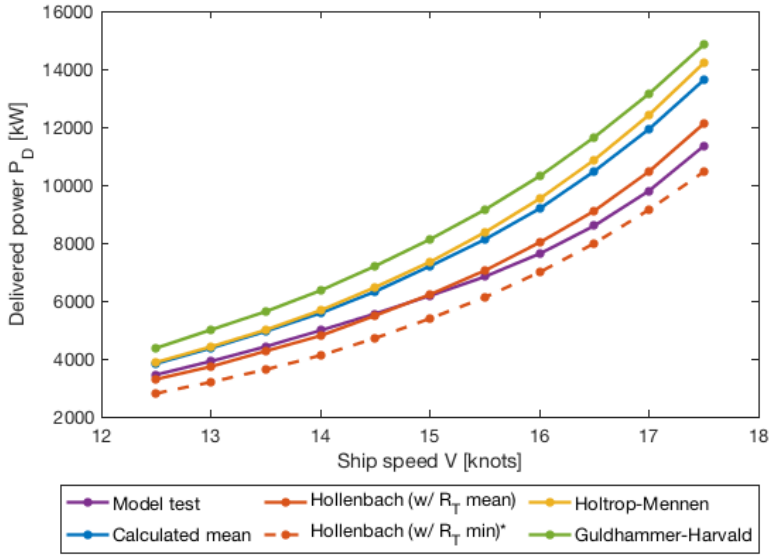

Figure 6.3: Validation of power prediction for Case 1 with design loading and estimated parameters. Model test results and calculated results.

Table 6.5 gives the deviation between the parameter estimates and the exact input. The transverse projected area deviates significantly by -44.7%, which gives an underpredicted air resistance. This may be the reason for the slightly lower power predicted.

Table 6.5: Deviation of estimated parameters for Case 1 with design loading condition

Parameter	Symbol	Unit	Ship	Estimated	Deviation
Length of waterline	L_{WL}	$[m]$	198.30	197.88	-0.2 %
Draught fore	T_F	$[m]$	12.00	12.00	0.0 %
Draught aft	T_A	$[m]$	12.00	12.00	0.0 %
Block coefficient	C_B	$[-]$	0.795	0.795	0.0 %
Wetted surface area	S	$[m^2]$	9,496.00	9,155.15	-3.6%
Prismatic coefficient	C_P	$[-]$	0.798	0.800	0.2%
Transverse projected area	A_{VT}	$[m^2]$	700.00	387.12	-44.7%
Propeller diameter	D_p	$[m]$	7.00	6.68	-4.6%

6.5.2 Case 2: Container Ship (13,000 TEU)

Case 2 is a 13,000 TEU container ship with main particulars as listed in Table 6.6. The validation data comprise calm water power predictions at heavy ballast loading from a sea trial report. This loading condition gives a sea trial draught of 7.25 m, while the design draught is 14.50 m. Further, the propeller is surface piercing in the sea trial, as seen in Table 6.6. An underlying assumption for the new model is design draught and submerged propeller, so the ballast loading condition is expected to give deviations in the predictions. Calculated results are presented in the following, both with the complete set of exact input parameters, and when the parameter estimates are included.

Table 6.6: Main particulars of Case 2: Container Ship (13,000 TEU) at ballast draught

Parameter	Symbol	Value	Unit
Length between perpendiculars	L_{pp}	350.00	$[m]$
Breadth	B	48.20	$[m]$
Draught	T	7.25	$[m]$
Volume displacement	∇	71,675.00	$[m^3]$
Block coefficient	C_B	0.582	$[-]$
Propeller diameter	D_P	8.80	$[m]$
No. of blades	Z	6	$[-]$
No. of propellers	-	1	$[-]$

Exact input parameters

Figure 6.4 presents the delivered power P_D, computed by each calm water method and by the sea trial. Only Holtrop-Mennen is applicable in this case, and the other computations are plotted in stapled lines. The small draught and displacement give too large ratios for $(L/\nabla^{1/3})$, (B/T) and (D_p/T), for Guldhammer-Harvald and Hollenbach.

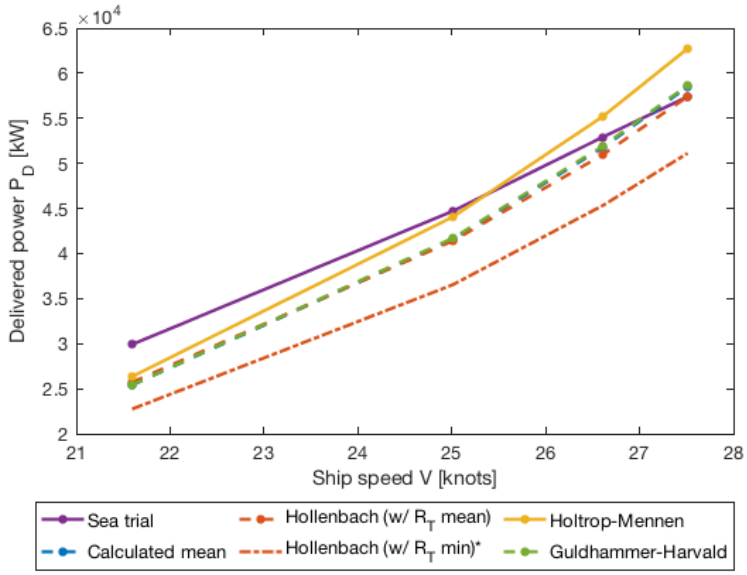

Figure 6.4: Validation of power prediction for Case 2 with heavy ballast loading and exact parameters. Sea trial results and calculated results.

Table 6.7 presents the deviation between the calculated results and the sea trial, expressed in terms of the mean deviation plus the standard deviation. Holtrop-Mennen's estimate is on average the most accurate with a mean deviation of 0%, although with a relatively large standard deviation of 9%. The other, non-valid methods, underpredict the delivered power. In this case, the modernised Guldhammer-Harvald is applicable and the results show that Guldhammer-Harvald's and Hollenbach's mean power predictions are similar.

Table 6.7: Deviation between calculated power and sea trial power for Case 2 (exact input parameters)

Method	Mean deviation	Std. deviation	Applicable
Hollenbach (w/ mean resistance)	-6%	6%	no
Holtrop-Mennen	0%	9%	yes
Guldhammer-Harvald	-6%	7%	no
Calculated mean	-6%	7%	no
Hollenbach (w/ minimum resistance)*	-17%	6%	no
* Not included in the calculated mean			

Estimated input parameters

Figure 6.5 presents the computed results including the parameter estimates. Compared to the results with exact input, there is a large difference in the predicted power. As Table 6.8 displays, the estimated propeller diameter deviates -50.5 % the program, due to the surface piercing condition. This result in a significantly underpredicted propeller efficiency of about 30% for all the methods. As a result, the delivered power is significantly overpredicted. In addition, the draught fore and aft deviate largely due to the trim. The transverse projected area is also overpredicted by 20.1%, which overpredicts the resistance.

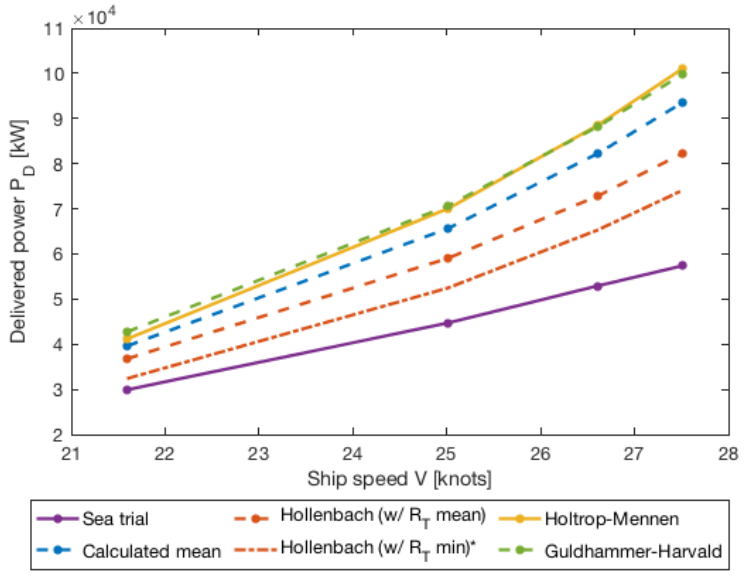

Figure 6.5: Validation of power prediction for Case 2 with heavy ballast loading and estimated parameters. Sea trial results and calculated results.

Table 6.8: Deviation of estimated parameters for Case 2 with heavy ballast loading condition

Parameter	Symbol	Unit	Ship	Estimated	Deviation
Draught fore	T_F	$[m]$	4.90	7.25	48.0 %
Draught aft	T_A	$[m]$	9.60	7.25	-24.5 %
Block coefficient	C_B	$[-]$	0.582	0.586	0.6%
Wetted surface area	S	$[m^2]$	14,216.20	14,681.89	3.3%
Midship section coefficient	C_M	$[-]$	0.975	0.977	0.2%
Prismatic coefficient	C_P	$[-]$	0.597	0.600	0.5%
Transverse projected area	A_{VT}	$[m^2]$	1,950.00	2,341.22	20.1%
Propeller diameter	D_p	$[m]$	8.80	4.36	-50.5%

Corrected propeller diameter

Figure 6.6 shows the results when the propeller diameter is corrected. As can be seen, the estimate is significantly improved. This indicate that the estimated propeller diameter affects the predicted power more than the other parameter estimates in this case. Note that the range on the y-axis is different in the plots.

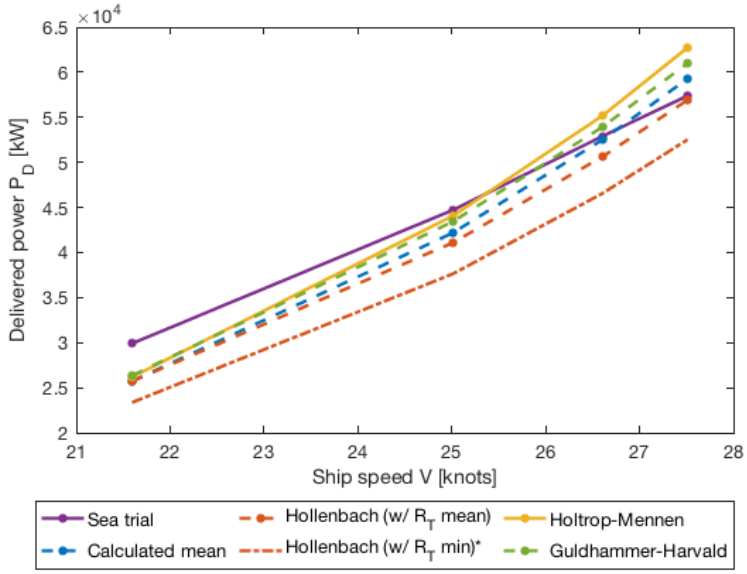

Figure 6.6: Validation of power prediction for Case 2 with heavy ballast loading and estimated parameters, with corrected propeller diameter. Sea trial results and calculated results.

6.5.3 Case 3: Vehicles Carrier

Case 3 is a vehicles carrier with main particulars as listed in Table 6.9. The validation data comprise full-scale power predictions at design draught from a model test report. This vessel is twin-screw, therefore, the underlying assumption in the method of single screw vessels is expected to give some deviations in the predictions. Calculated results are presented in the following, both with the complete set of exact input parameters, and when the parameter estimates are included.

Table 6.9: Main particulars of Case 3: Vehicles carrier at design draught

Parameter	Symbol	Value	Unit
Length between perpendiculars	L_{pp}	131.30	$[m]$
Breadth	B	22.70	$[m]$
Draught	T	6.50	$[m]$
Volume displacement	∇	11,094.30	$[m^3]$
Block coefficient	C_B	0.573	$[-]$
Propeller diameter	D_P	4.50	$[m]$
No. of blades	Z	4	$[-]$
No. of propellers	-	2	$[-]$

Exact input parameters

Figure 6.7 presents the delivered power P_D, computed by each calm water method and by the model test. Holtrop-Mennen and Hollenbach are applicable in this case, as well as the mean of the two. Guldhamer-Harvald is not applicable due to a too large slenderness ratio $(L/\nabla^{1/3})$.

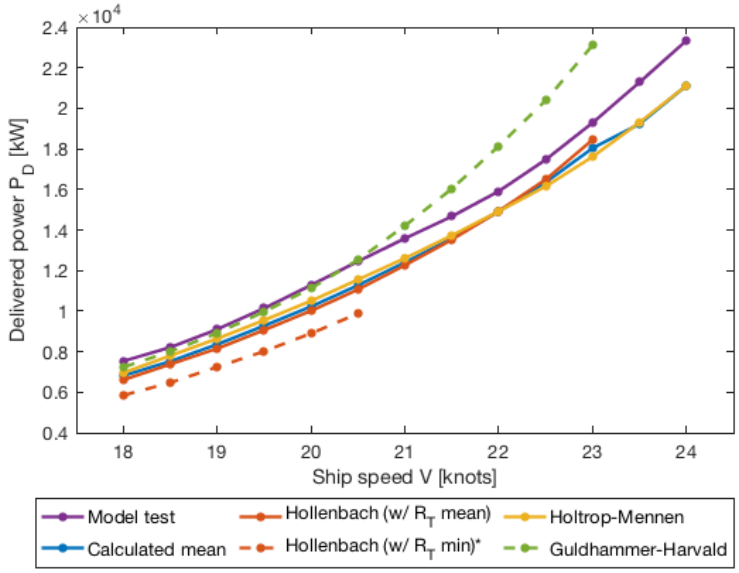

Figure 6.7: Validation of power prediction for Case 3 with design loading and exact parameters. Model test results and calculated results.

Table 6.10 presents the deviation between the calculated results and the model test, expressed in terms of the mean deviation plus the standard deviation. All the applicable methods underestimate the power, whereas Holtrop-Mennen's estimate is the most accurate. The applicable froude number range for Guldhammer-Harvald and Hollenbach is exceeded in this case.

Table 6.10: Deviation between calculated power and model test power for Case 3 (exact input parameters)

Method	Mean deviation	Std. deviation	Applicable
Hollenbach (w/ mean resistance)	-9%	3%	yes
Holtrop-Mennen	-7%	1%	yes
Guldhammer-Harvald	5%	9%	no
Calculated mean**	-8%	1%	yes
Hollenbach (w/ minimum resistance)*	-21%	1%	yes
* Not included in the calculated mean			
** Mean of Hollenbach and Holtrop-Mennen			

Estimated input parameters

Figure 6.8 presents the computed results including the parameter estimates. Compared to the results with exact input, the power is even more underpredicted. As Table 6.11 presents, the estimated wet surface area deviates by -15.4%, and the transverse projected area deviates by -19.6%. These deviations result in an underpredicted resistance, and further, an underpredicted power.

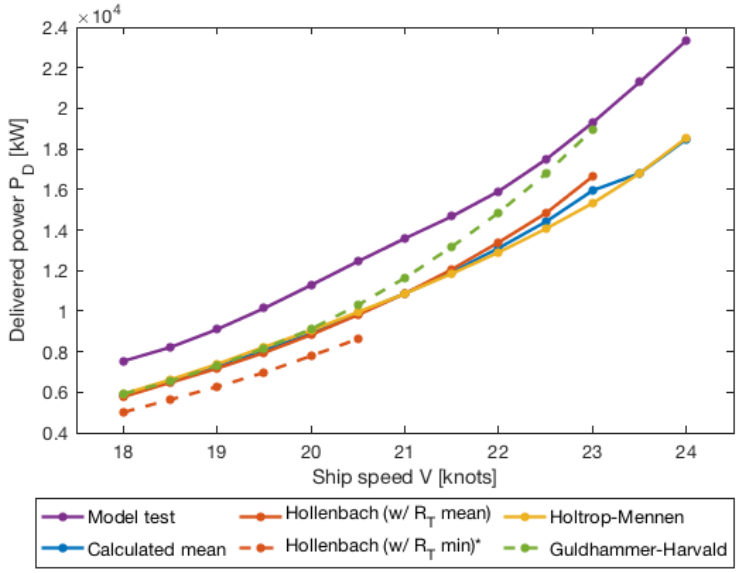

Figure 6.8: Validation of power prediction for Case 3 with design loading and estimated parameters. Model test results and calculated results.

Table 6.11: Deviation of estimated parameters for Case 3

Parameter	Symbol	Unit	Ship	Estimated	Deviation
Length of waterline	L_{WL}	$[m]$	134.60	133.93	-0.5 %
Draught fore	T_F	$[m]$	6.50	6.50	0.0 %
Draught aft	T_A	$[m]$	6.50	6.50	0.0 %
Block coefficient	C_B	$[-]$	0.573	0.572	-0.1 %
Wetted surface area	S	$[m^2]$	3826.45	3,235.50	-15.4%
Midship section coefficient	C_M	$[-]$	0.973	0.976	0.3%
Prismatic coefficient	C_P	$[-]$	0.589	0.586	-0.4%
Transverse projected area	A_{VT}	$[m^2]$	692.00	556.20	-19.6%
Propeller diameter	D_p	$[m]$	4.50	4.55	1.1%

6.5.4 Case 4: Wellboat

Case 4 is a wellboat with main particulars as listed in Table 6.12. The validation data comprise full-scale power predictions at design draught from a model test report. In contrast to the other vessels included in the case study, the wellboat is not a conventional ship in the fleet. As most of the empirical calculation methods are based on conventional hull forms, this may give some deviations in the predictions. Calculated results are presented in the following, both with the complete set of exact input parameters, and when the parameter estimates are included.

Table 6.12: Main particulars of Case 4: Wellboat at design draught

Parameter	Symbol	Value	Unit
Length between perpendiculars	L_{pp}	73.40	$[m]$
Breadth	B	16.00	$[m]$
Draught	T	6.40	$[m]$
Volume displacement	$\bigtriangledown$	5,575.80	$[m^3]$
Block coefficient	C_B	0.742	$[-]$
Propeller diameter	D_P	3.30	$[m]$
No. of blades	Z	4	$[-]$
No. of propellers	-	1	$[-]$

Exact input parameters

Figure 6.9 presents the delivered power P_D, computed by each calm water method and by the model test. Holtrop-Mennen is the only valid method for this case, and the other power predictions are plotted in stapled lines. Guldhammer-Harvald and Hollenbach is not applicable due to a too small slenderness ratio. As illustrated in the figure, Hollenbach's predictions are further limited by the froude number range.

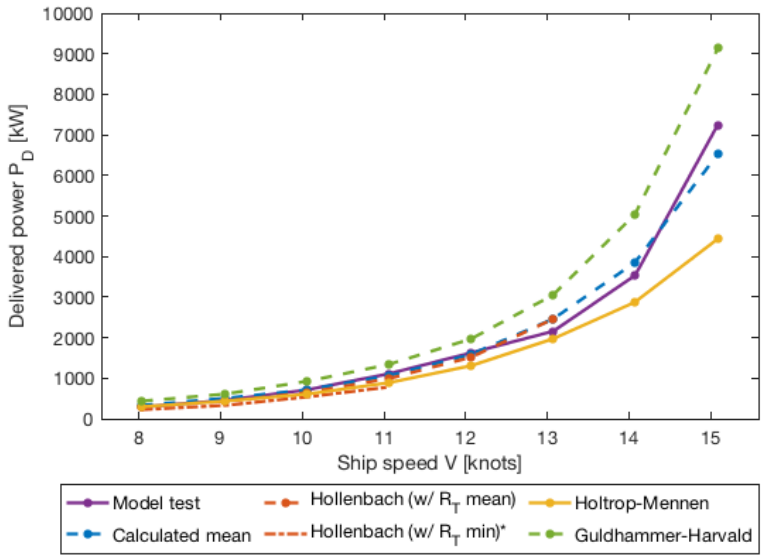

Figure 6.9: Validation of power prediction for Case 4 with design loading and exact parameters. Model test results and calculated results.

Table 6.13 presents the deviation between the calculated results and the model test, expressed in terms of the mean deviation plus the standard deviation. Of the calm water methods, Hollenbach's mean prediction is the most accurate, even though it is not applicable. Guldhammer-Harvald overpredicts the power, while Holtrop-Mennen underpredicts the power. As a result, the calculated mean is more accurate than the two latter methods.

Table 6.13: Deviation between calculated power and model test power for Case 4 (exact input parameters)

Method	Mean deviation	Std. deviation	Applicable
Hollenbach (w/ mean resistance)	-3%	9%	no
Holtrop-Mennen	-14%	13%	yes
Guldhammer-Harvald	32%	10%	no
Calculated mean	3%	9%	no
Hollenbach (w/ minimum resistance)*	-25%	3%	no
* Not included in the calculated mean			

Estimated input parameters

Figure 6.10 presents the computed results including the parameter estimates. Compared to the results with exact input, all the power predictions are somewhat reduced. As a result, the applicable prediction by Holtrop-Mennen deviates more. As displayed in Table 6.14, the prediction of the wet surface deviates -7.3%, which underpredicts the resistance. Further, the propeller diameter is overestimated by 35.8%. As a result the propulsive efficiency is overpredicted. Despite this, the final predicted power is still underestimated due to the resistance and the deviation increase for higher ship speed.

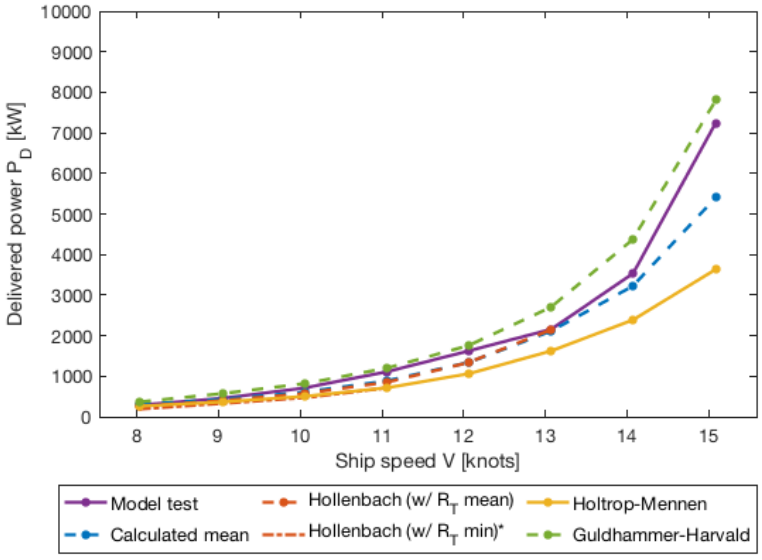

Figure 6.10: Validation of power prediction for Case 4 with design loading and estimated parameters. Model test results and calculated results.

Table 6.14: Deviation of estimated parameters for Case 4

Parameter	Symbol	Unit	Ship	Estimated	Deviation
Length of waterline	L_{WL}	$[m]$	75.29	74.87	-0.6%
Draught fore	T_F	$[m]$	6.40	6.40	0.0%
Draught aft	T_A	$[m]$	6.40	6.40	0.0%
Block coefficient	C_B	$[-]$	0.742	0.742	0.0%
Wetted surface area	S	$[m^2]$	1,845.58	1,711.56	-7.3%
Midship section coefficient	C_M	$[-]$	0.996	0.989	-0.6%
Prismatic coefficient	C_P	$[-]$	0.745	0.750	0.6%
Transverse projected area	A_{VT}	$[m^2]$	210.00	222.40	5.9%
Propeller diameter	D_p	$[m]$	3.30	4.48	35.8%

6.5.5 Case 5: Chemical Tanker

Case 5 is a chemical tanker with main particulars as listed in Table 6.15. The validation data comprise full-scale power predictions at design draught from a model test report. Calculated results are presented in the following, both with the complete set of exact input parameters, and when the parameter estimates are included.

Table 6.15: Main particulars of Case 5: Chemical tanker at design draught

Parameter	Symbol	Value	Unit
Length between perpendiculars	L_{pp}	142.00	$[m]$
Breadth	B	23.50	$[m]$
Draught	T	9.30	$[m]$
Volume displacement	∇	23,674.60	$[m^3]$
Block coefficient	C_B	0.763	$[-]$
Propeller diameter	D_P	5.80	$[m]$
No. of blades	Z	4	$[-]$
No. of propellers	-	1	$[-]$

Exact input parameters

Figure 6.11 presents the brake power P_B, computed by each calm water method and by the model test. All calm water methods are applicable in this case, and the Hollenbach minimum estimate is plotted as a stapled line as it is not included in the calculated mean.

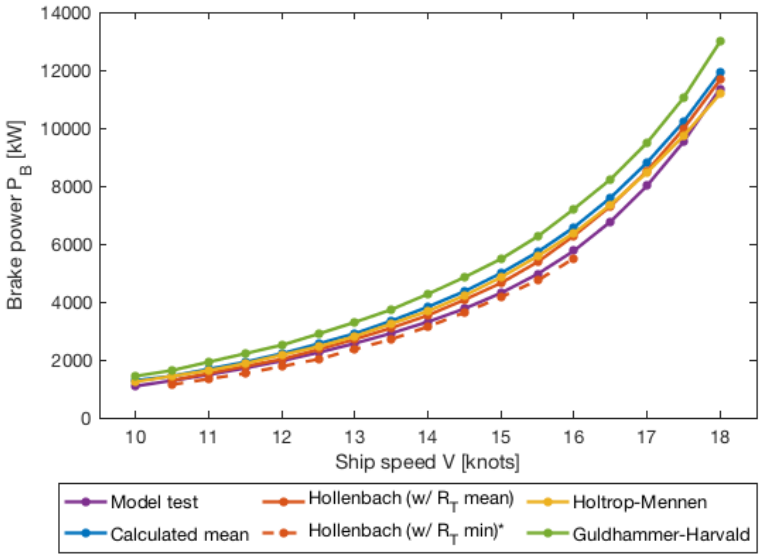

Figure 6.11: Validation of power prediction for Case 5 with design loading and exact parameters. Model test results and calculated results.

Table 6.16 presents the deviation between the calculated results and the model test, expressed in terms of the mean deviation plus the standard deviation. Hollenbach's mean estimate is the most accurate in this case, with a mean deviation of 6% and standard deviation of 2%. While all methods overestimate the power, Hollenbach's minimum estimate underestimates the power by -7% on average. Guldhammer-Harvald significantly overpredicts the power, on average by 26%. Similar to the cargo ship in case 1, the reason for this may be that chemical tankers are not included in the modernised Guldhammer-Harvald by Kristensen et al. (2017), so the calculations are computed without the bulb correction.

Table 6.16: Deviation between calculated power and model test power for Case 5 (exact input parameters)

Method	Mean deviation	Std. deviation	Applicable
Hollenbach (w/ mean resistance)	6%	2%	yes
Holtrop-Mennen	9%	4%	yes
Guldhammer-Harvald	26%	5%	yes
Calculated mean	13%	3%	yes
Hollenbach (w/ minimum resistance)*	-7%	3%	yes
* Not included in the calculated mean			

Estimated input parameters

Figure 6.12 presents the computed results including the parameter estimates. Compared to the results with exact input, there is little difference in the predicted power. In this case, the accuracy of Hollenbach and Holtrop-Mennen's predictions increases slightly. This may be due to the underestimated wetted surface area and transverse projected area, as presented in Table 6.17. Since both methods overestimate the power with exact input parameters, the underpredicted parameters reduce the calculated resistance and improve the estimate.

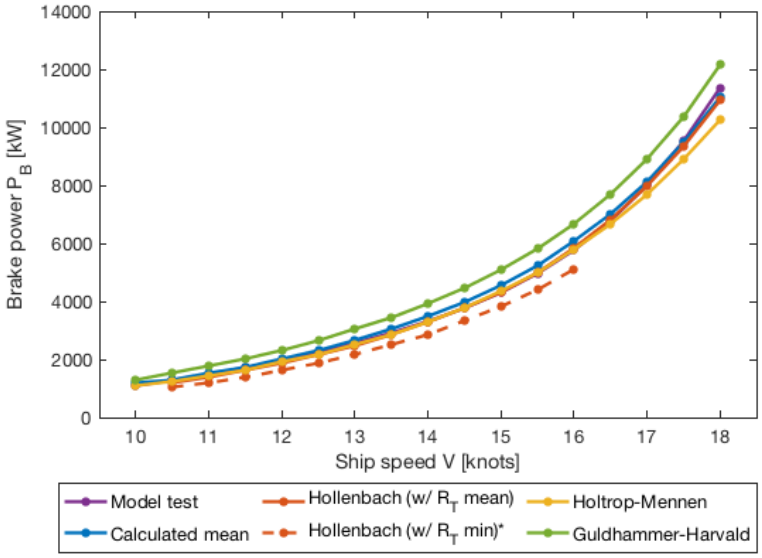

Figure 6.12: Validation of power prediction for Case 5 with design loading and estimated parameters. Model test results and calculated results.

Table 6.17: Deviation of estimated parameters for Case 5

Parameter	Symbol	Unit	Ship	Estimated	Deviation
Length of waterline	L_{WL}	$[m]$	145.84	144.84	-0.7%
Draught fore	T_F	$[m]$	9.30	9.30	0.0%
Draught aft	T_A	$[m]$	9.30	9.30	0.0%
Block coefficient	C_B	$[-]$	0.763	0.763	0.0%
Wetted surface area	S	$[m^2]$	5,156.80	4,910.44	-4.8%
Midship section coefficient	C_M	$[-]$	0.995	0.991	-0.3%
Prismatic coefficient	C_P	$[-]$	0.767	0.770	0.3%
Transverse projected area	A_{VT}	$[m^2]$	460.00	131.60	-71.4%
Propeller diameter	D_p	$[m]$	5.80	6.51	12.2%

6.5.6 Case 6: Container ship (3,500 TEU)

Case 6 is a 3,500 TEU container ship with main particulars as listed in Table 6.18. The validation data comprise full-scale power predictions at design draught from a model test report. Calculated results are presented in the following, both with the complete set of exact input parameters, and when the parameter estimates are included.

Table 6.18: Main particulars of Case 6: Container ship (3,500 TEU) at design draught

Parameter	Symbol	Value	Unit
Length between perpendiculars	L_{pp}	233.00	$[m]$
Breadth	B	32.20	$[m]$
Draught	T	11.00	$[m]$
Volume displacement	∇	47,202.30	$[m^3]$
Block coefficient	C_B	0.572	$[-]$
Propeller diameter	D_P	7.52	$[m]$
No. of blades	Z	4	$[-]$
No. of propellers	-	1	$[-]$

Exact input parameters

Figure 6.13 presents the delivered power P_D, computed by each calm water method and by the model test. Only Holtrop-Mennen is applicable in this case, and the other computations are plotted in stapled lines. The slenderness ratio and the length-breadth ratio are too large for Guldhammer-Harvald and Hollenbach.

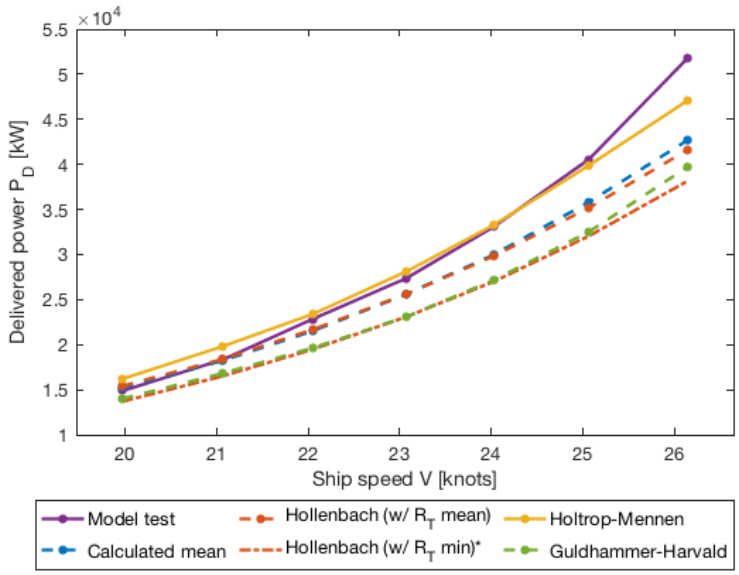

Figure 6.13: Validation of power prediction for Case 6 with design loading and exact parameters. Model test results and calculated results.

Table 6.19 presents the deviation between the calculated results and the model test, expressed in terms of the mean deviation plus the standard deviation. Holtrop-Mennen's estimate is on average the most accurate with a mean deviation of 2%, and a standard deviation of 6%. The other, non-valid methods, underestimate the delivered power. As for the other container ship in Case 2, the modernised Guldhammer-Harvald is applicable, and the results show that Guldhammer-Harvald's and Hollenbach's minimum power predictions are similar.

Table 6.19: Deviation between calculated power and model test power for Case 6 (exact input parameters)

Method	Mean deviation	Std. deviation	Applicable
Hollenbach (w/ mean resistance)	-7%	8%	no
Holtrop-Mennen	2%	6%	yes
Guldhammer-Harvald	-15%	6%	no
Calculated mean	-7%	7%	no
Hollenbach (w/ minimum resistance)*	-17%	6%	no
* Not included in the calculated mean			

Estimated input parameters

Figure 6.14 presents the computed results including the parameter estimates. Compared to the results with exact input, there is little difference in the predicted power, and the trend is the same. Table 6.20 gives the deviation between the parameter estimates and the exact input. The transverse projected area is overestimated by 48.5%, and the propeller diameter is underestimated by 11%. Although these deviations are significant, the predicted power is not significantly affected.

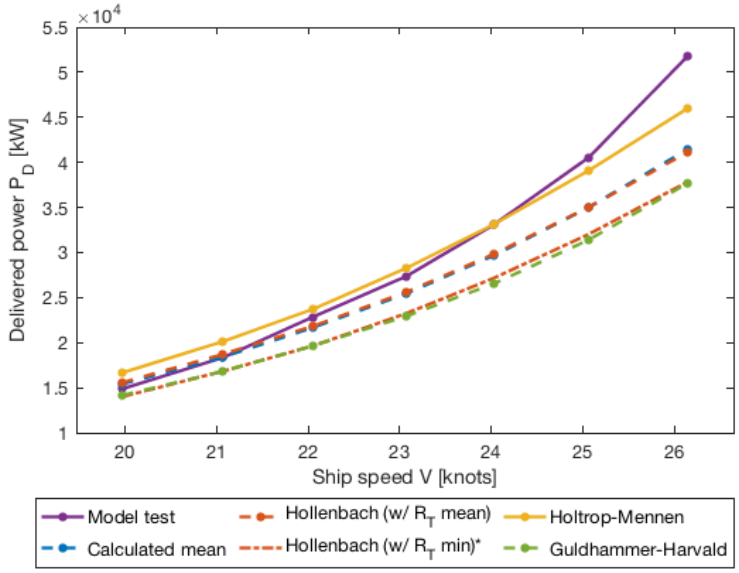

Figure 6.14: Validation of power prediction for Case 6 with design loading and estimated parameters. Model test results and calculated results.

Table 6.20: Deviation of estimated parameters for Case 6

Parameter	Symbol	Unit	Ship	Estimated	Deviation
Length of waterline	L_{WL}	$[m]$	226.66	235.33	3.8%
Draught fore	T_F	$[m]$	11.00	11.00	0.0%
Draught aft	T_A	$[m]$	11.00	11.00	0.0%
Block coefficient	C_B	$[-]$	0.572	0.572	0.0%
Wetted surface area	S	$[m^2]$	8,979.13	9,163.47	2.1%
Midship section coefficient	C_M	$[-]$	0.972	0.976	0.4%
Prismatic coefficient	C_P	$[-]$	0.589	0.586	-0.4%
Transverse projected area	A_{VT}	$[m^2]$	850.00	1,262.24	48.5%
Propeller diameter	D_p	$[m]$	7.52	6.69	-11.0%

6.5.7 Case 7: Bulk Carrier

Case 7 is a bulk carrier with main particulars as listed in Table 6.21. The validation data comprise calm water power predictions at heavy ballast loading from a sea trial report. This loading condition gives a sea trial draught of 8.15 m, while the design draught is 12.2 m. As discussed for the sea trial validation of Case 2, the underlying assumption for the new model is design draught, so the ballast loading condition is expected to give deviations in the predictions. Further, the sea trial report only provide three data points over a small speed range. Calculated results are presented in the following, both with the complete set of exact input parameters, and when the parameter estimates are included.

Table 6.21: Main particulars of Case 7: Bulk Carrier at ballast draught

Parameter	Symbol	Value	Unit
Length between perpendiculars	L_{pp}	226.15	$[m]$
Breadth	B	32.27	$[m]$
Draught	T	8.15	$[m]$
Volume displacement	∇	48,213.66	$[m^3]$
Block coefficient	C_B	0.810	$[-]$
Propeller diameter	D_P	7.20	$[m]$
No. of blades	Z	4	$[-]$
No. of propellers	-	1	$[-]$

Exact input parameters

Figure 6.15 presents the brake power P_B, computed by each calm water method and by the sea trial. Only Holtrop-Mennen is applicable in this case, and the other computations are plotted in stapled lines. Similar to Case 2, the small draught and displacement result in a too large slenderness ratio for Guldhammer-Harvald and Hollenbach.

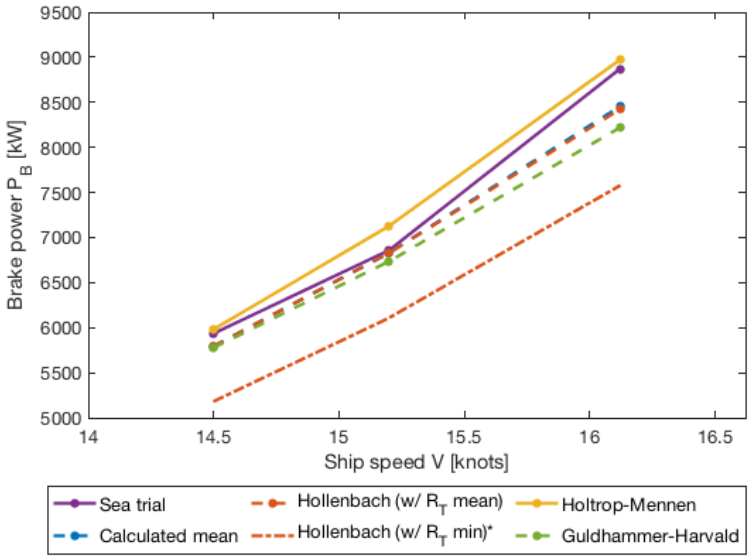

Figure 6.15: Validation of power prediction for Case 7 with heavy ballast loading and exact parameters. Sea trial results and calculated results.

Table 6.22 presents the deviation between the calculated results and the sea trial, expressed in terms of the mean deviation plus the standard deviation. Holtrop-Mennen's estimate is the only applicable and also the most accurate, with a mean deviation of 2%, and standard deviation of 2%. Hollenbach's mean estimate is slightly underestimated, on average by 3%. In this case, the modernised Guldhammer-Harvald is applied, and the results show that Guldhammer-Harvald's and Hollenbach's mean power predictions are similar. The minimum prediction by Hollenbach represents the most significant deviation of -13 %.

Table 6.22: Deviation between calculated power and sea trial power for Case 7 (exact input parameters)

Method	Mean deviation	Std. deviation	Applicable
Hollenbach (w/ mean resistance)	-3%	2%	no
Holtrop-Mennen	2%	2%	yes
Guldhammer-Harvald	-4%	3%	no
Calculated mean	-3%	2%	no
Hollenbach (w/ minimum resistance)	-13%	2%	no
* Not included in the calculated mean			

Estimated input parameters

Figure 6.16 presents the computed results including the parameter estimates. Compared to the results with exact input, there is a large difference in the predicted power. Note that the range on the y-axis is different in the plots. The tendency of the results is similar to the sea trial results from Case 2. As Table 6.23 displays, the estimated propeller diameter deviates -37.2 %, which is expected to result in an underestimated propeller efficiency. This is, however, not verified, as the sea trial report only provides brake power data. In addition, the draught fore and aft deviate largely due to the trim. The transverse projected area is also overpredicted by 41.2%, which overestimates the resistance. An underestimated propulsive efficiency, and an overestimated resistance results in a significantly overpredicted power.

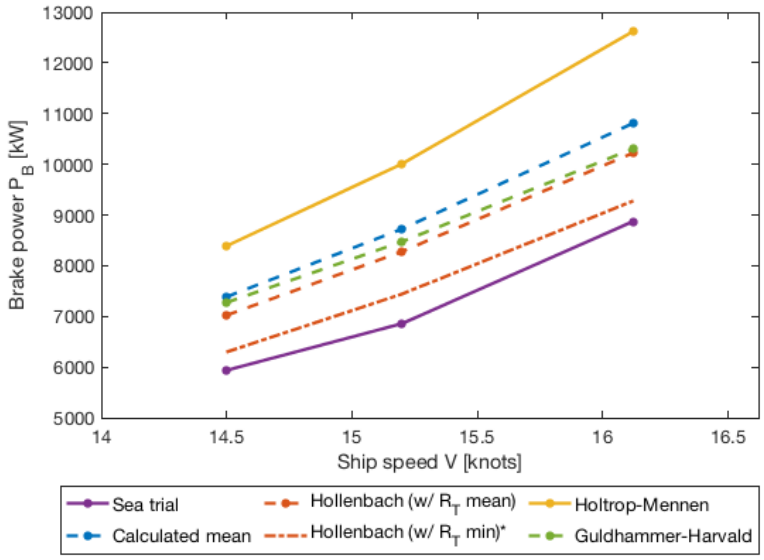

Figure 6.16: Validation of power prediction for Case 7 with heavy ballast loading and estimated parameters. Sea trial results and calculated results.

Table 6.23 lists less parameters than for the other cases. The number of estimated parameters in the calculations are naturally the same for all the cases, however, the sea trial report only provides the exact values for the parameters included below.

Table 6.23: Deviation of estimated parameters for Case 7

Parameter	Symbol	Unit	Ship	Estimated	Deviation
Draught fore	T_F	$[m]$	7.17	8.15	13.7%
Draught aft	T_A	$[m]$	8.96	8.15	-9.0%
Transverse projected area	A_{VT}	$[m^2]$	384.93	543.58	41.2%
Propeller diameter	D_p	$[m]$	7.20	4.52	-37.2%

Corrected propeller diameter

Figure 6.17 shows the results when the propeller diameter is corrected. As can be seen, the estimate is significantly improved. This indicates that the estimated propeller diameter affects the predicted power more than the other parameter estimates in this case. However, the power is still somewhat overestimated compared to the exact input results for each method.

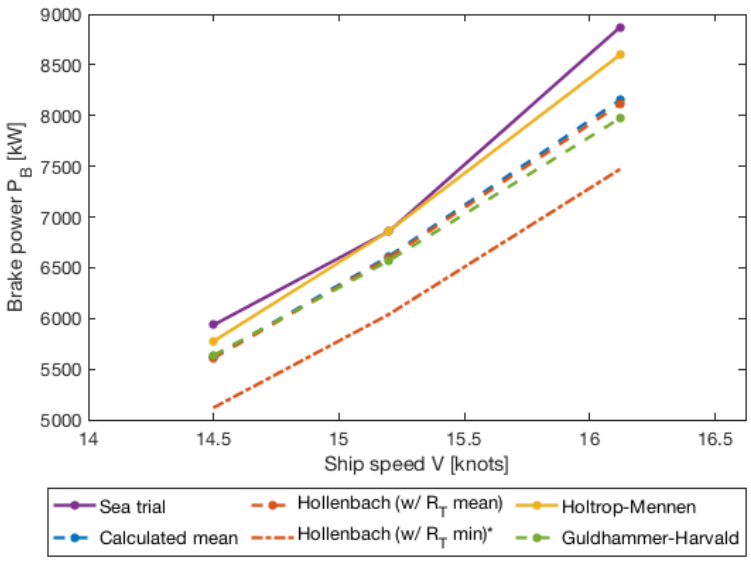

Figure 6.17: Validation of power prediction for Case 7 with heavy ballast loading, estimated parameters but corrected propeller diameter. Sea trial results and calculated results.

6.6 Validation of In-service Power Prediction

The second part of the validation includes the effects of wind and waves and compares the power predictions to the in-service data of Case 1 and Case 2. In addition to the computed mean added resistance, the performance of each added resistance method is assessed in each case. Further, the effect of varying loading conditions on the power prediction is analysed. Each case is analysed for both the in-service draught and the maximum draught provided by Sea-web, to investigate the difference. The root-mean-square error (RMSE) between the measured power and the calculated power is applied to assess the performance of the predictions.

For both the in-service cases, it is assumed that the power produced by the main engine corresponds to the propulsion power and that the other generators provide auxiliary power. Further, sea passage is the only state considered, while manoeuvring or anchor/waiting is disregarded.

6.6.1 Case 1: Cargo Ship

The voyage data of Case 1 include one month of measurements of ship speed, draught and power produced by the engines. In addition, the in-service displacement is made available by Gupta et al. (2019). The mean in-service draught and displacement is applied in the following calculations, together with the weather data variables from the voyage. Table 6.24 presents an overview of the weather characteristics. As displayed, the weather range from calm sea ($BN = 0$) to strong breeze and large waves ($BN = 6$). Both the wind and wave heading vary from head-to to following.

Table 6.24: In-service weather data range for Case 1

Parameter	Symbol	Range $[min, max]$	Unit
Significant wave height	H_s	[0.08,3.64]	$[m]$
Mean wave period	T_w	[0.37,12.35]	$[s]$
Relative mean wave direction	β_{wave}	[1.26, 180.0]	$[^\circ]$
True wind speed	U	[0.10, 11.75]	$[m/s]$
Beauforts number	BN	[0,6]	$[-]$
Relative wind speed	U_{rel}	[0.45, 13.79]	$[m/s]$
Relative wind direction	β_{wind}	[1.07, 358.90]	$[^\circ]$

Figure 6.18 presents the measured brake power (in dark blue), the calculated power by the new method (middle blue), and the computed calm water power (light blue). These results are calculated by applying the mean added resistance estimate. The predicted power follows the trend of the measured power over the speed range. There is, however, measured a constant in-service power for a range of speed. This is observed by the amount of in-service scatter points, forming the horizontal shape in the plot, which deviates from the typical cubic relation between power and speed. A reason for this may be uncertainties related to the on-board measurements of the ship speed. Also, the predicted power appears slightly overestimated in the lower speed range. This corresponds to the results from the calm water analysis of the model test.

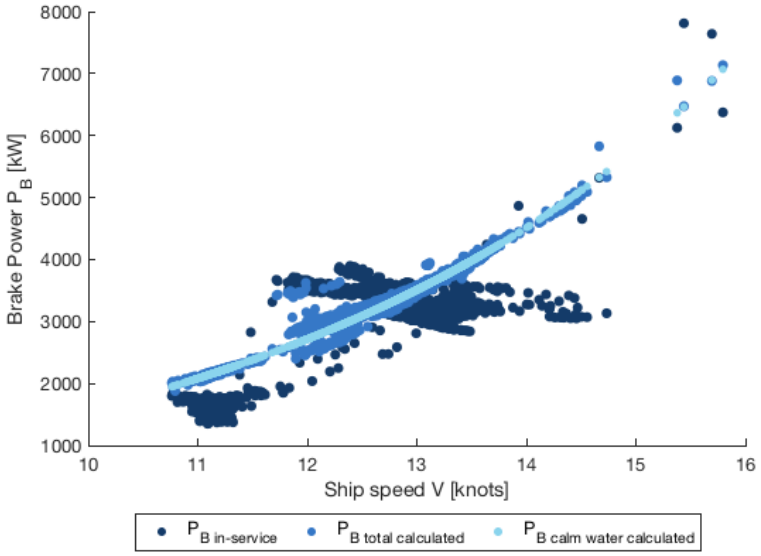

Figure 6.18: Validation of power prediction for Case 1 with in-service loading. In-service measurements and calculated results.

Added resistance module performance

Several combinations of methods to predict the added resistance in waves and wind are investigated. RMSE is computed for each combination and for the mean of all methods. As presented in Table 6.25, the RMSE of

the computed mean is 572.02 kW. Applying Kwon alone increases the error by 7%, to 610.83 kW. The most accurate prediction is obtained by applying STA-1 for wave resistance and Blendermann for wind resistance, improving the accuracy by 5% relative to the mean prediction. Figures 6.19a and 6.19b illustrate the most accurate and the least accurate prediction, respectively. There is a significant difference between the two, however, the other variations of RMSE are relatively small for the various combinations.

Table 6.25: RMSE for combinations of added resistance methods applied to Case 1 with in-service loading condition

Module combination	RMSE [kW]	Difference from 'mean of all methods'
Mean of all methods	572.02	-
Townsin & Kwon	610.83	7%
Mean wind + mean(STA-1, STA-2)	551.20	-4%
Mean wind + STA-1	550.24	-4%
Mean wind + STA-2	552.31	-3%
Mean wave + STAJIP wind	559.97	-2%
Mean wave + Blendermann	543.97	-5%
Best combination: STA-1 + Blendermann	**543.03**	**-5%**

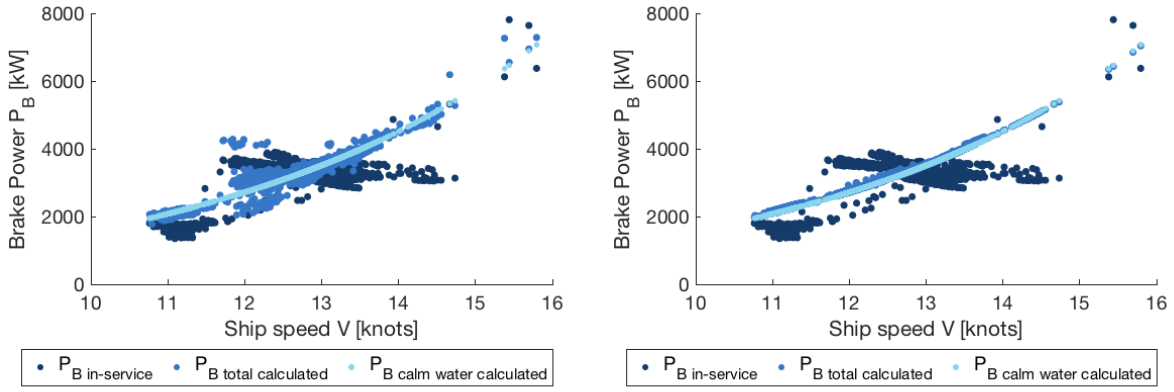

(a) STA-1 (wave) + Blendermann (wind)

(b) Townsin & Kwon (wind and waves combined)

Figure 6.19: The added resistance modules with highest accuracy (a) and lowest accuracy (b) in terms of RMSE

Effect of loading condition

For fleet-wide calculations, the exact in-service draught is unavailable. Sea-web only provides maximum draught, which is expected to affect the power predictions significantly. For Case 1, the the mean in-service draught is 7.91 m, and the maximum draught provided by Sea-web is 12.64 m. The maximum draught is applied to the calculations and the result is presented in Figure 6.20. The predicted power is overestimated, both relative to the in-service measurements and to the prediction on in-service draught. Table 6.26 presents the RMSE of the prediction, which is increased 197% relative to the in-service draught prediction. In this case, the loading condition affects the predicted power significantly more than the choice of added resistance method.

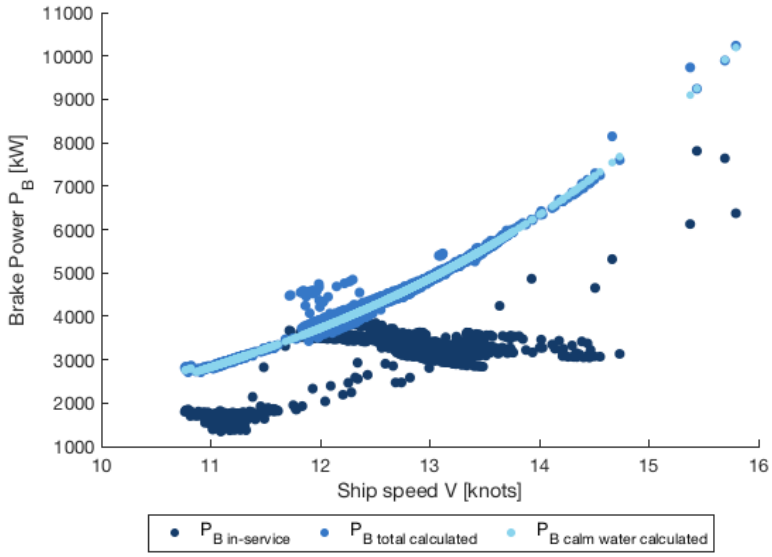

Figure 6.20: Validation of power prediction for Case 1 with maximum loading from Sea-web. In-service measurements and calculated results.

Table 6.26: Deviation of predicted power for in-service loading condition and for maximum loading condition

Loading condition	Draught	Added resistance calculation method	RMSE [kW]
In-service loading	7.91 m	Mean of all methods	572.02
Maximum loading	12.64 m	Mean of all methods	1699.30

6.6.2 Case 2: Container Ship

The voyage data of Case 2 include one month of measurements of ship speed, draught and power produced by the engines. In this case, the in-service displacement (and dwt) is not known. Therefore, the displacement is retrieved from Sea-web. The mean in-service draught is applied in the following calculations, together with the weather data variables from the voyage. Table 6.27 presents an overview of the weather characteristics. As displayed, the weather range from light conditions ($BN = 1$) to moderately strong conditions ($BN = 8$). It is observed that the maximum wave height does not correspond to typical values for $BN = 8$. In this case, the wind is measured onboard the ship, and may, therefore, include some effects of wind gusts. Both the wind and wave heading vary from head-to to following.

Table 6.27: In-service weather data range for Case 2

Parameter	Symbol	Range $[min, max]$	Unit
Significant wave height	H_s	[0.00,2.34]	$[m]$
Mean wave period	T_w	[0.10,14.00]	$[s]$
Relative mean wave direction	β_{wave}	[0.30, 180.0]	$[^\circ]$
True wind speed	U	[0.67,17.56]	$[m/s]$
Beauforts number	BN	[1,8]	$[-]$
Relative wind speed	U_{rel}	[0.15,24.41]	$[m/s]$
Relative wind direction	β_{wind}	[0.00,360.00]	$[^\circ]$

Figure 6.21 presents the measured brake power and the calculated power by the program. These results are calculated by applying the mean added resistance estimate. The predicted power is somewhat underestimated, but follows the trend of the measured power over the speed range. Even though the exact draught

is applied, the displacement is retrieved from Sea-web and is therefore probably overestimated. This is expected to overpredict the power, hence is not the reason for the underestimated result. A different reason may be that the container ship has significant growth of fouling or hull roughness contributing to the resistance. RMSE values are presented in the following.

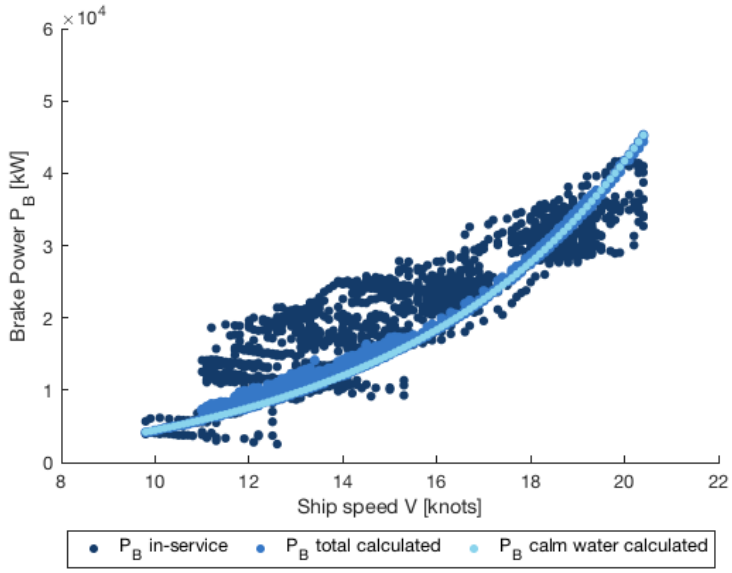

Figure 6.21: Validation of power prediction for Case 2 with in-service loading. In-service measurements and calculated results.

Added resistance module performance

Several combinations of methods to predict the added resistance in waves and wind are assessed. The RMSE is computed for each combination and for the mean of all methods. As presented in Table 6.28, the RMSE of the computed mean is 3,694.11 kW. Applying Kwon alone increases the error by 4%, to 3,827.74 kW. The most accurate prediction is obtained by applying STA-1 for wave resistance and STAJIP for wind resistance, improving the accuracy by 3% relative to the mean prediction. Figures 6.22a and 6.22b illustrate the most accurate and the least accurate prediction, respectively. Similar as for Case 1, there is a significant difference between the two, however, the other variations of RMSE are relatively small for the various combinations.

Table 6.28: RMSE for combinations of added resistance methods applied to Case 2 with in-service loading condition

Module combination	RMSE [kW]	Difference from 'mean of all methods'
Mean of all methods	3,694.11	-
Townsin & Kwon only	3,827.74	4%
Mean wind + mean(STA-1, STA-2)	3,615.02	-2%
Mean wind + STA-1	3,614.45	-2%
Mean wind + STA-2	3,628.23	-2%
Mean wave + STAJIP wind	3,586.54	-3%
Mean wave + Blendermann	3,650.42	-1%
Best combination: STA-1 + STAJIP wind	**3,585.89**	**-3%**

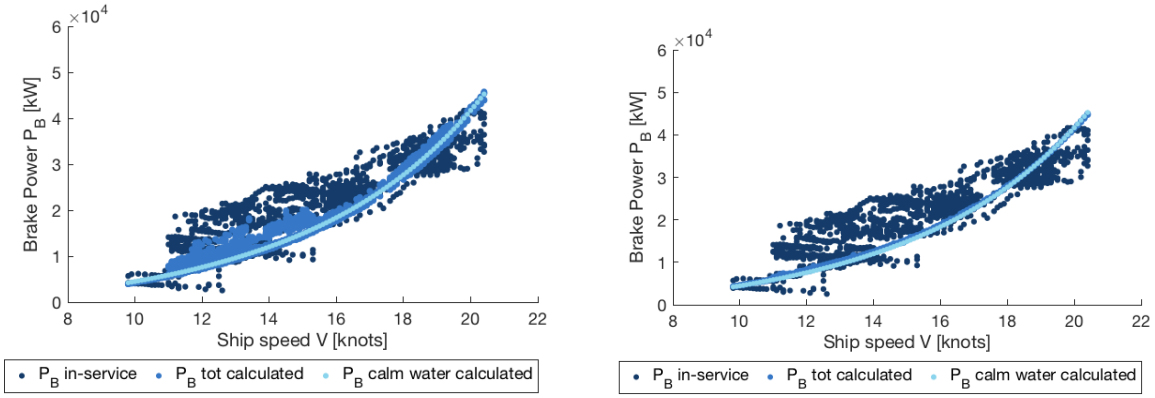

(a) STA-1 (wave) + STAJIP (wind)

(b) Townsin & Kwon (wind and waves combined)

Figure 6.22: The added resistance modules with highest accuracy (a) and lowest accuracy (b) in terms of RMSE

Effect of loading condition

The effect of varying loading conditions is not properly captured in this case, since the in-service displacement is unavailable. Even though the in-service draught is available, important parameters depend on the displacement such as the block coefficient and the wetted surface area. Therefore, a varying loading condition is not completely captured by only changing the draught. A power prediction is still computed for the maximum draught, presented in Figure 6.23.

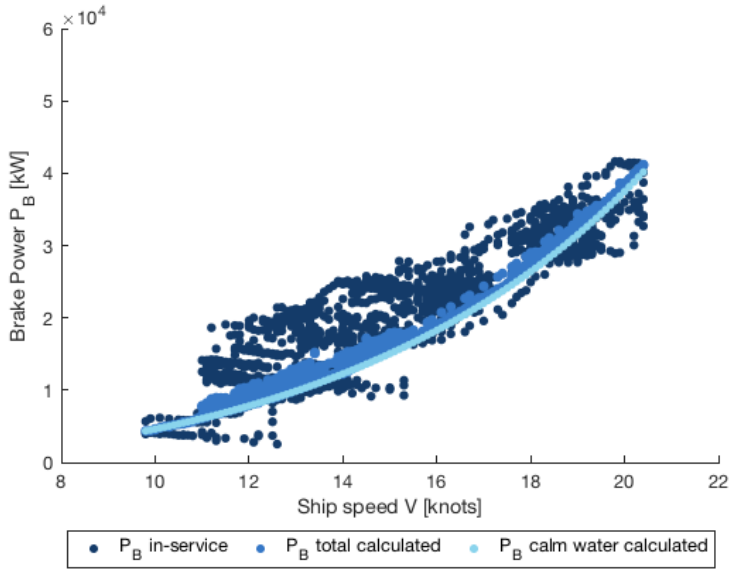

Figure 6.23: Validation of power prediction for Case 2 with maximum loading from sea-web. In-service measurements and calculated results.

In this case, the computed RMSE for the maximum loading is improved, as Table 6.29 displays. The reason for this may be that the overestimated draught contribute to increase the power which is initially underestimated, as discussed above. These results are, therefore, not considered to be significant.

Table 6.29: Deviation of predicted power for in-service loading condition and for maximum loading condition

Loading condition	Draught	Added resistance calculation method	RMSE [kW]
In-service loading	13.12 m	Mean of all methods	3,694.11
Maximum loading	15.52 m	Mean of all methods	3,367.78

6.7 Summary of Results and Validation

This section is dedicated to summarising the results from the validation of the new model. First, the results from the calm water power predictions are summarised, followed by the in-service predictions and finally, the parameter estimates. The objective is to give an overview of the performance of the program.

6.7.1 Performance of the Calm Water Resistance Methods

In the validation of the calm water power predictions, all methods are included for each case. However, not all methods are applicable, and Table 6.30 summarises the applicability. Holtrop-Mennen applies to all the cases (indicated in green), while Hollenbach only applies to three ships, and Guldhammer-Harvald to two. As most of the ships analysed are conventional vessel types, all methods were expected to apply. However, Case 2 (container ship), and Case 7 (bulk carrier) have ballast loading conditions which are outside the applicable area of Hollenbach. Further, the wellboat in Case 4 does not represent a conventional hull form.

Table 6.30: Applicable methods for Case 1 - Case 7

Case	Ship type	Hollenbach	Holtrop-Mennen	Guldhammer-Harvald
1	Cargo ship			
2	Container (13,000 TEU)			
3	Vehicles carrier			
4	Wellboat			
5	Chemical tanker			
6	Container (3,500 TEU)			
7	Bulk carrier			

In order to assess the accuracy of the calm water resistance methods, the results for exact input are evaluated, excluding any error of the parameter estimates. Table 6.31 presents the mean deviation and mean standard deviation for all cases. The mean deviation for all cases indicates whether the method on average underestimates or overestimates the results. Cancellation effects may not be captured in the final mean; however, the variability is expressed in terms of the standard deviation. The presented results include deviation of predicted calm water resistance, propulsive efficiency and final power. All methods are included, even in the cases where they are not applicable.

Hollenbach's mean resistance estimate is on average the most accurate with only 1% deviation, even though the method is not applicable for all the ships. Holtrop-Mennen follows with a mean deviation of 5%. Guldhammer-Harvald overestimate the resistance on average by 11%. This may be explained by the limited applicability of the modernised method, only applied to 3 out of 7 cases. Hollenbach's minimum estimate underestimate the resistance, on average by 8%. These large variations are cancelled out for the calculated mean, which on average deviates only 5%.

The propulsive efficiency is predicted within an accuracy of 3% for all the cases. This indicate that the estimated thrust and wake factors from the calm water methods are reasonably reliable and that the simplified Wageningen-B series perform well. As highlighted in the Table, Holtrop-Mennen and Hollenbach's estimates for the final predicted power are evidently the most accurate in the comparison.

Table 6.31: Mean deviation and mean std. deviation for the calculated resistance, propulsive efficiency and power. Results include all cases.

	Resistance		Propulsive efficiency		Power	
	Mean deviation	Std. deviation	Mean deviation	Std. deviation	Mean deviation	Std. deviation
Hollenbach (w/ mean resistance)	1%	4%	2%	2%	**-3%**	**5%**
Holtrop-Mennen	5%	5%	3%	2%	**2%**	**6%**
Guldhammer-Harvald	11%	6%	3%	2%	**11%**	**6%**
Calculated mean	5%	5%	2%	2%	**2%**	**5%**
Hollenbach (w/ min. resistance)	-8%	3%	3%	2%	**-16%**	**4%**

The results in Table 6.32 only include the applicable cases. Since Holtrop-Mennen is valid for all cases, these results are equal as for Table 6.31. However, for Hollenbach, both the mean and the minimum predictions are improved. Guldhammer-Harvald's average deviations increase significantly. The reason may be that Guldhammer-Harvald is only valid for two cases, Case 1 (cargo ship) and Case 5 (chemical tanker), and both cases are only valid to analyse with the old Guldhammer-Harvald method. The modernised corrections by Kristensen et al. (2017) are therefore not applied in these cases.

Table 6.32: Mean deviation and mean std. deviation for the calculated resistance, propulsive efficiency and power. Results only include cases where the respective methods are valid.

	Resistance		Propulsive efficiency		Power	
	Mean deviation	Std. deviation	Mean deviation	Std. deviation	Mean deviation	Std. deviation
Hollenbach (w/ mean resistance)	1%	3%	0%	1%	**0%**	**3%**
Holtrop-Mennen	5%	5%	3%	2%	**2%**	**6%**
Guldhammer-Harvald	22%	4%	-8%	1%	**31%**	**5%**
Calculated mean	7%	3%	-1%	1%	**8%**	**3%**
Hollenbach (w/ min. resistance)	-3%	3%	0%	1%	**-13%**	**3%**

To summarise these results, Hollenbach's mean estimate is the most accurate overall, followed by Holtrop-Mennen. Both Guldhammer-Harvald and Hollenbach's minimum power predictions deviate significantly, on average more than 10%.

6.7.2 Performance of the In-service Prediction

The in-service power predictions for Case 1 (cargo ship) and Case 2 (13,000 TEU container ship) correspond relatively well to the voyage measurements when the correct loading condition is applied. As demonstrated for Case 1, the effect of varying the added resistance methods is less significant than varying the loading condition. However, when comparing the individual methods, Townsin & Kwon underestimates the added resistance relative to the other methods. The application of Townsin & Kwon alone only increases the resistance slightly from the calm water resistance.

In Case 2, the calculated power is underestimated relative to the measured power. One reason may be the effects of roughness or fouling on the hull, which should be investigated further in future work. Another reason may be that the calm water power is underpredicted for the ship in this case. The latter is difficult to verify without more information from model tests for the ship.

6.7.3 Performance of the Parameter Estimates

This section presents the deviations of the results when the parameter estimates are included in the computations. Mean deviation and standard deviation for the computed resistance, propulsive efficiency and final power are presented. In addition, the mean deviation of each parameter estimate is calculated. The objective

is to assess whether errors in the parameter estimates significantly influences the results.

Table 6.33 displays the mean deviation of each parameter estimate in the case study. The most significant errors include the transverse projected area, the propeller diameter, effects of trim on the draught, and the wet surface area.

Table 6.33: Mean deviation and mean standard deviation of the estimated parameters

Parameter	Symbol	Unit	Mean deviation	Std. deviation
Length of waterline	L_{WL}	$[m]$	0 %	2 %
Draught fore	T_F	$[m]$	9 %	18 %
Draught aft	T_A	$[m]$	-5 %	9 %
Block coefficient	C_B	$[-]$	0 %	0 %
Wetted surface area	S	$[m^2]$	-4 %	7 %
Midship section coefficient	C_M	$[-]$	0 %	1 %
Prismatic coefficient	C_P	$[-]$	0 %	0 %
Transverse projected area	A_{VT}	$[m^2]$	-3 %	45 %
Propeller diameter	D_p	$[m]$	-8 %	29 %

While the fore and aft draught deviations are due to the assumption of zero trim, the other parameter estimates are based on empirical formulas. The deviations indicate these formulas are not reliable for all ship types. However, it should be noted that the propeller diameter is estimated based on the maximum draught, and all the analysed ships have design draught or ballast draught in the case study. This is a weakness of the calculations in the case study. However, the parameter estimate is intended to supplement Sea-web parameters, which applies maximum draught. Table 6.34 outlines the results obtained with the estimated parameters. All cases are included, even when the calm water method is not applicable.

Table 6.34: Mean deviation and mean std. deviation for the calculated resistance, propulsive efficiency and power. Results include all cases with estimated parameters.

	Resistance		Propulsive efficiency		Power	
	Mean deviation	Std. deviation	Mean deviation	Std. deviation	Mean deviation	Std. deviation
Hollenbach (w/ mean resistance)	-3%	5%	-1%	2%	**2%**	**5%**
Holtrop-Mennen	2%	5%	-1%	2%	**10%**	**6%**
Guldhammer-Harvald	6%	5%	-8%	2%	**17%**	**7%**
Calculated mean	2%	4%	-3%	2%	**8%**	**6%**
Hollenbach (w/ min. resistance)	-16%	3%	-1%	2%	**-12%**	**4%**

Compared to the results with exact input parameters, the tendency is that most of the predictions are less accurate. However, apart from Hollenbach's minimum estimate, all the method's resistance predictions are still within 6% on average. Holtrop-Mennen and Guldhammer-Harvald's power prediction deviates signifcantly more, 10% and 17% respectively. In contrast, the deviation of Hollenbach's mean and minimum power estimate is improved, to 2 % and -12% on average. The propulsive efficiency is generally underestimated by including the parameter estimates. As demonstrated in the case study, deviations in the propeller diameter affects the propulsive efficiency considerably.

6.8 Comparing the New Model to the Current MariTEAM Model

This section is dedicated to comparing the performance of the new model to the current MariTEAM model. Power predictions are computed by both methods, for all the ships in the case study. Both methods include

their respective parameter estimates. The current MariTEAM model is implemented as outlined previously in Section 4.2.

6.8.1 Case 1: Cargo Ship

Case 1 is a cargo ship with main particulars as listed previously in Table 6.3. The validation data comprise full-scale power predictions at design draught from a model test report, and one month of in-service data. Calculated results are presented in the following, both by the new model and the current MariTEAM model.

Calm-water power prediction

Figure 6.24 presents the computed power together with the model test results. As displayed in Table 6.35, the current MariTEAM model's prediction overestimates the power by 22% on average, and deviates largely from the minimum resistance estimate by Hollenbach in the new model. These two estimates were expected to be similar, since the current MariTEAM model applies Hollenbach's minimum resistance estimate. However, in the new model, Hollenbach is modified as presented in Section 3.1.3 and the resistance prediction is therefore different. Further, the propulsive efficiency is underestimated in this case by the current MariTEAM model, contributing to an increased power.

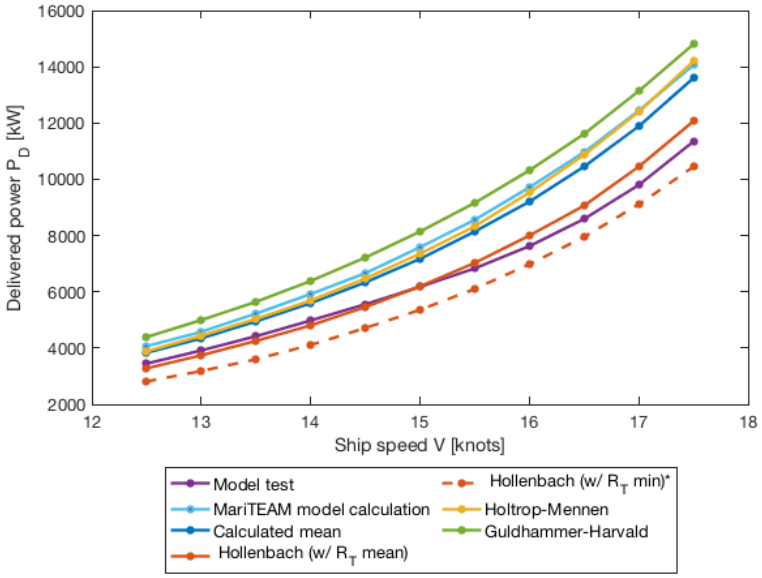

Figure 6.24: Comparison of power predicted by the model test, new model, and the current MariTEAM model for Case 1 (parameter estimates included).

Table 6.35: Deviation of power predicted by the model test, new model, and the current MariTEAM model for Case 1 (parameter estimates included).

Method	Mean deviation	Std. deviation	Applicable
Hollenbach (w/ mean resistance)	1%	5%	yes
Holtrop-Mennen	19%	6%	yes
Guldhammer-Harvald	31%	3%	yes
Calculated mean	16%	4%	yes
Hollenbach (w/ minimum resistance)*	-13%	5%	yes
Current MariTEAM model	22%	4%	yes

In-service power prediction

Figures 6.25a and 6.25b present the in-service power prediction by both models. In both cases the predicted power follows the trend of the in-service measurements. Similar to the calm water results, the current MariTEAM model overpredicts the power relative to the new model. Further, Townsin & Kwon predicts less added resistance than the methods implemented in the new model. Table 6.36 shows that the RMSE is higher for the current MariTEAM model than the new model. Hence, the accuracy of the predicted added resistance is improved for this case.

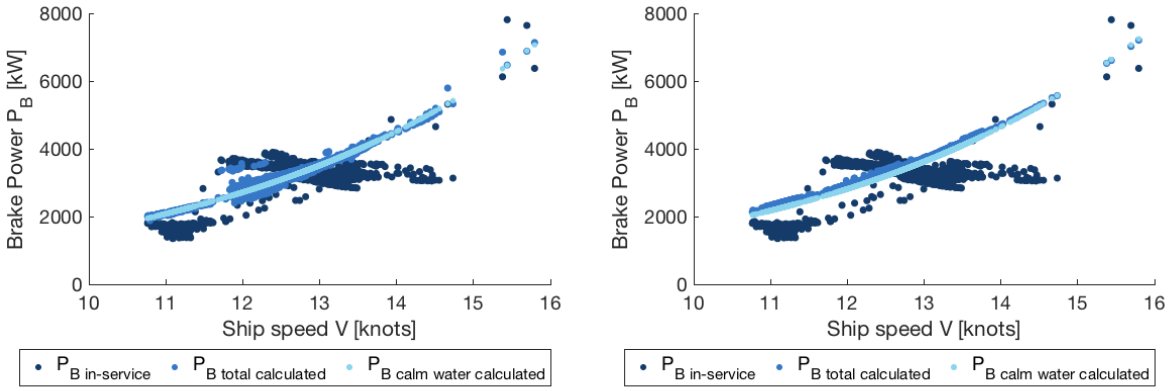

(a) New model **(b)** Current MariTEAM model

Figure 6.25: Comparison of measured in-service power to the power predicted by the new model (a) and the current MariTEAM model (b) for Case 1

Table 6.36: Deviation of power measured in-service, predicted by the new model, and the current MariTEAM model for Case 1.

Model	Added resistance calculation method	RMSE [kW]
New model	Mean of all methods	572.02
Current MariTEAM model	Townsin and Kwon	713.03

6.8.2 Case 2: Container Ship (13,000 TEU)

Case 2 is a 13,000 TEU container ship with main particulars as listed previously in Table 6.6. The validation data comprise calm water power predictions at heavy ballast draught from a sea trial report, and one month of in-service data. Calculated results are presented in the following, both by the new model and the current MariTEAM model.

Calm-water power prediction

Figure 6.26 presents the computed power together with the sea trial results. Only Holtrop-Mennen is valid to apply in this case. The results are presented without any correction of the propeller diameter, which is underestimated by 50 % in the new model due to the surface piercing propeller. As discussed previously, this result in a largely underestimated propeller efficiency, and correspondingly an overpredicted power.

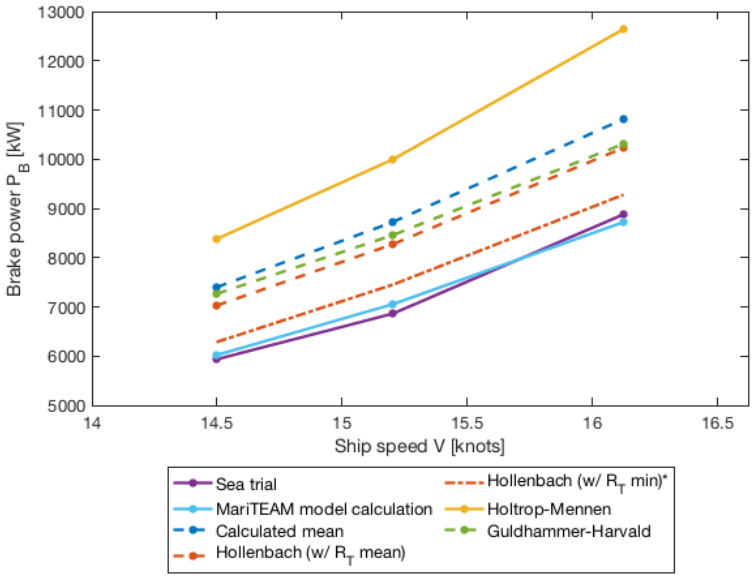

Figure 6.26: Comparison of power predicted by the sea trial, new model, and the current MariTEAM model for Case 2 (parameter estimates included).

As Table 6.37 displays, the prediction by the current MariTEAM model is significantly more accurate than by the new model. The current model applies a constant value for the propeller efficiency, resulting in an improved prediction of the propulsive efficiency, which is independent of the propeller diameter.

Table 6.37: Deviation of power predicted by the sea trial, new model, and the current MariTEAM model for Case 2 (parameter estimates included).

Method	Mean deviation	Std. deviation	Applicable
Hollenbach (w/ mean resistance)	34%	9%	no
Holtrop-Mennen	59%	17%	yes
Guldhammer-Harvald	60%	13%	no
Calculated mean	49%	13%	no
Hollenbach (w/ minimum resistance)*	19%	9%	no
Current MariTEAM model	-9%	5%	no

Calm-water resistance prediction

Due to the relatively large deviations in predicted power between the two models, the predicted resistance is further investigated. Figure 6.27 presents the computed resistance and the sea trial resistance. In this case, the predicted resistance by the current MariTEAM model and by Hollenbach's minimum procedure in the new model correspond more closely. As Table 6.38 demonstrates, Hollenbach's mean estimate gives the most accurate resistance prediction. The results indicate that the current MariTEAM model's prediction of the propulsive efficiency is better than the Wageningen-B procedure in cases where the propeller diameter is inaccurately estimated.

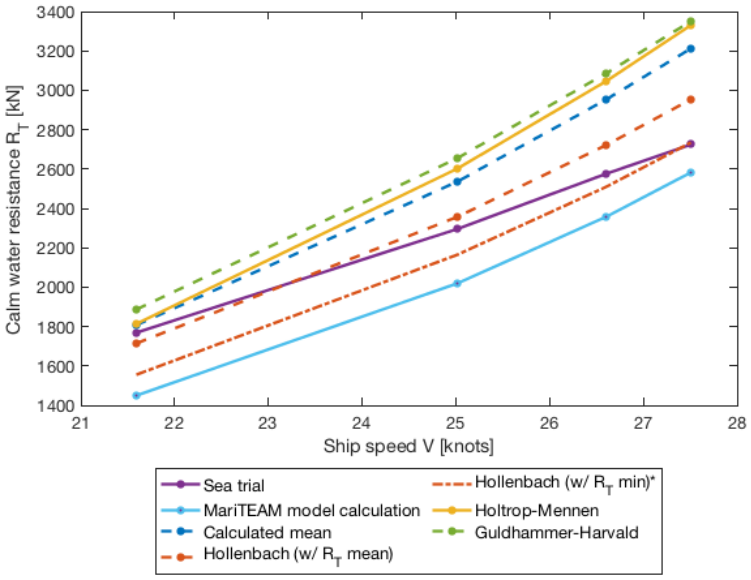

Figure 6.27: Comparison of calm water resistance predicted by the sea trial, new model, and the current MariTEAM model for Case 2 (parameter estimates included).

Table 6.38: Deviation of calm water resistance predicted by the sea trial, new model, and the current MariTEAM model for Case 2 (parameter estimates included).

Method	Mean deviation	Std. deviation	Applicable
Hollenbach (w/ mean resistance)	3%	5%	no
Holtrop-Mennen	14%	9%	yes
Guldhammer-Harvald	16%	7%	no
Calculated mean	11%	7%	no
Hollenbach (w/ minimum resistance)*	-5%	5%	no
Current MariTEAM model	-11%	5%	no

In-service power prediction

Figures 6.28a and 6.28b present the in-service power prediction by both models. In both cases the predicted power follows the trend of the in-service measurements, although somewhat underestimated. Similar to Case 1, Townsin & Kwon predicts less added resistance than the methods implemented in the new model. Table 6.39 shows that the RMSE is higher for the current MariTEAM model relative to the new model.

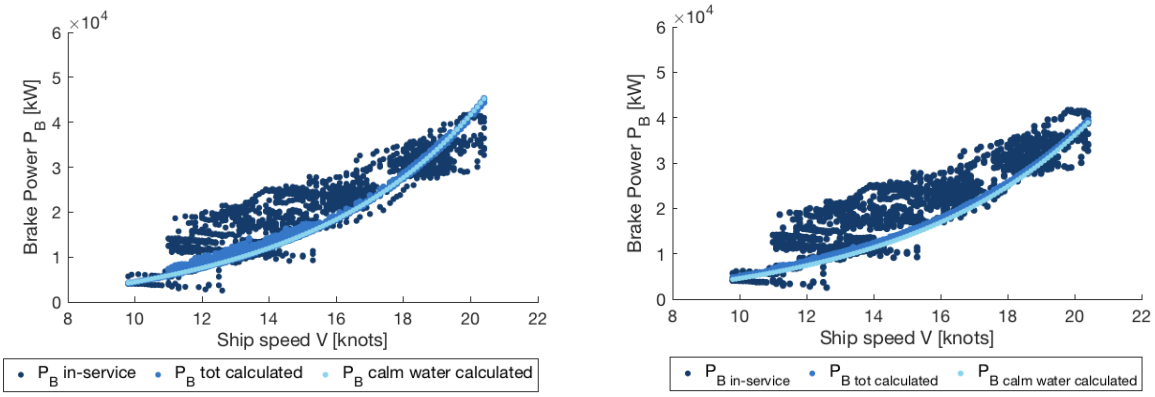

(a) New model

(b) Current MariTEAM model

Figure 6.28: Comparison of measured in-service power to the power predicted by the new model (a) and the current MariTEAM model (b) for Case 2

Table 6.39: Deviation of power measured in-service, predicted by the new model, and the current MariTEAM model for Case 2.

Model	Added resistance calculation method	RMSE [kW]
New model	Mean of all methods	3694.11
Current MariTEAM model	Townsin and Kwon	4185.94

6.8.3 Case 3: Vehicles Carrier

Case 3 is a vehicles carrier with main particulars as listed previously in Table 6.9. The validation data comprise full-scale power predictions at design draught from a model test report. Figure 6.29 presents the computed power by both models, together with the model test results. Only Holtrop-Mennen and Hollenbach are valid in this case.

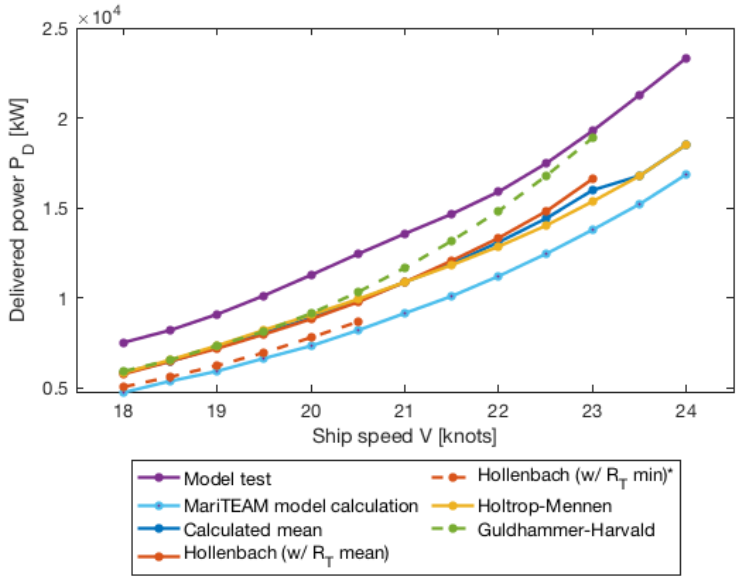

Figure 6.29: Comparison of power predicted by the model test, new model, and the current MariTEAM model for Case 3 (parameter estimates included).

In this case, the current MariTEAM model prediction is close to the Hollenbach minimum prediction. Both underestimate the power, on average by 32 % and 31 % as displayed in Table 6.40. As discussed in Section 6.5.3, the wet surface is underestimated by 15.4% in this case, which underestimates the resistance. Both the current MariTEAM model and the new model applies the same parameter estimate for the wetted surface.

Table 6.40: Deviation of power predicted by the model test, new model, and the current MariTEAM model for Case 3 (parameter estimates included).

Method	Mean deviation	Std. deviation	Applicable
Hollenbach (w/ mean resistance)	-19%	3%	yes
Holtrop-Mennen	-20%	1%	yes
Guldhammer-Harvald	-14%	7%	no
Calculated mean	-20%	2%	yes
Hollenbach (w/ minimum resistance)	-31%	1%	yes
Current MariTEAM model	-32%	3%	yes

6.8.4 Case 4: Wellboat

Case 4 is a wellboat with main particulars as listed previously in Table 6.12. The validation data comprise full-scale power predictions at design draught from a model test report. Figure 6.30 presents the computed power by both models, together with the model test results. Only Holtrop-Mennen is valid in this case.

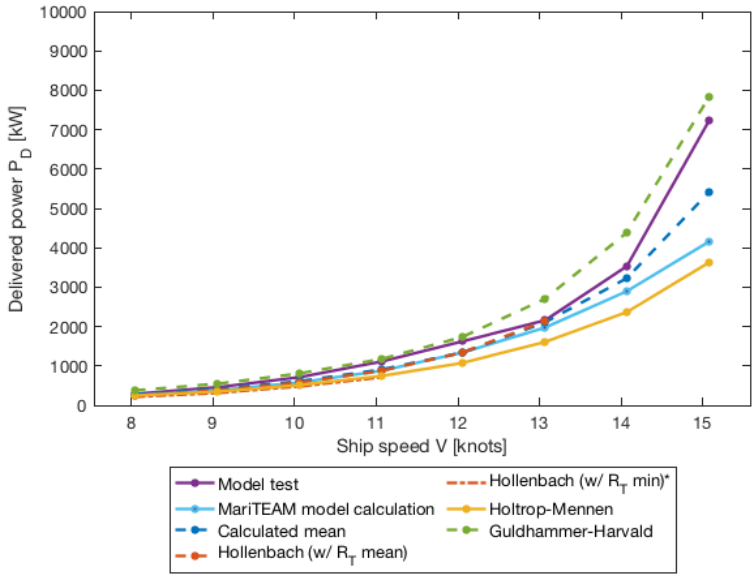

Figure 6.30: Comparison of power predicted by the model test, new model, and the current MariTEAM model for Case 4 (parameter estimates included).

In this case, all predictions show significant deviations, as presented in Table 6.41. As discussed previously, the wellboat represents the least conventional ship type in the study. The wetted surface area is underestimated in both the new and the current MariTEAN model. Note that the froude limitation range is not applied in the current MariTEAM model.

Table 6.41: Deviation of power predicted by the model test, new model, and the current MariTEAM model for Case 4 (parameter estimates included).

Method	Mean deviation	Std. deviation	Applicable
Hollenbach (w/ mean resistance)	-14%	7%	no
Holtrop-Mennen	-30%	10%	yes
Guldhammer-Harvald	17%	9%	no
Calculated mean	-12%	8%	no
Hollenbach (w/ minimum resistance)	-32%	3%	no
Current MariTEAM model	-18%	11%	no

6.8.5 Case 5: Chemical Tanker

Case 5 is a chemical tanker with main particulars as listed previously in Table 6.15. The validation data comprise full-scale power predictions at design draught from a model test report. Figure 6.31 presents the computed power by both models, together with the model test results. All methods are applicable in this case.

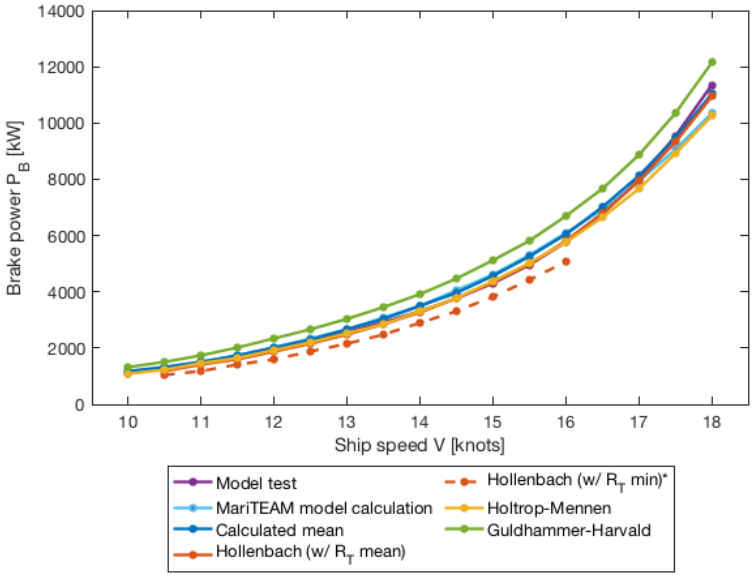

Figure 6.31: Comparison of power predicted by the model test, new model, and the current MariTEAM model for Case 5 (parameter estimates included).

In this case, the current MariTEAM model prediction is significantly more accurate than the minimum prediction by Hollenbach. As displayed in Table 6.42, the average deviation is 3 %, against -15 % for Hollenbach's minimum estimate. The reason that these results deviate, is the underestimated propulsive efficiency in the current MariTEAM model. The current model underestimates the resistance by 5%, and since the propulsive efficiency also is underestimated by 9 %, the final power prediction increases.

Table 6.42: Deviation of power predicted by the model test, new model, and the current MariTEAM model for Case 5 (parameter estimates included).

Method	Mean deviation	Std. deviation	Applicable
Hollenbach (w/ mean resistance)	-2%	3%	yes
Holtrop-Mennen	-2%	3%	yes
Guldhammer-Harvald	16%	4%	yes
Calculated mean	3%	3%	yes
Hollenbach (w/ minimum resistance)*	-15%	3%	yes
Current MariTEAM model	3%	4%	yes

6.8.6 Case 6: Container Ship (3,500 TEU)

Case 6 is a 3,500 TEU container ship with main particulars as listed previously in Table 6.18. The validation data comprise full-scale power predictions at design draught from a model test report. Figure 6.32 presents the computed power by both models, together with the model test results. Only Holtrop-Mennen is valid in this case.

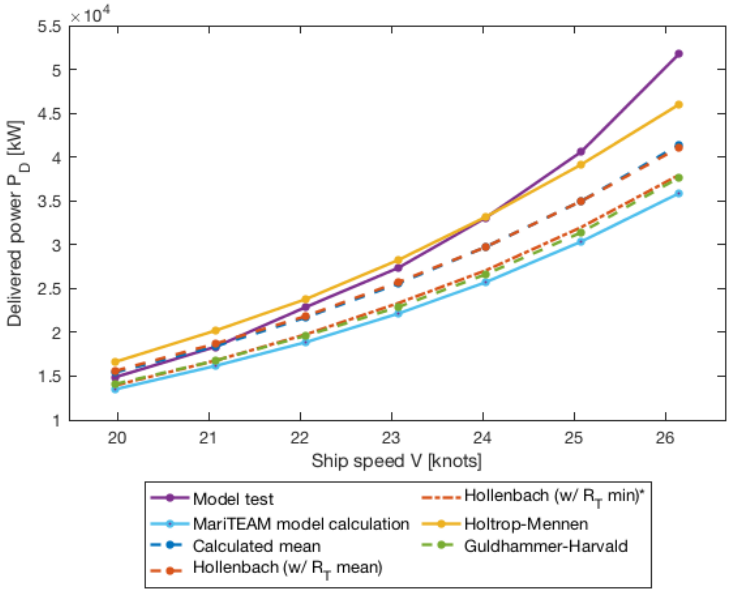

Figure 6.32: Comparison of power predicted by the model test, new model, and the current MariTEAM model for Case 6 (parameter estimates included).

As Table 6.43 presents, the prediction by the current MariTEAM model is close to the minimum Hollenbach prediction. Both predictions underestimate the power significantly, on average by 17 % and 19 % respectively.

Table 6.43: Deviation of power predicted by the model test, new model, and the current MariTEAM model for Case 6 (parameter estimates included).

Method	Mean deviation	Std. deviation	Applicable
Hollenbach (w/ mean resistance)	-7%	8%	no
Holtrop-Mennen	2%	6%	yes
Guldhammer-Harvald	-15%	6%	no
Calculated mean	-7%	7%	no
Hollenbach (w/ minimum resistance)*	-17%	6%	no
Current MariTEAM model	-19%	7%	no

6.8.7 Case 7: Bulk Carrier

Case 7 is a bulk carrier with main particulars as listed previously in Table 6.21. The validation data comprise calm water power predictions at heavy ballast draught from a sea trial report. Calculated results are presented in Figure 6.33, both by the new model and the current MariTEAM model. Only Holtrop-Mennen is valid to apply in this case. The results are presented without any correction of the propeller diameter, which is underestimated by 37.2 % in the new model. Similar to Case 2, this result in a largely underestimated propeller efficiency, and correspondingly an overpredicted power.

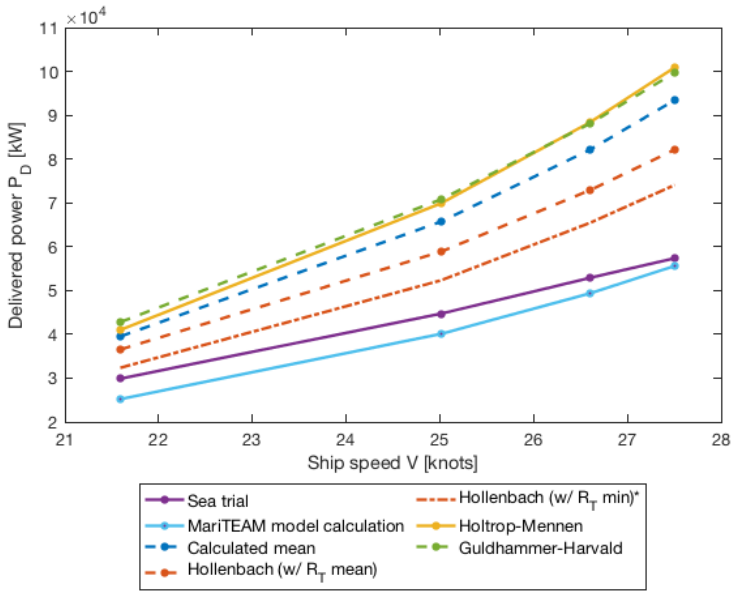

Figure 6.33: Comparison of power predicted by the sea trial, new model, and the current MariTEAM model for Case 7 (parameter estimates included).

As Table 6.44 displays, the prediction by the current MariTEAM model is significantly more accurate than by the new model, on average with 1 % deviation. The current MariTEAM model predicts the propulsive efficiency with less error, as the calculation is independent of propeller diameter.

Table 6.44: Deviation of power predicted by the sea trial, new model, and the current MariTEAM model for Case 7 (parameter estimates included).

Method	Mean deviation	Std. deviation	Applicable
Hollenbach (w/ mean resistance)	18%	3%	no
Holtrop-Mennen	43%	2%	yes
Guldhammer-Harvald	21%	4%	no
Calculated mean	25%	3%	no
Hollenbach (w/ minimum resistance)	6%	2%	no
* Not included in the calculated mean			
Current MariTEAM model	1%	2%	no

6.8.8 Summary of Comparison

Table 6.45 summarises the mean deviations for Case 1-7. The table include all results, even when the respective methods are not applicable. When comparing the resistance predictions, the current MariTEAM model is close to the minimum prediction by Hollenbach. This corresponds with the expectation, since the current MariTEAM model applies the Hollenbach minimum prediction, although not the modified version as described in Section 3.1.3.

In the current MariTEAM model, the propulsive efficiency is computed by the empirical formula by Lindstad et al. (2011). On average for the seven cases, the prediction deviates by -5%, which is less accurate than the Wageningen B-series estimate with Hollenbach minimum prediction. However, Case 2 and Case 7 demonstrate that the formula by Lindstad et al. (2011) is more accurate than the Wageningen B-series in the cases where the propeller diameter is inaccurately estimated. The propulsive efficiency predictions in the new model is not as reliable for surface piercing propellers or ballast draught conditions.

The final power predicted by the current MariTEAM model deviates on average by -7%, which is more accurate than the prediction by Hollenbach's minimum estimate, and less accurate than Hollenbach's mean prediction. In some of the cases, the current MariTEAM model benefits from underpredicting the propulsive efficiency, since it results in an increased power when the resistance is underestimated. This cancellation effect may improve the final power prediction, although it is not considered to increase the reliability of the results.

Table 6.45: Deviations for the calculated resistance, propulsive efficiency and power. Results include all cases with estimated parameters, for the new model and the current MariTEAM model.

	Resistance		Propulsive efficiency		Power	
	Mean deviation	Std. deviation	Mean deviation	Std. deviation	Mean deviation	Std. deviation
Hollenbach (w/ mean resistance)	-3%	5%	-1%	2%	**2%**	**5%**
Holtrop-Mennen	2%	5%	-1%	2%	**10%**	**6%**
Guldhammer-Harvald	6%	5%	-8%	2%	**17%**	**7%**
Calculated mean	2%	4%	-3%	2%	**8%**	**6%**
Hollenbach (w/ min. resistance)	-16%	3%	-1%	2%	**-12%**	**4%**
Current MariTEAM model	-13%	5%	-5%	4%	**-7%**	**5%**

Chapter 7

Discussion

This thesis has identified, developed, and validated a ship powering performance method suitable for the MariTEAM model. The current state of knowledge in the field of global fleet-wide power predictions has been reviewed. In line with the literature, various empirical methods are implemented in the model. The new method requires few input parameters and can predict the propulsion power in realistic sea states, for a wide range of ships in the fleet.

7.1 The New Performance Prediction Method

Based on a comprehensive literature study, a wide range of empirical methods are reviewed and narrowed down to the most relevant. These are included in the model, which is subdivided into five main modules:

- Module 1: Estimate missing input parameters
- Module 2: Calm water resistance
- Module 3: Added resistance in wind and waves
- Module 4: Propulsive efficiency
- Module 5: Final power

Three calm water resistance methods are considered to be suitable for fleet-wide calculations today, including Hollenbach, Holtrop-Mennen, and the modernised Guldhammer-Harvald by Kristensen et al. (2017). Each method is valid for ships with characteristics within a defined range. Module 2 returns the calm water resistance as an average of the valid methods, which is based on the assumption that the three methods are equally reliable. The work presented by Tillig (2020) and Kristensen et al. (2017) forms the basis for this assumption. Both studies present power predictions of good accuracy by the application of Hollenbach and the updated Guldhammer-Harvald procedure. Besides, Holtrop-Mennen is widely applied in the literature and represents the method with the greatest applicable range. As Chapter 5 demonstrates, only 53.4% of the fleet can be analysed by either Hollenbach or Guldhammer-Harvald, while the number of ships increases to 72.8 % if Holtrop-Mennen is included. These numbers include the applicable range defined in the original Guldhammer-Harvald method. The updated Guldhammer-Harvald procedure by Kristensen et al. (2017) only applies to tankers, bulk carriers and container ships, which is currently not reflected in the defined valid range. This is considered a weakness in the model, although easy to improve in further work.

Module 3 includes Townsin & Kwon, as well as two methods to predict added resistance in waves, STAWAVE-1 and -2, and two methods to predict added resistance in wind, STAJIP wind and Blendermann. Townsin & Kwon represents the most straightforward method and applies to all ships and sea states without restrictions, which is suitable for fleet-wide calculations. However, the method calculates a combined added resistance in wind and waves based on only the Beaufort number as an environmental parameter. Significant resistance contributions from large superstructures or wave-induced motions are not captured; therefore, additional methods are implemented. MARIN (2006) presents accurate predictions of added wave resistance for both STAWAVE methods. STA-JIP wind is recommended for modern ships in ISO 15016, and Blendermann applies to an extensive range of ship types. The average added resistance from these methods is expected to provide a reliable prediction. However, the accuracy of the prediction depends on accurate input parameters, which has proven to be a challenge. STA-1 requires the length of the bow to 95 % of the maximum breadth on the

waterline, L_{BWL}, which is difficult to determine based on limited input. In the current work, comparison ships are applied to estimate the value; however, a suggestion for further work is to develop a parameter estimate based on typical hull forms within the ship types.

7.2 Validation Results

A validation study, including seven cases, has been conducted for the new model. The predicted power for each ship is compared to the actual ship power from model tests, sea trials or in-service measurements. Model test reports include detailed information on the ship powering performance for various loading conditions, and represent the most reliable validation data source for calm water power predictions. Model test reports are available for five out of seven cases, and sea trial reports are applied for the two remaining cases. The sea trial reports contain fewer details about hull and propeller performance, relative to model test reports. Also, the trials are performed on heavy ballast loading, which is an unconventional loading condition for ships in the fleet. Therefore, model test reports serve as a significantly more solid validation data source than sea trial reports.

7.2.1 Calm Water Powering Performance

The study evaluates the performance of each method implemented in the model as well as the parameter estimates. In order to assess the accuracy of the calm water resistance methods, the results for exact input are evaluated, excluding any error of the parameter estimates. The computed propulsive efficiency was on average, predicted within 3% and with a mean standard deviation of 2% for all the cases analysed. This indicates that the Wageningen B-series procedure is highly reliable when the propeller diameter is known. Further, the power predictions reflect the performance of the calm water resistance prediction, since errors in the propulsive efficiency are small. Table 7.1 summarises the mean deviation and mean standard deviation for the calculated power in the study. The first column includes all cases, while the second only includes cases where the particular method was applicable.

Table 7.1: Mean deviation and mean std. deviation for the calculated power (Results are computed with exact input parameters).

	All cases		Valid cases		
	Mean deviation	Std. deviation	Mean deviation	Std. deviation	No. of valid cases
Hollenbach (w/ mean resistance)	-3%	5%	0%	3%	3
Holtrop-Mennen	2%	6%	2%	6%	7
Guldhammer-Harvald	11%	6%	31%	5%	2
Calculated mean	2%	5%	8%	3%	3
Hollenbach (w/ min. resistance)	-16%	4%	-13%	3%	3

Holtrop-Mennen was the only method applicable to all the cases. On average, Holtrop-Mennen's power prediction deviates 2% with a standard deviation of 6% for all the cases. Hollenbach was only applicable to three cases, and for the particular cases, Hollenbach's mean power prediction deviates on average by 0%, with a standard deviation of 3%. If Hollenbach's mean power predictions are evaluated for all the seven cases, the average deviation is -3% with a standard deviation of 5%. These results demonstrate that both methods are highly accurate, although the number of cases is too few to make any definite conclusions. Hollenbach's minimum power prediction deviates on average -13% for the three applicable cases, and -16% for all the cases in the study. As expected, the mean prediction by Hollenbach is more accurate, and the results confirm the decision of not including the minimum estimate in the calculated mean.

Guldhammer-Harvald's power prediction was only valid for two cases and deviated on average by 31% with a standard deviation of 5% for the respective cases. However, the updated Guldhammer-Harvald did not apply

to the particular ship types (cargo ships and chemical tankers). Hence the corrections by Kristensen et al. (2017) are not applied in the calculations. The results indicate that the original Guldhammer-Harvald method significantly overestimates the power. The updated Guldhammer-Harvald procedure applies to the ship types in Case 1, 6 and 7, the two container ships and the bulk carrier. For these cases, the average deviation of the predicted power is -8% with an average standard deviation of 5%. Hence there is a significant effect of including the modernised corrections in the procedure. Although the results are underestimated, the deviation is reduced relative to the original method. However, both the container ships and the bulk carrier have ship dimensions outside the valid range for Guldhammer-Harvald. As a result, the modernised procedure did not apply to any of the ships in the case study.

There were only three cases where more than one calm water method was applicable, and the mean power prediction was calculated. On average, for the respective cases, the deviation is 8% with a standard deviation of 3%. The inclusion of Guldhammer-Harvald contribute to significant deviations in the calculated mean, and as a result, the individual performance of Hollenbach (mean) and Holtrop-Mennen is better. The results of the case study suggest that Guldhammer-Harvald is less reliable than Hollenbach and Holtrop-Mennen, even with the corrections by Kristensen et al. (2017). Based on these results, it should be considered to exclude the method, or at least only include the updated procedure restricted to tankers, bulk carriers and containers. This is expected to increase the accuracy of the predictions. Further, excluding Guldhammer-Harvald from the model will not affect the applicable range for fleet-wide calculations.

Overall, Hollenbach (mean) and Holtrop-Mennen provide accurate results and can apply to a large range of ships, 72.8% of the current fleet. Hollenbach includes the most restricted applicable range, despite this, the method provides accurate predictions for the cases outside the valid range. The valid range for ship dimensions defined by Hollenbach (1997) correspond to the mean value of the ships analysed, ± 1.5 standard deviation. In future work, it may be reasonable to increase the range and allow for larger applicability. The mean powering prediction will be further improved by excluding Guldhammer-Harvald, although it may be reasonable to only apply Hollenbach (mean) and use Holtrop-Mennen in cases where Hollenbach is not applicable.

The performance of the parameter estimates influences the power predictions significantly in the case study. Among the estimated parameters, the propeller diameter deviates on average -8 % with a standard deviation on 29% and introduces the most substantial error in the calculations. In cases where the propeller diameter is significantly underestimated, the propulsive efficiency is underpredicted, and the final power prediction is correspondingly overestimated. This is a weakness in the model. However, the estimation formulas for propeller diameter are based on maximum draught, and in the case study, all vessels have design draught or ballast draught. Fleet-wide calculations apply maximum draught from Sea-web, which is expected to provide less underpredicted propeller diameter estimates.

7.2.2 In-service Powering Performance

The validation against in-service measurements demonstrates good prediction accuracy for exact loading conditions, with some variations between the different added resistance methods. The computed RMSE shows that the applied loading condition affects the power predictions more than varying the added resistance methods. Sea-web provides maximum draught and displacement for all ships, which is not expected to be a representative loading condition for the fleet at all times. For future work, this should be further investigated and corrected to achieve accurate fleet-wide powering predictions.

For both the cargo ship and the container ship, Townsin & Kwon underestimates the added resistance. The power predictions are improved in both cases by including the additional methods to predict resistance in wind and waves. In the model, the mean resistance is computed for the valid methods, and the RMSE for each combination shows that the prediction accuracy is improved by excluding Townsin & Kwon. A recommendation for improving the model is to exclude Townsin & Kwon, and further develop a parameter estimate for L_{BWL} in STA-1 to apply this method. Besides, the parameter estimate for the transverse projected area A_{VT} should be improved as it shows a significant variability, with an average deviation of -3% and standard deviation of 45%.

7.2.3 Comparing the New and Current MariTEAM model

The powering performance of the new and current MariTEAM model is compared, including the parameter estimates. Table 6.45 summarises the mean deviations for resistance, propulsive efficiency and power in the validation study. As expected, Hollenbach's minimum resistance prediction is close to the current MariTEAM model's. However, for most cases, the propulsive efficiency is underestimated in the current MariTEAM model, which result in a less underestimated power. The results indicate that the Wageningen-B series procedure is more accurate than the propulsive efficiency procedure by Lindstad et al. (2011), if the propeller diameter is properly estimated. However, the Lindstad formula applies a constant propeller efficiency, which is a better prediction if the propeller diameter is inaccurately predicted.

Overall, the current MariTEAM model underestimates the calm water power. The mean deviation is, however, less than for Guldhammer-Harvald. Based on these results, and the results for exact input parameters, it is recommended to apply the new model, including Hollenbach (mean) and Holtrop-Mennen. A larger validation study is needed to make any definite conclusions. However, the seven cases investigated represent various ship types, and there is a clear tendency of more accurate results with Hollenbach's mean procedure and Holtrop-Mennen relative to the other methods. In addition, it is recommended to replace the current Townsin & Kwon added resistance procedure by the four suggested methods, as argued in Section 7.2.2.

Chapter 8

Conclusion

A new ship powering performance method for the MariTEAM model is developed and validated in the current work. The method requires few input parameters and can provide fleet-wide powering predictions in realistic sea-states. Based on reviewing the current state of knowledge in the field of powering predictions, the most relevant empirical methods were implemented in the model.

The performance of each method was assessed and validated in a case study of seven different vessels. Based on the study, it is recommended to apply Holtrop-Mennen and Hollenbach (mean) for calm water powering predictions. On average, for all the cases, these methods provided powering predictions with a mean deviation of $\pm$ 3 % for exact input parameters, which is a significant improvement to the current MariTEAM model. Further, by including both methods, 72.8% of the fleet is valid to analyse. Alongside these methods, Guldhammer-Harvald was suggested, including the updated version of the procedure by Kristensen et al. (2017). However, the procedure showed a significantly higher deviation, on average, 31 % for the two cases where it was applicable, and 11 % if all cases are included. Ideally, more cases should be investigated to make definite conclusions. However, the results demonstrate a clear tendency for seven diverse ship types which represent large segments of the fleet.

The recommended methods for added resistance in wind and waves include STAJIP wind, Blendermann (wind) and both STAWAVE procedures. In-service validation of two ships demonstrates an improved powering prediction for these methods relative to the Townsin & Kwon method currently applied in the current MariTEAM model. Therefore, it is recommended to exclude Townsin & Kwon. The prediction of the propulsive efficiency is further improved for the current model by implementing the Wageningen B-series procedure. On average for all the cases, the procedure provided propulsive efficiency predictions with a mean deviation of 3 %, when Hollenbach and Holtrop-Mennen were applied. The new model is subdivided into modules, which makes it easy to apply the current recommendations and implement new procedures in future work.

Chapter 9

Recommendations for Further Work

In addition to the specific recommendations presented in the conclusion, the following suggestions are given for further work.

Parameter estimates

As the case study demonstrates, the accuracy of the parameter estimates affects the performance of the powering prediction. A new parameter estimate for L_{BWL} (the length of the bow to 95 % of the maximum breadth on the waterline), is required for STA-1. This may be developed by investigating typical bow designs for the main ship types in the fleet. Further, the estimate of the transverse projected area A_{VT} deviates significantly and should be improved. In addition, the propulsive efficiency computed by the Wageningen B-series is sensitive to errors in the estimated propeller diameter, which should be further investigated. As discussed, the estimate is expected to improve for maximum draught input, although this must be confirmed.

Loading conditions

Both the calm water validation study and the in-service study demonstrated significant variations in the powering predictions for varying loading conditions. Applying a maximum loading condition to all vessels in the fleet is expected to overpredict fleet-wide powering and fuel consumption significantly. As Sea-web provides maximum draught and displacement, a fleet-wide study of typical loading conditions is necessary to develop a correction to the current powering predictions. AIS data containing draught may be utilised in the investigation.

Valid range for Hollenbach

The valid range for Hollenbach (1997) is defined in terms of several dimensionless ship characteristics. The range for each dimension is defined as the mean value of all the ships analysed in Hollenbach's study, $\pm$ 1.5 standard deviation. The range is significantly more restrictive than the range defined in Holtrop-Mennen. Results from the case study indicate that Hollenbach provides accurate powering predictions for vessels outside the range. Although the case study is limited to seven ships, it may be reasonable to increase the range and allow for larger applicability in future work.

Bibliography

Alte, R. and Baur, M. V. (1986). Propulsion. Handbuch der Werften. *Hansa*, 18(S 132).

Andersen, P. and Guldhammer, H. E. (1986). A Computer-Oriented Power Prediction Procedure. In *International Conference on Computer Aided Design, Manufacture and Operation in the Marine and Offshore IndustriesComputational Mechanics Publications*.

Auf'm Keller, W. (1973). Extended diagrams for determining the resistance and required power for single-screw ships. *International Shipbuilding Progress*, 20:133–142.

Bertram, V. (2012). *Practical Ship Hydrodynamics*. Elsevier, 2 edition.

Bertram, V. and Wobig, M. (1999). Simple empirical formulae to estimate main form parameter. *Schiff Hafen*, 11(1):118–121.

Birk, L. (2019). *Fundamentals of Ship Hydrodynamics*. Wiley, 1 edition. Publication Title: ISBN: 978-1-118-85551-5.

Blendermann, W. (1986). The wind forces on ships. In *Rep. 467*. Institut für Schiffbau Hamburg.

Blendermann, W. (1994). Parameter identification of wind loads on ships. *Journal of Wind Engineering and Industrial Aerodynamics*, 51(3):339–351. ISBN: 0167-6105 Publisher: Elsevier.

Blendermann, W. (1995). Estimation of wind loads on ships in wind with a strong gradient. *Proceedings of the 14th International Conference on Offshore Mechanics and Arctic Engineering (OMAE), New York, ASMW*, 1-A:271–277.

Blendermann, W. (2004). Ships may encounter high wind loads—a statistical assessment. *Proceedings of the Institution of Mechanical Engineers, Part M: Journal of Engineering for the Maritime Environment*, 218(1):1–10. Publisher: SAGE Publications.

Boswell, R. J. (1971). Design, cavitation performance, and open-water performance of a series of research skewed propellers. Technical report, David W Taylor Naval Ship Research and Development Center Bethesda MD.

Bouman, E. A., Lindstad, H. E., and Stromman, A. H. (2016). Life-Cycle Approaches for Bottom-Up Assessment of Environmental Impacts of Shipping. In *SNAME Maritime Convention*. The Society of Naval Architects and Marine Engineers.

Breslin, J. P. and Andersen, P. (1994). Hydrodynamics of Ship Propellers. ISBN: 9780521413602 9780521574709 9780511624254 Library Catalog: www.cambridge.org Publisher: Cambridge University Press.

Brix, J., Blendermann, W., Grensemann, K., Norrbin, N. H., Pieper, W., Schwanecke, H., Sharma, S. D., Söding, H., Wagner, B., and Weiss, F. (1993). *Manoeuvring technical manual*, volume 36. Seehafen Verlag, Hamburg. ISBN: 0036-603X.

Clarksons (2020). Sea/net - Clarksons Research Portal.

Co, W. a. (1985). Prediction of Windloads on Large Liquified Gas Carriers by Witherby & Co. London for Oil Companies International Marine Forum (OCIMF) and Society of International Gas Tanker & Terminal Operators Ltd. (SIGTO). Technical report, Witherby & Co.

Dale, T. (2020). *Development of Simplified Methods for Ship Powering Performance Calculations*. Project Thesis, NTNU, Trondheim.

Danckwardt, E. C. M. (1969). *Ermittlung des Widerstandes von Frachtschiffen und Hecktrawlern beim Entwurf*. Schiffbauforschung.

Digernes, T. (1982). *An analytical approach to evaluating fishing vessel design and operation*. Norges tekniske høgskole.

ECMWF (2014). ERA-Interim. Library Catalog: www.ecmwf.int.

Edenhofer, O. (2014). Climate change 2014: mitigation of climate change: Working Group III contribution to the Fifth Assessment Report of the Intergovernmental Panel on Climate Change. Technical report, Cambridge University Press, New York, NY. OCLC: ocn892580682.

EU-council (2019). CO2 emissions from ships: Council agrees its position on a revision of EU rules. Library Catalog: www.consilium.europa.eu.

Faltinsen, O. (1993). *Sea loads on ships and offshore structures*, volume 1. Cambridge university press.

Faltinsen, O. M., Minsaas, K., Skjørdal, O, S., and Liapis, N. (1980). Prediction of Resistance and Propulsion of a Ship in a Seaway. In Proceeding of 13th Symposium on Naval Hydrodynamics. In *Prediction of Resistance and Propulsion of a Ship in a Seaway. In Proceeding of 13th Symposium on Naval Hydrodynamics*, pages 505–529.

Fujiwara, T. (2005). A New Estimation Method of Wind Forces and Moments Acting on Ships on the Basis of Physical Components Models. *Journal of the Japan society of naval architects and ocean engineers*, 2:243–255.

Fujiwara, T., Kitamura, F., Ueno, M., and Sogihara, N. (2017). Estimation of above water structural parameters and wind loads on ships. *Ships and Offshore Structures*, 12(8):1100–1108.

Gawn, R. and Burrill, L. (1957). Effect of Cavitation on the Performance of a Series of 16 in. Model Propellers. In *Meeting of the Institution of Naval Architects, TINA, London, 1954, Published in: RINA Transactions: 1957-32, Paper 3*.

Gawn, R. W. L. (1953). Effect of pitch and blade width on propeller performance. In *Autumn Meeting of the Institution of Naval Architects, TINA, Rome, Italy, 1953, pp. 157-193, RINA Transactions 1953-09*.

Gertler, M. (1954). A reanalysis of the original test data for the Taylor Standard Series. Technical report, David Taylor Model Basin Washington.

Guldhammer, H. E. and Harvald, S. A. (1974). Ship Resistance - Effect of form and principal dimensions. (Revised). *Danish Technical Press, Danmark, Danmarks Tekniske Hojskole, kademisk Forlag, St. kannikestrade 8, DK 1169 Copenhagen*.

Gupta, P., Steen, S., and Rasheed, A. (2019). Big Data Analytics As a Tool to Monitor Hydrodynamic Performance of a Ship. In *Volume 7A: Ocean Engineering*, page V07AT06A059, Glasgow, Scotland, UK. American Society of Mechanical Engineers.

Harvald, S. A. (1992). *Resistance and propulsion of ships*. Krieger Publishing Company.

Helm, G. (1964). Systematic (model) investigations on the resistance of boats and small ships. *Hansa*, 101(22):p. 2179.

Hoegh-Guldberg, O., Lovelock, C., Caldeira, K., Howard, J., Chopin, T., and Gaines, S. (2019). The Ocean as a Solution to Climate Change: Five Opportunities for Action. Technical report, World Resources Institute, Washington DC. Publisher: World Resources Institute.

Hollenbach, K. U. (1997). *Beitrag zur abschätzung von widerstand und propulsion von ein-und zweischraubenschiffen im vorentwurf*. PhD thesis, Inst. für Schiffbau.

Hollenbach, K. U. (1998). Estimating resistance and propulsion for single-screw and twin-screw ships. *Schiffstechnik*, 45(2):72.

Holtrop, J. (1977). A Statistical Analysis of Performance Test Results. *International Shipbuilding Progress*, 24(270).

Holtrop, J. (1984). A statistical re-analysis of resistance and propulsion data. *International shipbuilding progress*, 31(363):272–276. ISBN: 0020-868X.

Holtrop, J. and Mennen, G. (1982). An approximate power prediction method. *International Shipbuilding Progress*, 29(335):166–170.

IHS (2020). Maritime Sea-web Online Ship Register | IHS Markit. Library Catalog: ihsmarkit.com.

IMO (2020). Automatic Identification Systems (AIS).

IndEcol (2019). IndEcol - Industrial Ecology Programme - NTNU.

ISO Technical Committee (2015). ISO 15016:2015 Ships and marine technology — Guidelines for the assessment of speed and power performance by analysis of speed trial data.

ITTC (2014). ITTC Analysis of Speed/Power Trial Data (ITTC - Recommended Procedures 7.5-04-01-01.2).

ITTC (2017). 1978 ITTC Performance Prediction Method (ITTC - Recommended Procedures 7.5-02-03-01.4).

ITTC (2017). Description and Rules of the ITTC.

ITTC (2018). ITTC Calculation of the weather factor (fw) for decrease of ship speed in wind and waves (ITTC - Recommended Procedures 7.5-02-07-02.8).

ITU (2018). List of Ship Stations and Maritime Mobile Service Identity Assignments (List V) - Compilation of amendments.

Jalkanen, J.-P., Johansson, L., Kukkonen, J., Brink, A., Kalli, J., Stipa, T., and Kerminen, V.-M. (2012). Extension of an assessment model of ship traffic exhaust emissions for particulate matter and carbon monoxide. *Atmospheric Chemistry & Physics*, 12(5). ISBN: 1680-7316.

Johansson, L., Jalkanen, J.-P., and Kukkonen, J. (2017). Global assessment of shipping emissions in 2015 on a high spatial and temporal resolution. *Atmospheric Environment*, 167:403–415.

Kim, Y. (2020). PhD Project (in-progress): Develop new models for hull resistance, engine emissions, driveline, propeller efficiency and fuel production that enables efficient fleetwide modelling (CLIMMS WP2).

Kristensen, H. O., Lützen, M., and Bingham, H. (2017). Prediction of Resistance and Populsion Power of Ships (Work Package 2, Report no. 4). Technical report, Technical University of Denmark.

Kwon, Y. J. (2008). Speed loss due to added resistance in wind and waves. *The Naval Architect, RINA*, 3:14–16.

Lackenby, H. (1963). The effect of shallow water on ship speed. *Shipbuilder and Marine Engineer*, 70:446–450.

Lap, A. J. W. (1954). Diagrams for determining the resistance of single-screw ships. *International Shipbuilding Progress*, 1(4):179–193. ISBN: 0020-868X Publisher: IOS Press.

Lindstad, H., Asbjørnslett, B. E., and Jullumstrø, E. (2013). Assessment of profit, cost and emissions by varying speed as a function of sea conditions and freight market. *Transportation Research Part D: Transport and Environment*, 19:5–12. ISBN: 1361-9209 Publisher: Elsevier.

Lindstad, H., Asbjørnslett, B. E., and Strømman, A. H. (2011). Reductions in greenhouse gas emissions and cost by shipping at lower speeds. *Energy Policy*, 39(6):3456–3464. Publisher: Elsevier.

Lindstad, H., Sandaas, I., and Steen, S. (2014). Assessment of profit, cost, and emissions for slender bulk vessel designs. *Transportation Research Part D: Transport and Environment*, 29:32–39. ISBN: 1361-9209 Publisher: Elsevier.

Liu, S. and Papanikolaou, A. (2016). Fast approach to the estimation of the added resistance of ships in head waves. *Ocean Engineering*, 112:211–225.

Lloyd's (2020). Shipping and maritime intelligence - Lloyd's List Intelligence.

Lu, R., Turan, O., Boulougouris, E., Banks, C., and Incecik, A. (2015). A semi-empirical ship operational performance prediction model for voyage optimization towards energy efficient shipping. *Ocean Engineering*, 110:18–28.

Lützen, M. and Kristensen, H. O. H. (2012). A Model for Prediction of Propulsion Power and Emissions – Tankers and Bulk Carriers. In *World Maritime Technology Conference WMTC 2012*, page 13.

MAN (2018). Marine Engines & Systems.

MARIN (2006). Sea Trial Analysis (STA) - JIP. Issued Reports.

MarineTraffic (2018). Four ways MarineTraffic ensures AIS data accuracy. Library Catalog: www.marinetraffic.com Section: AIS – essential knowledge.

MARINTEK (2020). MARINTEK, Norwegian Marine Technology Research Institute, Trondheim, Norway.

Molland, A. F. (2011). *The maritime engineering reference book: a guide to ship design, construction and operation*. Elsevier.

Molland, A. F., Turnock, S. R., and Hudson, D. A. (2017). *Ship resistance and propulsion*. Cambridge university press.

Moor, D. I., Parker, M. N., and Pattullo, R. N. M. (1961). The BSRA Methodical Series–An Overall Presentation. *Transactions of the Royal Institution of Naval Architects*, 103(329-419):1. Publisher: The Institution.

Muri, H., Strømman, A. H., Ringvold, A. L., Lonka, R., and Bouman, E. (2019a). Influence of weather on emissions from the global shipping fleet. In *Geophysical Research Abstracts*, volume 21.

Muri, H., Strømman, A. H., Ringvold, A. L., Lonka, R., Lindstad, E., and Bouman, E. A. (2019b). A new emission inventory of the global maritime fleet; the effect of weather. *AGUFM*, 2019:A21W–2637.

Newton, R. and Rader, H. (1961). Performance data of propellers for high speed craft. *Admiralty Experiment Works, Haslar, UK, Published by: The Royal Institution of Naval Architects, RINA Transactions 1961-07, Volume 103, No. 2, Quarterly Transactions, pp. 93-129*.

Olmer, N., Comer, B., Roy, B., Mao, X., and Rutherford, D. (2017). Greenhouse gas emissions from global shipping, 2013-2015 Detailed methodology. *ICCT (The International Council on Clean Transportation)*, page 52.

Oosterveld, M. W. C. (1970). Wake adapted ducted propellers. Technical report, NSBM.

Oosterveld, M. W. C. and van Oossanen, P. (1975). Further computer-analyzed data of the Wageningen B-screw series. *International shipbuilding progress*, 22(251):251–262. ISBN: 0020-868X Publisher: IOS Press.

Papanikolaou, A. (2014). *Ship Design: Methodologies of Preliminary Design*. Springer. Google-Books-ID: WACKBAAAQBAJ.

Ringvold, A. (2017). *Prospective Life Cycle Assessment of Container Shipping*. PhD thesis, NTNU.

Schneekluth, H. and Bertram, V. (1998). *Ship design for efficiency and economy*. Butterworth-Heinemann, Oxford, 2nd ed. edition. Pages: 220.

SFI, S. M. (2016). Sub Project 4 - Performance in a Seaway. Library Catalog: www.smartmaritime.no.

Smith, Jalkanen, J. P., Anderson, B. A., Corbett, J. J, Faber, J., Hanayama, S., O'Keeffe, E., Parker, S., Johansson, L., Aldous, L., Raucci, C., and Traut, M. (2014). Third IMO Greenhouse Gas Study 2014. Technical report, International Maritime Organization, London.

Steen, S. (2011). *TMR4247 Marin teknikk 3-Hydrodynamikk: Motstand og propulsjon, propell og foilteori*. volume UK-2011-99. Department of marine technology, Trondheim.

Steen, S. (2020). Personal communication with Sverre Steen, Professor in marine hydrodynamics, Norwegian University of Science and Technology.

Steen, S., Koushan, K., and Minsaas, K. (2016). *Ship Resistance - Lecture notes TMR4220 Naval hydrodynamics*. Department of Marine Technology, NTNU.

Tillig, F. (2017). *A Generic Model for Simulation of the Energy Performance of Ships – from Early Design to Operational Conditions*. PhD thesis, Chalmers University of Technology.

Tillig, F. (2020). *Simulation model of a ship's energy performance and transportation costs*. PhD thesis, Chalmers University of Technology.

Tillig, F., Ringsberg, J. W., Mao, W., and Ramne, B. (2018). Analysis of uncertainties in the prediction of ships' fuel consumption – from early design to operation conditions. *Ships and Offshore Structures*, 13(sup1):13–24. Publisher: Taylor & Francis _eprint: https://doi.org/10.1080/17445302.2018.1425519.

Todd, F. H. (1957). Series 60-The Effect upon Resistance and Power of Variation in Ship Propotions. *Trans. SNAME*, 65:445–589.

Townsin, R. L. and Byrne, D. (1980). Speed, power and roughness: the economics of outer bottom maintenance. Technical report, Royal Institution of Naval Architects. ISBN: 0306-0209.

Townsin, R. L. and Kwon, Y. J. (1983). Approximate formulae for the speed loss due to added resistance in wind and waves. *Transactions of the Royal Institution of Naval Architects*.

Townsin, R. L. and Kwon, Y. J. (1993). Estimating the influence of weather on ship performance. *Transactions of the Royal Institution of Naval Architects*.

Townsin, R. L. and Mosaad, M. A. (1985). The ITTC Line - Its genesis and Correlation Allowance. *Naval Arcitech*.

Troost, L. (1951). Open water test series with modern propeller forms. *Netherlands Ship Model Basin, Wageningen, Paper presented at: The North East Coast Institution of Engineers and Shipbuilders in Newcastle upon Tyne, UK, Institution Transactions Volume 67*.

UNCTAD (2018). Review of Maritime Transport - United Nations Conference on Trade and Development, UNCTAD/RMT/2018. In *Review of Maritime Transport - United Nations Conference on Trade and Development, UNCTAD/RMT/2018*, New York and Geneva. United Nations Publications. OCLC: 1083029692.

Valanto, P. and Hong, Y. (2017). Wave Added Resistance and Propulsive Performance of a Cruise Ship in Waves. In *Proceedings of the Twenty-seventh (2017) International Ocean and Polar Engineering Conference*, page 9. ISOPE.

Van Oortmerssen, G. (1971). A power prediction method and its application to small ships. *International Shipbuilding Progress*, 18(207):397–415. ISBN: 0020-868X Publisher: IOS Press.

Wartsila (2019). Ship Resistance.

Watson, D. G. (1998). *Practical ship design*, volume 1. Elsevier.

Appendix A

Hollenbach Coefficients

Residuary resistance

$$
\begin{aligned}
C_{R_{\mathrm{std}}} &= b_{11} + b_{12}F_N + b_{13}F_N^2 \\
&+ \left(b_{21} + b_{22}F_N + b_{23}F_N^2\right) C_B \\
&+ \left(b_{31} + b_{32}F_N + b_{33}F_N^2\right) C_B^2
\end{aligned}
\tag{A.1}
$$

	mean residuary resistance			minimum residuary resistance	
	single screw		twin screw	single screw	twin screw
	design draft	ballast draft	design draft	design draft	design draft
b_{11}	−0.57424	−1.50162	−5.3475	−0.91424	3.27279
b_{12}	13.3893	12.9678	55.6532	13.3893	−44.1138
b_{13}	90.596	−36.7985	−114.905	90.596	171.692
b_{21}	4.6614	5.55536	19.2714	4.6614	−11.5012
b_{22}	−39.721	−45.8815	−192.388	−39.721	166.559
b_{23}	−351.483	121.82	388.333	−351.483	−644.456
b_{31}	−1.14215	−4.33571	−14.3571	−1.14215	12.4626
b_{32}	−12.3296	36.0782	142.738	−12.3296	−179.505
b_{33}	459.254	−85.3741	−254.762	459.254	680.921

Figure A.1: Coefficients for computing C_R in Hollenbach as presented by Birk (2019)

Appendix B

Guldhammer-Harvald Coefficients

Residuary resistance

Kristensen et al. (2017) presents coefficients for the original C_R curves in Guldhammer-Harvald, based on extensive regression analysis. The details are outlined in the following. Note that in the current work, the residuary resistance coefficient without corrections is denoted $C_{R,\text{diagram}}$.

$$
\begin{aligned}
&10^3 \cdot \mathrm{C_{R,diagram}} = \mathrm{E} + \mathrm{G} + \mathrm{H} + \mathrm{K} \\
&\text{where:} \\
&\mathrm{E} = \left(\mathrm{A_0} + 1.5 \cdot \mathrm{Fn}^{1.8} + \mathrm{A_1} \cdot \mathrm{Fn}^{\mathrm{N_1}}\right) \cdot \left(0.98 + \tfrac{2.5}{(\mathrm{M}-2)^4}\right) + (\mathrm{M}-5)^4 \cdot (\mathrm{Fn}-0.1)^4 \\
&\mathrm{A_0} = 1.35 - 0.23 \cdot \mathrm{M} + 0.012 \cdot \mathrm{M}^2 \\
&\mathrm{A_1} = 0.0011 \cdot \mathrm{M}^{9.1} \\
&\mathrm{N_1} = 2 \cdot \mathrm{M} - 3.7 \\
&\mathrm{G} = \tfrac{\mathrm{B_1} \cdot \mathrm{B_2}}{\mathrm{B_3}} \\
&\mathrm{B_1} = 7 - 0.09 \cdot \mathrm{M}^2 \\
&\mathrm{B_2} = (5 \cdot \mathrm{C_P} - 2.5)^2 \\
&\mathrm{B_3} = \left(600 \cdot (\mathrm{Fn} - 0.315)^2 + 1\right)^{1.5} \\
&\mathrm{H} = \exp\left(80 \cdot (\mathrm{Fn} - (0.04 + 0.59 \cdot \mathrm{C_P}) - 0.015 \cdot (\mathrm{M}-5))\right) \\
&\mathrm{K} = 180 \cdot \mathrm{Fn}^{3.7} \cdot \exp\left(20 \cdot \mathrm{C_P} - 16\right)
\end{aligned}
\tag{B.1}
$$

Hull-propeller interaction parameters

Harvald (1992) present estimates for t and w as outlined by Lützen and Kristensen (2012), presented in Equation B.2

$$
\begin{aligned}
w &= w_1\left(\tfrac{B}{L}, C_B\right) + w_2\left(\text{form}, C_B\right) + w_3\left(\tfrac{D_\text{p}}{L}\right) \\
t &= t_1\left(\tfrac{B}{L}, C_B\right) + t_2(\text{form}) + t_3\left(\tfrac{D_\text{p}}{L}\right)
\end{aligned}
\tag{B.2}
$$

The parameters of Equation B.2 can be approximated in accordance with diagrams from Harvald (1992). Lützen and Kristensen (2012) presents approximated values from these diagrams by the following regression formulas. Wake fraction is estimated by Equation B.3

$$
w = w_1 + w_2 + w_3 \tag{B.3}
$$

where

$$w_1 = a + \frac{b}{c \cdot (0.98 - C_B)^3 + 1}$$

$$w_2 = \frac{0.025 \cdot F_a}{100 \cdot (C_B - 0.7)^2 + 1}$$

$$w_3 = -0.18 + \frac{0.00756}{\frac{0.00756}{L} + 0.002} \text{ and } w_3 \leq 0.1$$

and

$$a = \frac{0.1 \cdot B}{L} + 0.149$$

$$b = \frac{0.05 \cdot B}{L} + 0.449$$

$$c = 585 - \frac{5027 \cdot B}{L} + 11700 \cdot \left(\frac{B}{L}\right)^2$$

F_a is a form parameter defined as [-2,0,2] respectively for the hull shapes [U, N, V]. The thrust deduction is estimated by Equation B.4

$$t = t_1 + t_2 + t_3 \tag{B.4}$$

where

$$t_1 = d + \frac{e}{f \cdot (0.98 - C_B)^3 + 1}$$

$$t_2 = -0.01 \cdot F_a$$

$$t_3 = 2 \cdot \left(\frac{D_p}{L} - 0.04\right)$$

and

$$d = \frac{0.625 \cdot B}{L} + 0.08$$

$$e = 0.165 - \frac{0.25 \cdot B}{L}$$

$$f = 525 - \frac{8060 \cdot B}{L} + 20300 \cdot \left(\frac{B}{L}\right)^2$$

Appendix C

Holtrop-Mennen Coefficients

Full scale wake fraction coefficients

Coefficients for the full scale wake fraction in Equation 3.22, as presented by Birk (2019).

$$c_8 = \begin{cases} \frac{S}{L_{WL}D}\left(\frac{B}{T_A}\right) & \text{if } B/T_A \leq 5 \\ \frac{S\left(7\frac{B}{T_A}-25\right)}{L_{WL}D\left(\frac{B}{T_A}-3\right)} & \text{if } B/T_A > 5 \end{cases} \tag{C.1}$$

$$c_9 = \begin{cases} c_8 & \text{if } c_8 \leq 28 \\ 32 - \frac{16}{c_8-24} & \text{if } c_8 > 28 \end{cases} \tag{C.2}$$

$$c_{11} = \begin{cases} \frac{T_A}{D} & \text{if } T_A/D \leq 2 \\ 0.0833333\left(\frac{T_A}{D}\right)^3 + 1.33333 & \text{if } T_A/D > 2 \end{cases} \tag{C.3}$$

$$c_{19} = \begin{cases} \frac{0.12997}{(0.95-C_B)} - \frac{0.11056}{(0.95-C_P)} & \text{if } C_P \leq 0.7 \\ \frac{0.18567}{(1.3571-C_M)} - 0.71276 + 0.38648C_P & \text{if } C_P > 0.7 \end{cases} \tag{C.4}$$

$$\begin{aligned} c_{20} &= 1 + 0.015C_{\text{stern}} \\ C_{P1} &= 1.45C_P - 0.315 - 0.0225\ell_{CB} \end{aligned} \tag{C.5}$$

Holtrop'84 hull form factor

$$k = -0.07 + 0.487118c_{14}\left[\left(\frac{B}{L_{WL}}\right)^{1.06806}\left(\frac{T}{L_{WL}}\right)^{0.46106}\left(\frac{L_{WL}}{L_R}\right)^{0.121563}\left(\frac{L_{WL}^3}{V}\right)^{0.36486}(1-C_P)^{-0.604247}\right] \tag{C.6}$$

Wave resistance coefficients

Coefficients for computing the wave resistance if $Fn \leq 0.4$ according to Birk (2019).

$$c_7 = \begin{cases} 0.229577 \left(\frac{B}{L_{WL}}\right)^{(1/3)} & \text{if } B/L_{WL} \leq 0.11 \\ \frac{B}{L_{WL}} & \text{if } 0.11 < B/L_{WL} \leq 0.25 \\ 0.5 - 0.0625 \frac{L_{WL}}{B} & \text{if } B/L_{WL} > 0.25 \end{cases} \tag{C.7}$$

$$\begin{aligned} c_1 &= 2223105 c_7^{3.78613} \left(\frac{T}{B}\right)^{1.07961} (90 - i_E)^{-1.37565} \\ c_3 &= 0.56 \frac{A_{BT}^{1.5}}{\left[BT\left(0.31\sqrt{A_{BT}} + T_F - h_B\right)\right]} \\ c_2 &= \mathrm{e}^{(-1.89\sqrt{c_3})} \\ c_5 &= 1 - 0.8 \frac{A_T}{BTC_M} \end{aligned} \tag{C.8}$$

$$c_{15} = \begin{cases} -1.69385 & \text{if } \frac{L_{WL}^3}{V} \leq 512 \\ -1.69385 + \frac{\frac{L_{WL}}{V^{(1/3)}} - 8}{2.36} & \text{if } 512 < \frac{L_{WL}^3}{V} \leq 1726.91 \\ 0 & \text{if } \frac{L_{WL}^3}{V} > 1726.91 \end{cases} \tag{C.9}$$

$$c_{16} = \begin{cases} 8.07981 C_P - 13.8673 C_P^2 + 6.984388 C_P^3 & \text{if } C_P \leq 0.8 \\ 1.73014 - 0.7067 C_P & \text{if } C_P > 0.8 \end{cases} \tag{C.10}$$

$$d = -0.9$$

$$\lambda = \begin{cases} 1.446 C_P - 0.03 \frac{L_{WL}}{B} & \text{if } \frac{L_{WL}}{B} \leq 12 \\ 1.446 C_P - 0.36 & \text{if } \frac{L_{WL}}{B} > 12 \end{cases} \tag{C.11}$$

$$\begin{aligned} m_1 &= 0.0140407 \frac{L_{WL}}{T} - 1.75254 \frac{V^{(1/3)}}{L_{WL}} - 4.79323 \frac{B}{L_{WL}} - c_{16} \\ m_4 &= 0.4 c_{15} \mathrm{e}^{\left(-0.034 \mathrm{Fn}^{-3.29}\right)} \end{aligned} \tag{C.12}$$

Appendix D

Sea-web Parameters

Aux. Engine builder
Aux. engine design
Aux. engine model
Aux. engine stroke type*
Aux. Engine Total kW*
Aux engines number
Bale
Bollard pull
Bow discharge
Bow loading
Bow stoppers
Bow stoppers no
Bow stoppers swl
Bow to centre manifold
Breadth*
Breadth extreme
Breadth moulded
Built*
Cabins
Callsign
Cancel data
Cargo tank coating
Cargo tanks
Cars
Class
Clean ballast
Closed loading
Cont hull survey
Converted (last/only)
Country of build
Crew
Crude oil washing
Deadweight*
Decks
Delivery date
Depth
Displacements
DOC company
DOC company code
DOC control
DOC domicile
DOC registration
Docking survey
Draught*
Engine bore
Engine builder
Engine cylinders*
Engine design
Engine model*
Engine stroke
Engine stroke type*
Engine type
Engines number
Engines RPM*
Est. Comp. Date
Ex-flag
ExName
Fairplay ID
Fishing No.
Flag
Flash Point < 60
Flash point > 60
Formula DWT
Fuel capacity 1
Fuel capacity 2
Fuel consumption Main Engines
Fuel Consumption Total
Fuel Type 1*
Fuel Type 2
Gas Capacity
Gear No Largest
Gear SWL Largest
Gir Type Largest
Gearless
Generators kW
Grades
Grain
Group Owner
Group Owner Code
Group Owner Control
Group Owner Domicile
Group Owner Registration
GT*
Hatches
Heating Coil Material
Heating Coils
Heating Coils Slop
Holds
Hull material
Hull Type
Ice Capable
IMO chemical class I
IMO chemical class II
IMO chemical class III
Inert gas system
Insulated capacity
Keel Laid
Keel to Mast height
Last update
Launch date
LDT*
Leadship
Length
Length BP*
Length Registered
Lines per side
Liquid
Manifold
Maniful diameter
Marpol 13G Phaseout
Mid point manifold aft ballast
Mid point manifold aft laden
Mid point manifold aft light
Mid point manifold fwd ballast
Mid point manifold fwd laden
Mid point manifold fwd light
MMSI*
Movements
Newbuilding price
NRT
Official No.
Operator
Operator Code
Operator Control
Operator Domicile
Operatior Registration
Order Date
P and I Club
Parallel Body Length Ballast
Parallel Body Length Laden
Parallel Body Length Light

Passengers
PCNT
Permanent Ballast
Photo
Port
Propeller Manufacturer
Propeller Type
Propulsion Type*
Propulsion Units
Recycling Arrival
Recycling Commenced
Recycling Country
Recycling LDT Price
Recycling Price
Recycling Yard
Reefer Points*
Registered Owner
Registered Owner Code
Registered Owner Control
Registered Owner Domicile
Registered Owner Registration
Retirement
RORO Lanes Height
RORO Lanes Length
RORO Lanes Number
RORO Lanes Width
RORO Ramp Position
RORO Ramp SWL
Sale Date
Sale Price (US$)
SCNT
Segregated ballast
Segregated ballast – Protected
Segregated ballast Capacity
Service Speed*
Ship Type*
Ship Type Group*
Shipbuilder
Shipbuilder code
Shipmanager
Shipmanager code
Shipmanager control
Shipmanager domicile
Shipmanager registration
Slop capacity
Slop tank coating
Slop tanks
SMC Auditor
SMC Date Expires
SMC Date Issued
SMC Issuer
Special Survey
SPM Equipped
Standard Design
Statcode 5
Status
Status Date
Stern Discharge
Stern Loading
Sub Contractor
Sub Contractor Yard No
Tank Heat Exchanger Material
Tank Heat Exchangers
Tanks
Technical Manager
Technical Manager Code
Technical Mgr Control
Technical Mgr Domicile
Technical Mgr Registration
Temperature Max
Temperature Min
TEU*
TEU 14
Thruster Largest kW
Thruster Largest Type
Thrusters Number
Thrusters Total kW
Total HP Main Eng
Total kW Main Eng*
TPC
TVE Expiry Date
Vapour Recovery
Yard No.
Year

*In the current MariTEAM database

Appendix E

Blendermann Wind Coefficients

Wind forces and moments in dimensionless form are presented in the diagrams by Blendermann (Brix et al., 1993). The longitudinal dimensionless wind resistance coefficient C_X is retrieved from the diagram and tabulated for each ship. Note that the diagrams present the wind resistance coefficient as $-C_X$ according to the definitions in the current work.

E.1 Car Carrier

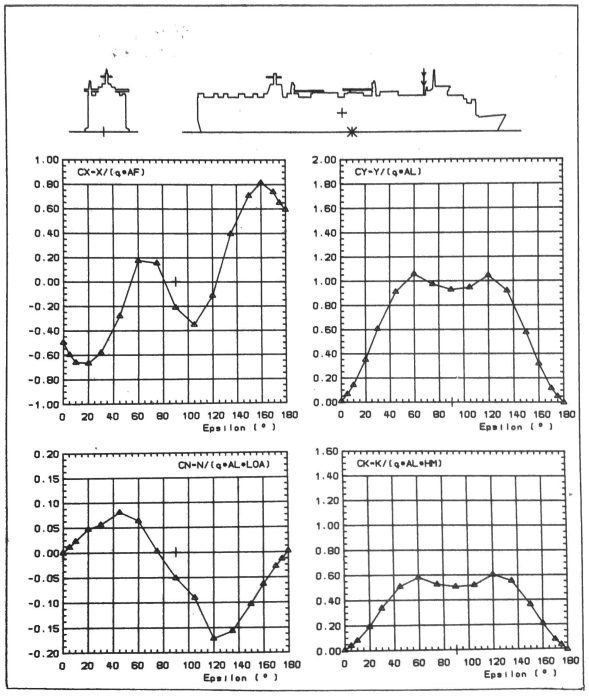

Table E.1: Car carrier wind coefficients

Angle of Attack	$-C_X$
0	-0.55
10	-0.65
20	-0.65
30	-0.60
40	-0.40
50	-0.10
60	0.18
70	0.15
80	0.00
90	-0.20
100	-0.30
110	-0.25
120	-0.12
130	0.20
140	0.50
150	0.70
160	0.80
170	0.74
180	0.60

E.2 Container Vessel

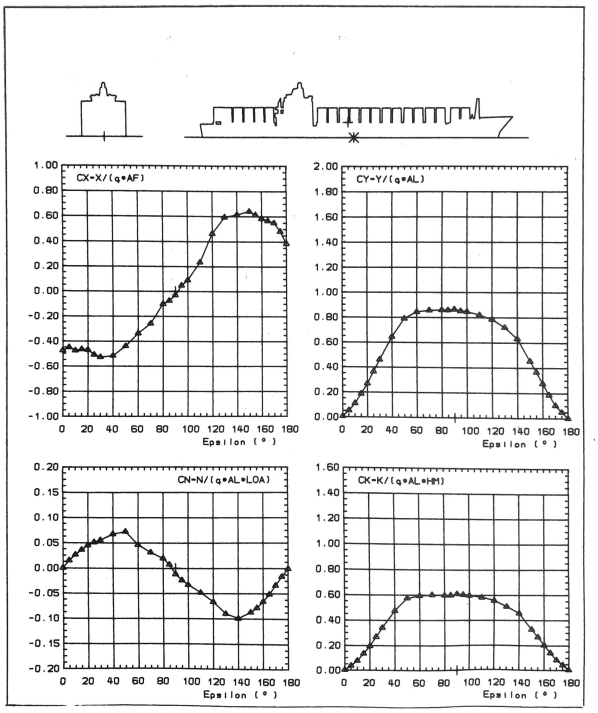

Table E.2: Container vessel wind coefficients

Angle of Attack	$-C_X$
0	-0.55
10	-0.47
20	-0.46
30	-0.52
40	-0.52
50	-0.44
60	-0.34
70	-0.26
80	-0.11
90	-0.03
100	0.08
110	0.22
120	0.44
130	0.58
140	0.60
150	0.63
160	0.58
170	0.54
180	0.40

E.3 Tanker (loaded)

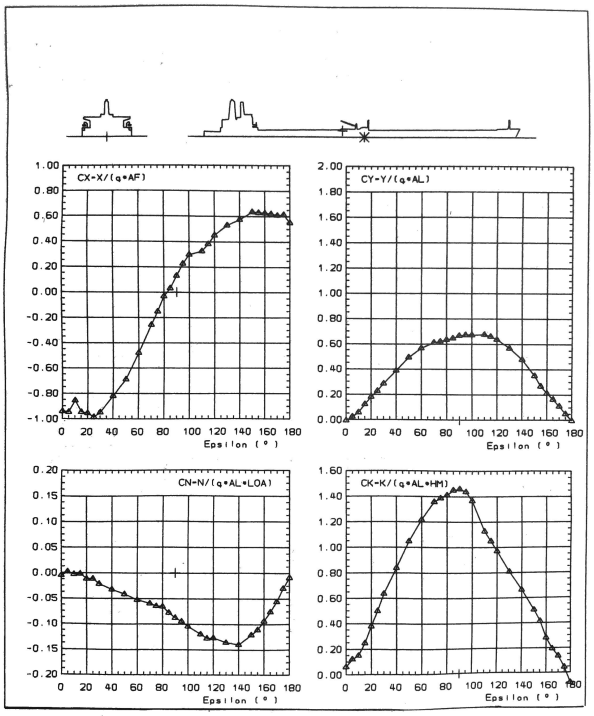

Table E.3: Tanker (loaded) wind coefficients

Angle of Attack	$-C_X$
0	-0.90
10	-0.87
20	-0.95
30	-0.95
40	-0.85
50	-0.72
60	-0.51
70	-0.29
80	-0.03
90	0.10
100	0.26
110	0.32
120	0.42
130	0.51
140	0.57
150	0.62
160	0.61
170	0.60
180	0.55

E.4 Cargo Vessel

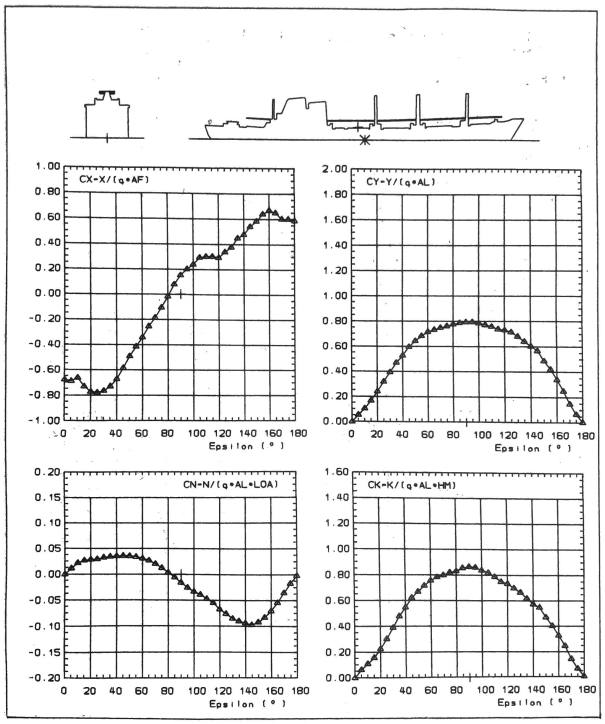

Table E.4: Cargo vessel wind coefficients

Angle of Attack	$-C_X$
0	-0.65
10	-0.67
20	-0.77
30	-0.77
40	-0.70
50	-0.52
60	-0.37
70	-0.21
80	-0.05
90	0.15
100	0.22
110	0.29
120	0.29
130	0.37
140	0.47
150	0.57
160	0.65
170	0.59
180	0.60

E.5 Passenger Ship

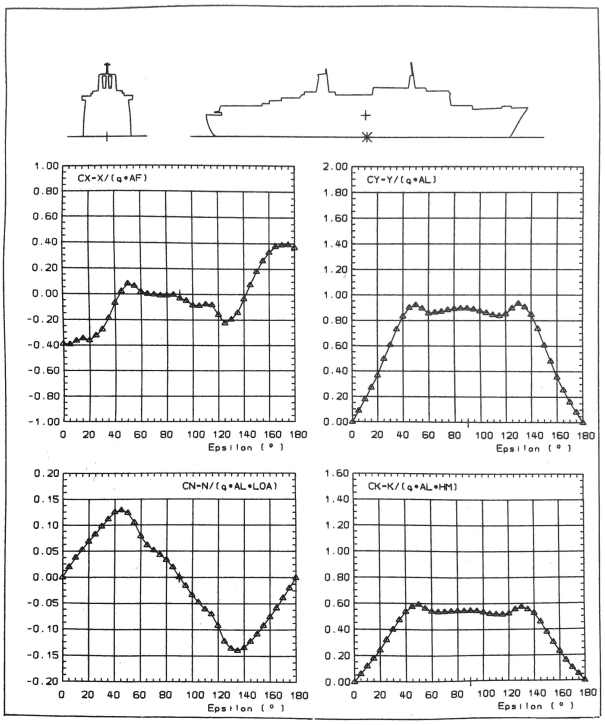

Table E.5: Passenger ship wind coefficients

Angle of Attack	$-C_X$
0	-0.40
10	-0.37
20	-0.35
30	-0.27
40	-0.08
50	0.09
60	0.04
70	0.00
80	-0.01
90	-0.03
100	-0.08
110	-0.08
120	-0.16
130	-0.18
140	-0.06
150	0.21
160	0.33
170	0.38
180	0.37

E.6 Offshore Supply Vessel

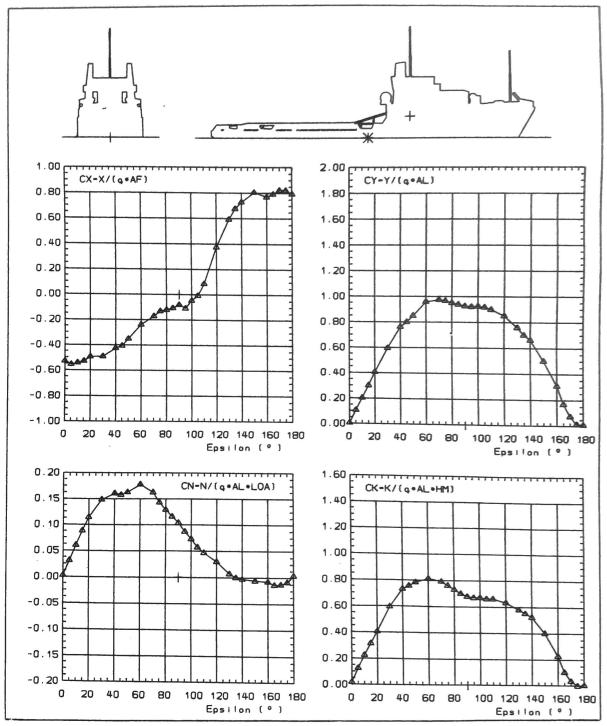

Table E.6: Offshore supply vessel wind coefficients

Angle of Attack	$-C_X$
0	-0.55
10	-0.55
20	-0.51
30	-0.50
40	-0.43
50	-0.33
60	-0.25
70	-0.17
80	-0.12
90	-0.10
100	-0.07
110	0.07
120	0.37
130	0.59
140	0.71
150	0.79
160	0.75
170	0.81
180	0.81

E.7 Ro-Ro/Lo-Lo

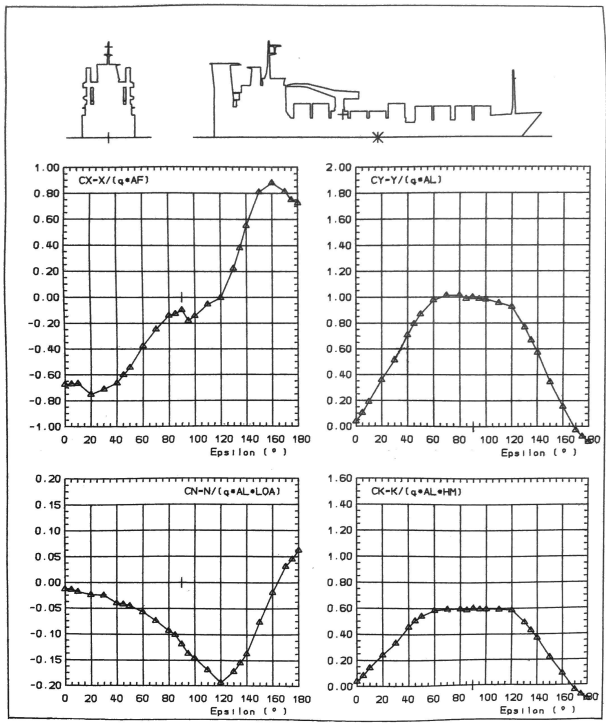

Table E.7: Ro-Ro/Lo-Lo wind coefficients

Angle of Attack	$-C_X$
0	-0.66
10	-0.66
20	-0.74
30	-0.71
40	-0.67
50	-0.55
60	-0.40
70	-0.25
80	-0.14
90	-0.09
100	-0.15
110	-0.05
120	0.00
130	0.26
140	0.52
150	0.81
160	0.88
170	0.79
180	0.70

E.8 Deep Sea Drilling Vessel

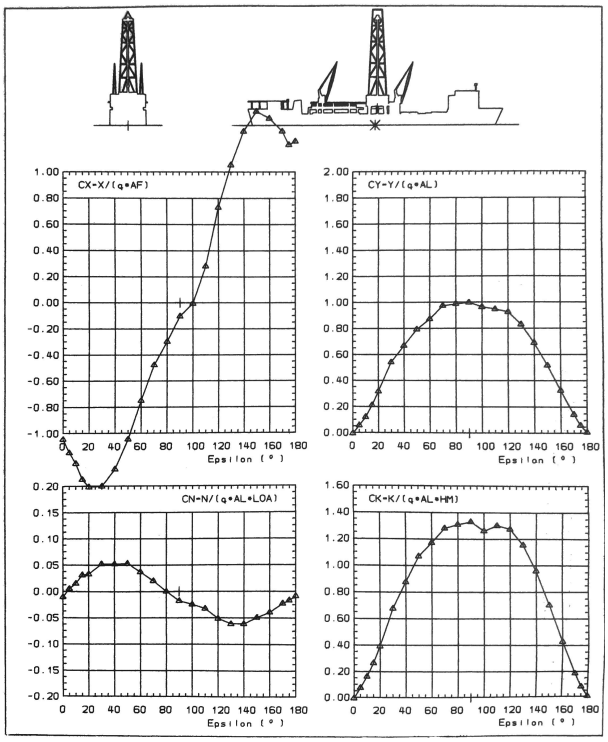

Table E.8: Deep sea drilling vessel wind coefficients

Angle of Attack	$-C_X$
0	-1.05
10	-1.22
20	-1.39
30	-1.38
40	-1.27
50	-1.08
60	-0.78
70	-0.56
80	-0.34
90	-0.15
100	-0.04
110	0.23
120	0.67
130	1.01
140	1.23
150	1.37
160	1.34
170	1.25
180	1.25

E.9 Research Vessel

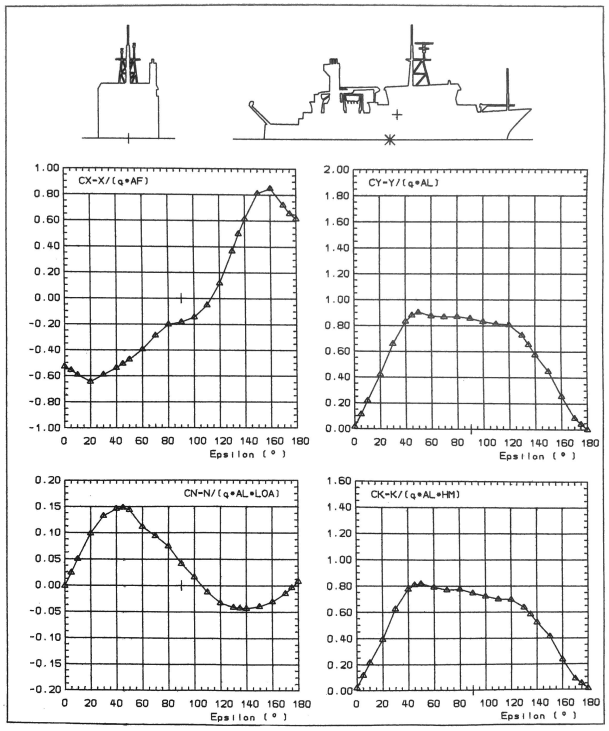

Table E.9: Research vessel wind coefficients

Angle of Attack	$-C_X$
0	-0.55
10	-0.59
20	-0.64
30	-0.59
40	-0.54
50	-0.47
60	-0.40
70	-0.29
80	-0.21
90	-0.18
100	-0.15
110	-0.06
120	0.10
130	0.39
140	0.62
150	0.82
160	0.83
170	0.71
180	0.60

Appendix F

The New Program (MATLAB code)

Main

```
%-------------------------------------------------------------------------%
% main.m - Empirical ship powering prediction method
%
% Other m-files required: import_ship_data.m, import_weather_data.m
%
% Subfunctions: air_resistance.m, beaufort.m, blendermann_wind.m,
% estimate_hull_char.m, estimate_prop_char.m, GH.m, HM.m, hollenbach.m,
% kwon.m, requirements.m, STA1.m, STA2.m, STAJIP_wind.m, wageningen.m
%
% Inputs (from Sea-web):
% B          -       Breadth (moulded)
% T          -       Draught
% dwt        -       Dead weight
% ldt        -       Lightship weight
% Loa        -       Length over all
% Lpp        -       Length between perpendiculars
% ship_type -       Ship type (string)
% D          -       Depth from keel to uppermost continuous deck
% no_decks   -       Number of decks
% Pin        -       Installed power
% ME_n       -       Main engine rpm
% Vd         -       Design speed
% bulb       -       Either 'yes' or 'no'
% teu        -       TEU if containership
%
% Inputs (Weather):
% Hs             -       Significant wave height
% Twave          -       Wave period
% wave_angle     -       Relative wave direction
% U              -       Relative wind speed
% U_angle        -       Relative wind direction
% U_true         -       True wind speed
%
% Outputs:
%    PB - Total brake power
%
% Author: Tone Dale
% Department of Marine technology, NTNU
% email address: tonedale@stud.ntnu.no
% April 2020; Last revision: 14-July-2020
%-------------------------------------------------------------------------%

%----------------------------- Import data -------------------------------%


% Constants
rho = 1026.0210;
rho_air = 1.250; % Dry air 15 degrees
```

```
g = 9.81;
nu = 1.1892E-6;
p_v = 1.6709E3;

% Import ship data from Sea-web
[B,T,D,no_decks,dwt,ldt,Loa,Lpp,Pin,ME_n,Vd,ship_type,sub_type,teu,bulb]...
    = import_ship_data();


% Import weather data (and in-service data for validation)
[Vsog,V,Hs,H,wave_angle,Twave,U,U_angle,U_true,P_aux_is,P_shaft_is,...
    shaft_rpm_is,ME_load_is,P_DG1_is,P_DG2_is,P_DG3_is]...
    = import_weather_data();

%----------------------- MODULE 1: Estimate input ------------------------%


% Estimate missing hull input parameters
[Lwl,Los,Lfn,TA,TF,voldisp,S,SB,Sapp,AVT,AVL,CB,CM,CP,CWP] ...
    = estimate_hull_char(B,T,D,no_decks,teu,dwt,ldt,Lpp,ship_type,rho);


% Estimate missing propulsion input parameters
[Dp] = estimate_prop_char(T,ship_type);


%--------------------- MODULE 2: Calm water resistance ---------------------%

% Calculate calm water resistance as mean of applicable methods

    % Check which methods fulfill the respective requirements
    [GH_req,HM_req,HB_req] = requirements(Lpp,Lwl,Los,B,T,TA,CB,CP,Dp,...
        voldisp,bulb);



    % Guldhammer Harvald (updated by Kristensen 2017)
    [RT_GH,etaH_GH,t_GH,w_GH] = GH(V,Vd,voldisp,Lwl,Lpp,Los,B,T,S,AVT,...
        CB,CP,Dp,ship_type,sub_type,teu,bulb,rho,g,nu);

    RT_GH = RT_GH*GH_req;
    etaH_GH = etaH_GH*GH_req;
    t_GH = t_GH*GH_req;
    w_GH = w_GH*GH_req;


    % Holtrop-Mennen
    [RT_HM,etaH_HM,t_HM,w_HM] = HM(V,Vd,voldisp,Lwl,Lpp,B,TA,TF,S,Sapp,...
        CB,CP,CM,CWP,Dp,rho,g,nu,ship_type,sub_type,AVT,teu);

    RT_HM = RT_HM*HM_req;
    etaH_HM = etaH_HM*HM_req;
    t_HM = t_HM*HM_req;
    w_HM = w_HM*HM_req;


    % Hollenbach (mean)
    [RT_HB,etaH_HB,t_HB,w_HB] = hollenbach(V,Lwl,Lpp,Los,Lfn,B,TA,TF,S,...
        CB,Dp,rho,g,nu,ship_type,sub_type,AVT,teu);

    RT_HB = RT_HB*HB_req;
    etaH_HB = etaH_HB*HB_req;
    t_HB = t_HB*HB_req;
    w_HB = w_HB*HB_req;



RT = mean_value(RT_HB,RT_GH,RT_HM);
etaH = mean_value(etaH_HB,etaH_GH,etaH_HM);
t = mean_value(t_HB, t_GH, t_HM);
w = mean_value(w_HB, w_GH, w_HM);
```

```
 % Plot results from calm water resistance predictions
    plot_calm_water_resistance(RT_HB,RT_GH,RT_HM,RT,V,g,Lpp);


%------------------ MODULE 3: Added weather resistance -------------------%

% Calculate added resistance due to weather

% Wave resistance

    % STA 1
    R_wave_STA1 = STA1(rho,g,Hs,wave_angle,B,Lpp);


    % STA 2
    [R_wave_STA2,STA2_req] = STA2(rho,g,Hs,H,B,Lwl,Lpp,Twave,V,CB,T,...
        wave_angle);
    R_wave_STA2 = R_wave_STA2.*STA2_req;


R_wave = mean_value(R_wave_STA1,R_wave_STA2,0);


% Wind resistance

    % STA-JIP wind (ISO 15016)
    R_wind_STAJIP = STAJIP_wind(ship_type,sub_type,AVT,rho_air,U,...
        U_angle,Vsog);


    % Blendermann wind
    R_wind_blendermann = blendermann_wind(ship_type,sub_type,AVT,...
        rho_air,U,U_angle,V);


R_wind = mean_value(R_wind_STAJIP,R_wind_blendermann,0);


% Total added resistance

    % Kwon
    R_added_kwon = kwon(CB,Lwl,V,H,wave_angle,U_true,U_angle,g,voldisp,...
        ship_type,RT);

    % Find mean added resistance
    R_added = mean_value(R_wave+R_wind,R_added_kwon,0);


 Rtot = RT + R_added;



%-------------------- MODULE 4: Propulsive efficiency --------------------%


    % Wageningen-B series by Breslin and Andersen (1994) and updated
    % according to Kristensen (2017)

    [etaD_cw] = wageningen(V,RT,etaH,t,w,Dp,rho); % Calm water
    [etaD] = wageningen(V,Rtot,etaH,t,w,Dp,rho);  % Total



%------------------------- MODULE 5: Final power -------------------------%

% Final propulsion power

PB_cw = ((1./etaD_cw).*(RT).*V)/1000;   % Calm water power
PB = ((1./etaD).*(Rtot).*V)/1000;       % Total power
```

Estimate missing input

```
function [Lwl,Los,Lfn,TA,TF,voldisp,S,SB,Sapp,AVT,AVL,CB,CM,CP,CWP] ...
            = estimate_hull_char(B,T,D,no_decks,teu,dwt,ldt,Lpp,ship_type,rho)

%-------------------------------------------------------------------------%
% estimate_hull_char.m - Estimate missing hull parameter input
%
% Other m-files required: main.m
% Subfunctions: none
%
% Inputs:
% B          -       Breadth (moulded)
% T          -       Draught
% dwt        -       Dead weight
% ldt        -       Lightship weight
% Loa        -       Length over all
% Lpp        -       Length between perpendiculars
% ship_type -       Ship type (string)
% rho        -       Sea water density 1025 kg/m^3
%
% Outputs:
% Lwl        -       Length of waterline
% Los        -       Length of surface
% TA         -       Molded draught aft perpendicular
% TF         -       Molded draught fore perpendicular
% voldisp    -       Volume displacement
% S          -       Wetted surface area
% SB         -       Wetted base/transom area
% Sapp       -       Wetted surface area of appendages
% AVT        -       Area of ship and cargo above waterline (transverse)
% AVL        -       Area of ship and cargo above waterline (longitudinal)
% ABT        -       Transverse cross section area of bulb
% CB         -       Block coefficient
% CM         -       Midship section coefficient
% CP         -       Prismatic coefficient
% CWP        -       Waterplane area coefficient
% Cstern     -       Shape parameter in Holtrop-Mennen
% LCB        -       Longitudinal centre of buoyancy
%
% Author: Tone Dale
% Department of Marine technology, NTNU
% email address: tonedale@stud.ntnu.no
% April 2020; Last revision: 19-May-2020
%-------------------------------------------------------------------------%

% Approximated parameters calculated directly by design parameters

% Lwl from Kristensen (2013) and Tillig (2020)

if contains(ship_type,'container')
    Lwl = 1.01*Lpp;
else
    Lwl = 1.02*Lpp;
end

% Los from TMR4220 Naval Hydrodynamics matlab code
Los   = 1.04*Lwl;

% Calculation of 'Froude length', Lfn for Hollenbach (from TMR4220):
if Los/Lpp < 1
   Lfn = Los;
elseif (Los/Lpp >= 1) & (Los/Lpp < 1.1)
   Lfn = Lpp+2/3*(Los-Lpp);
elseif Los/Lpp >= 1.1
   Lfn = 1.0667*Lpp;
end

% TA and TF assumed to be equal to T
```

```
TA = T;
TF = T;

% Volume displacement [m^3]
 voldisp = ((ldt+dwt)*1000/rho);


% Block coefficient w.r.t Lpp, breadth moulded and max draught
CB = voldisp/(Lpp*B*T);
if CB > 0.9
    disp('Error: CB > 0.9')
end

% Wetted surface area by Mumfords formula updated by Kristensen (2013)
if contains(ship_type,{'bulk dry', 'oil','other bulk'})
    S = 0.99*(voldisp/T + 1.9*Lwl*T);
elseif contains(ship_type,'container')
    S = 0.995*(voldisp/T + 1.9*Lwl*T);
else
    S = 1.025*Lpp*(CB*B + 1.7*T);
end

% Wetted base/transom area
SB = 0;

% Wetted surface area of appendages
Sapp = 0;

% Area of ship and cargo above waterline (transverse and longitudinal)
% According to Kristensen (2017) for tankers/bulk/container
if contains(ship_type,'container')
    if teu <= 3000
        h = interp1(1:300:3000,11:1:20.6,teu);
    elseif (teu > 3000) & (teu <= 6000)
        h = 24.2;
    elseif (teu > 6000) & (teu <= 16000)
        h = interp1(6000:2000:16000,24.2:0.5:26.8,teu);
    else
        disp(' Estimate transverse cross section area error. TEU > 16000')
    end
else
    h = 3*no_decks + 2; % 2 m for equipment
end

    AVT = B*(D-T+h);
    AVL = Lpp*(D-T+h);

% Midship section coefficient by Schneekluth and Bertram (1998) Tillig 2020
% NB! CM > 1 for CB >0.9
CM = 0.93 + 0.08*CB;

% Prismatic coefficient
CP = CB/CM;

% Waterplane area coefficient by Bertram and Wobig (Tillig 2020)
% Found in Birk p. 613
% General formula from Papanikolao Ship design: methodologies of
% preliminary design (book) (2014)
if contains(ship_type,{'bulk dry', 'oil','other bulk', 'cargo'})
    CWP = 0.763*(CP + 0.34);
elseif contains(ship_type,'container')
    CWP = 3.226*(CP - 0.36);
else
    CWP = (1+2*CB)/3;
end %if

if CWP > 1
    disp('Error: CWP > 1. Set to 0.9')
    CWP = 0.9;
end
```

```
end


function [Dp] = estimate_prop_char(T,ship_type)
%-------------------------------------------------------------------------%
% estimate_prop_char.m - Estimate missing propeller characteristics
%
% Other m-files required: main.m
% Subfunctions: none
%
% Inputs:
% T          -       Draught (max)
% ship_type -       Ship type (string)
%
% Outputs:
% Dp         -       Propeller diameter
%
% Author: Tone Dale
% Department of Marine technology, NTNU
% email address: tonedale@stud.ntnu.no
% April 2020; Last revision: 19-May-2020
%-------------------------------------------------------------------------%
    if contains(ship_type,{'bulk dry', 'oil','other bulk'})
        Dp = 0.395*T + 1.30;                                % Kristensen 2017
    elseif contains(ship_type,'container')
        Dp = 0.623*T - 0.16;                                % Kristensen 2017
    elseif contains(ship_type, 'ro-ro')
        Dp = 0.713*T - 0.08;                                % Kristensen 2017
    else
        Dp = 0.7*T;                                         % (MAN)
    end

end
```

Calm-water methods requirements

```
function [GH_req,HM_req,HB_req] = requirements(Lpp,Lwl,Los,B,T,TA,CB,CP,Dp,voldisp,bulb)
%-------------------------------------------------------------------------%
% requirements.m - Check if input fulfills calm-water methods requirement
%
% Other m-files required: main.m
% Subfunctions: none
%
% Inputs:
% B          -       Breadth (moulded)
% Lpp        -       Length between perpendiculars
% Lwl        -       Waterline length
% Los        -       Length over surface
% Lfn        -       Computational Froude length
% T          -       Draught
% TA         -       Molded draught aft perpendicular
% voldisp    -       Volume displacement
% CB         -       Block coefficient
% CP         -       Prismatic coefficient
% Dp         -       Propeller diameter
% g          -       Constant of gravity
% bulb       -       yes or no
%
% Outputs:
% GH_req     -      Guldhammer-Harvald dimensions requirement
% HM_req     -      Holtrop-Mennen dimensions requirement
% HB_req     -      Hollenbach dimensions requirement
%
% Author: Tone Dale
% Department of Marine technology, NTNU
% email address: tonedale@stud.ntnu.no
% April 2020; Last revision: 22-May-2020
%-------------------------------------------------------------------------%
```

```
% Guldhammer-Harvald requirements

    % Define computational length, L
    if contains(bulb, 'yes')
        L = Los;
    elseif contains(bulb, 'no')
        L = Lwl;
    end %if

    M = L/(voldisp^(1/3)); % Length-displacement ratio or slenderness

    if (L/B >= 5.0) & (L/B < 8.0) & (CB >= 0.55) & (CB < 0.85)...
            & (M >= 4.0) & (M < 6.0)
        GH_req = 1;
    else
        GH_req = 0;
        disp('Guldhammer-Harvald requirement not fulfilled')
    end

% Holtrop-Mennen requirements

    % CP based on Lpp not Lwl
    CP = (Lpp/Lwl)*CP;

    if  (CP >= 0.55) & (CP < 0.85) & (Lwl/B >= 3.9) & (Lwl/B < 9.5)
        HM_req = 1;
    else
        HM_req = 0;
        disp('Holtrop-Mennen requirement not fulfilled')
    end


% Hollenbach requirements

     if  (Lpp/B >= 4.71) & (Lpp/B < 7.11) & ... % Length - beam ratio
         (B/T >= 1.99) & (B/T < 4) & ...        % Breadth - draught ratio
         (Dp/TA >= 0.43) & (Dp/TA < 0.84) & ... % Dp - draught ratio
         (CB >= 0.49) & (CB < 0.83) & ...       % Block coefficient
         (Lpp/((voldisp)^(1/3)) >= 4.49) & ...  % Length - disp ratio
         (Lpp/((voldisp)^(1/3)) < 6.01)
         HB_req = 1;
     else
         HB_req = 0;
         disp('Hollenbach requirement not fulfilled')
     end % if


end
```

Guldhammer-Harvald

```
function [RT,etaH,t,w] = GH(V,Vd,voldisp,Lwl,Lpp,Los,B,T,S,AVT,CB,CP,Dp,...
    ship_type,sub_type,teu,bulb,rho,g,nu)
%--------------------------------------------------------------------------%
% GH.m - Calculate calm water resistance with new Guldhammer-Harvald method
%
% Other m-files required: main.m
% Subfunctions: air_resistance.m
%
% Inputs:
% V         -       Ship actual speed
% Vd        -       Ship design speed
% voldisp   -       Volume displacement
% Lwl       -       Length of waterline
% Lpp       -       Length between perpendiculars
% Los       -       Length over surface
% B         -       Breadth (moulded)
```

```
% T          -       Draught
% S          -       Wetted surface area
% AVT        -       Area of ship and cargo above waterline (transverse)
% CB         -       Block coefficient
% CP         -       Prismatic coefficient
% Dp         -       Propeller diameter
% rho        -       Seawater density
% g          -       Constant of gravity
% nu         -       Viscosity
% teu        -       No of containers (in twenty-foot equivalent units)
% ship type -       Ship type
% sub_type   -       Sub type for container ships
% bulb       -       Either 'yes' or 'no'
%
% Outputs:
% CR         -      Residual resistance coefficient
% RT         -      Total calm water resistance
% etaH       -      Hull efficiency
% t          -      Thrust deduction factor
% w          -      Wake fraction
%
% Author: Tone Dale
% Department of Marine technology, NTNU
% email address: tonedale@stud.ntnu.no
% April 2020; Last revision: 16-April-2020:
%-------------------------------------------------------------------------%

%Revised Harvald (1983) method defined in accordance with Kristensen (2017)
weightdisp = rho*voldisp/1000; % In tons

% Form factor is excluded in the CF part but corrected by hull form U/V
Re = V*Lwl./nu;
CF = 0.075./(log10(Re)-2).^2;

% Incremental resistance coefficient
% CA includes the effects of roughness of the ship hull (Kristensen 2017)
CA = (max(-0.1, 0.5*log10(weightdisp)-0.1*(log10(weightdisp)).^2))*10^-3;

% Axial calm water air resistance CAA (kristensen 2017 and skipshydro comp)
CAA = air_resistance(ship_type,sub_type,AVT,S,teu);

% Residuary resistance (Regression analysis of curves from Harvald, 1983)
% CR is f(M,CP,Fn,constants)

    % Define computational length, L
    if contains(bulb, 'yes')
        L = Los;
    elseif contains(bulb, 'no')
        L = Lwl;
    end %if

    M = L/(voldisp^(1/3)); % Length-displacement ratio or slenderness
    Fn = V./sqrt(g*Lpp);   % Froude number according to Guldhammer-Harvald
    AM = voldisp/(Lpp*CP); % Midship section area
    CP = voldisp/(L*AM);   % Prismatic coefficient based on computational L

    A0 = 1.35 - 0.23*M + 0.012*M^2;
    A1 = 0.0011*M^9.1;
    N1 = 2*M - 3.7;

    E = (A0 + 1.5*Fn.^1.8 + A1*Fn.^N1).*(0.98 + (25/((M-2)^4))) + ...
        ((M-5)^4).*((Fn-0.1).^4);

    B1 = 7 - 0.09*M^2;
    B2 = (5*CP - 2.5)^2;
    B3 = (600*(Fn - 0.315).^2 + 1).^1.5;

    G = B1*B2./B3;

    H = exp(80.*(Fn-(0.04+0.59*CP) - 0.015*(M-5)));
```

```
    K = 180*Fn.^(3.7).*exp(20*CP-16);

    CR_diagram = (E + G + H + K).*10^-3; % Valid for Fn <= 0.33;

    % Corrections:

    % Correction for B/T ratio deviating from 2.5
    if (B/T <= 2.4) || (B/T >= 2.6)
        dCR_BT = 0.16*(B/T - 2.5)*10^-3;
    else
        dCR_BT = 0;
    end

    % Correction for LCB not placed amidships
    dCR_LCB = 0; % Suggested neglected by Kristensen 2017 (Birk 2019)

    % Correction for shape/hull form according to Birk 2019
    % Modern tankers/bulk carriers with large CB often got U-fore body
    % Fast container ships often have entrances with V-shaped stations
    % Assuming fast is a design speed above 20 knots

    if (contains(ship_type,{'bulk dry', 'oil','other bulk'})) & (CB > 0.85)
        dCR_form = -0.1*10^-3;
    elseif (contains(ship_type, 'container')) & (Vd > 10)
        dCR_form = 0.1*10^-3;
    else
        dCR_form = 0;
    end %if

    CR_nobulb = CR_diagram + dCR_BT + dCR_LCB + dCR_form;

    % Bulb correction as function of Fn, according to Kristensen 2017
    % Only presented for tankers/bulk carriers
    % Correction for container ships is presented as a fraction
    % A factor of 10^-3 is missing in Kristensen 2017

    if contains(ship_type,{'bulk dry', 'oil','other bulk'})
        dCR_bulb = (max(-0.4,-0.1-1.6.*Fn)).*10^-3;
    elseif contains(ship_type, 'container')
        dCR_bulb = ((250.*Fn-90)./100).*CR_nobulb;
    else
        dCR_bulb = 0;
    end % if

    CR = CR_diagram + dCR_BT + dCR_LCB + dCR_form + dCR_bulb;

% CT by ITTC method
CT = CF + CA + CAA + CR;
RT = CT.*0.5*rho*S.*V.^2;

% Hull-propeller interaction parameters

    % Wake fraction
    % Fa = [ -2 0 2 ]; Form in the aft body
    Fa = 0; % Temporarily assumption

    a = 0.1*B/L + 0.149;
    b = 0.05*B/L + 0.449;
    c = 585 - 5027*B/L + 11700*(B/L)^2;

    w1 = a + b/(c*(0.98-CB)^3+1);
    w2 = 0.025*Fa/(100*(CB-0.7)^2+1);
    w3 = min(0.1,-0.18 + 0.00756/(Dp/L + 0.002));

    w_harvald = w1 + w2 + w3;
    w = (0.7*w_harvald - 0.45 + 0.08*M).*ones(1,length(V));

    % Thrust deduction factor
    d = 0.625*B/L + 0.08;
    e = 0.165 - 0.25*B/L;
    f = 825 - 8060*B/L + 20300*(B/L)^2;
```

```
    t1 = d + e/(f*(0.98-CB)^3+1);
    t2 = -0.01*Fa;
    t3 = 2*(Dp/L - 0.04);

    t_harvald = t1 + t2 + t3;
    t = (t_harvald - 0.26 + 0.04*M).*ones(1,length(V));

    etaH = (1-t)./(1-w);


% Froude number limitations
RT(Fn > 0.33) = 0;
w(Fn > 0.33) = 0;
t(Fn > 0.33) = 0;
etaH(Fn > 0.33) = 0;


end
```

Holtrop-Mennen

```
function [RT,etaH,t,w] = HM(V,Vd,voldisp,Lwl,Lpp,B,TA,TF,S,Sapp,CB,CP,...
    CM,CWP,Dp,rho,g,nu,ship_type,sub_type,AVT,teu)
%-------------------------------------------------------------------------%
% HM.m - Calculate calm water resistance with Holtrop-Mennen
%
% Other m-files required: main.m
% Subfunctions: air_resistance.m
%
% Inputs:
% V          -       Ship actual speed
% Vd         -       Ship design speed
% voldisp    -       Volume displacement
% Lwl        -       Length of waterline
% Lpp        -       Length between perpendiculars
% B          -       Breadth (moulded)
% T          -       Draught
% S          -       Wetted surface area
% Sapp       -       Wetted surface area of appendages (= 0)
% AVT        -       Area of ship and cargo above waterline (transverse)
% CB         -       Block coefficient
% CP         -       Prismatic coefficient
% CM         -       Midship section coefficient
% CWP        -       Waterplane area coefficient
% Dp         -       Propeller diameter
% rho        -       Seawater density
% g          -       Constant of gravity
% nu         -       Viscosity
% teu        -       No of containers (in twenty-foot equivalent units)
% ship type -       Ship type
% sub_type   -       Sub type for container ships
%
% Outputs:
% RT         -      Total calm water resistance
% etaH       -      Hull efficiency
% t          -      Thrust deduction factor
% w          -      Wake fraction
%
% Author: Tone Dale
% Department of Marine technology, NTNU
% email address: tonedale@stud.ntnu.no
% April 2020; Last revision: 16-June-2020:
%-------------------------------------------------------------------------%
% Method implemented as described by Birk 2019 p.613-616
Fn = V./sqrt(g*Lwl);
Fn_design = Vd/sqrt(g*Lwl);
Re = V*Lwl./nu;
```

```
% CP and CB defined with Lwl
CP = (Lpp/Lwl)*CP;
CB = (Lpp/Lwl)*CB;

T = (TA+TF)/2;

% Transverse area of bulbous bow
% Kracht 1978 gives C_ABT (Tillig 2020)
C_ABT = (40*Fn_design-3.5)/100;
AMS = B*T*CM;
ABT = C_ABT*AMS;

%Height of centre of bulb area max 0.6*TF according to Birk 2019 p. 612
hB = 0.6*TF;

% Assumption: Area of immersed transom =  0 birk p.623
AT = 0;

% Optimum LCB: lcb estimated by Guldhammer Harvald (Birk p.613)
% [%] aft of Lwl/2
lcb = -(0.44*Fn_design - 0.094);

LR = Lwl*(1-CP + (0.06*CP*lcb)/(4*CP-1)); % Length of run

% Waterline entrance angle iE [degrees]
a = -( ((Lwl/B)^0.80856)*((1-CWP)^0.30484)*((1-CP-0.0225*lcb)^0.6367)*...
    ((LR/B)^0.34574)*((100*voldisp/(Lwl^3))^0.16302) );

iE = 1 + 89*exp(a);

Cstern = 0; % Assuming normal sections
c14 = 1.0 + 0.011*Cstern; % Constant of stern shape

% Hull form factor
k = -0.07 + 0.487118*c14*(((B/Lwl)^1.06806)*((T/Lwl)^0.46106)*...
    ((Lwl/LR)^0.121563)*((Lwl^3/voldisp)^0.36486)*(1-CP)^-0.604247);

% Frictional resistance by ITTC 1957 line
CF = 0.075./(log10(Re)-2).^2;
RF = CF.*0.5*rho*S.*V.^2;


%% % Wave resistance defined according to Froude number range

if B/Lwl <= 0.11
    c7 = 0.229577*(B/Lwl)^(1/3);
elseif (B/Lwl > 0.11) & (B/Lwl <= 0.25)
    c7 = B/Lwl;
else
    c7 = 0.5-0.0625*Lwl/B;
end

c1 = 2223105*(c7^3.78613)*((T/B)^1.07961)*(90-iE)^-1.37565;
c3 = 0.56*(ABT^1.5)/(B*T*(0.31*sqrt(ABT) + TF - hB));
c2 = exp(-1.89*sqrt(c3));
c5 = 1-0.8*AT/(B*T*CM);

if (Lwl^3)/voldisp <= 512
    c15 = -1.69385;
elseif ((Lwl^3)/voldisp > 512) & ((Lwl^3)/voldisp <= 1726.91)
    c15 = -1.69385 + ((Lwl/(voldisp^(1/3))) - 8)/2.36;
else
    c15 = 0;
end

if CP <= 0.8
    c16 = 8.07981*CP - 13.8673*CP^2 + 6.984388*CP^3;
else
    c16 = 1.73014 - 0.7067*CP;
end
```

```
d = -0.9;

if Lwl/B <= 12
    lambda = 1.446*CP - 0.03*Lwl/B;
else
    lambda = 1.446*CP - 0.36;
end

m1 = 0.0140407*Lwl/T - 1.75254*(voldisp^(1/3))/Lwl - 4.79323*B/Lwl - c16;

m4 = 0.4*c15.*exp(-0.034*Fn.^-3.29);



RW = c1*c2*c5*rho*g*voldisp.*exp(m1.*Fn.^d + m4.*cos(lambda.*Fn.^-2));

%% Other resistance contributions
% Neglecting effect of appendage resistance
RAPP = 0;

% Neglecting the bulb correction
RB = 0;

% Neglecting transom resistance
RTR = 0;

% Correlation coefficient includes roughness

if TF/Lwl <= 0.04
    c4 = TF/Lwl;
else
    c4 = 0.04;
end

CA = 0.006*((Lwl+100)^-0.16) - 0.00205 + 0.003*sqrt(Lwl/7.5)*(CB^4)*c2*(0.04-c4);

% Additional correction for surface roughness > 150 um
ks = 150; % Assumption

if ks == 150
    dCA = 0;
else
    dCA = (0.105*(ks*10^-6)^(1/3) - 0.005579)/(Lwl^(1/3));
end

% Correlation resistance
RA = 0.5*rho.*(V.^2)*(CA+dCA)*(S+Sapp);

% Air resistance
CAA = air_resistance(ship_type,sub_type,AVT,S,teu);
RAA = 0.5*rho*S.*(V.^2)*CAA;

%% Total Resistance

RT = (1+k).*RF + RW + RAA + RA + RAPP  + RB + RTR;

%% Hull-propeller interation parameters

% Viscous resistance coefficient
CV = ((1+k).*RF + RA + RAPP)./(0.5*rho.*(V.^2)*(S+Sapp));

% Wake fraction

if B/TA <= 5
    c8 = (S/(Lwl*Dp))*(B/TA);
else
    c8 = (S*(7*B/TA - 25))/(Lwl*Dp*(B/TA - 3));
end

if c8 <= 28
    c9 = c8;
```

```
else
    c9 = 32 - 16/(c8-24);
end

if TA/Dp <= 2
    c11 = TA/Dp;
else
    c11 = 0.0833333*((TA/Dp)^3) + 1.33333;
end

if CP <= 0.7
    c19 = 0.12997/(0.95-CB) - 0.11056/(0.95-CP);
else
    c19 = 0.18567/(1.3571-CM) - 0.71276 + 0.38648*CP;
end

c20 = 1+0.015*Cstern;

CP1 = 1.45*CP - 0.315 - 0.0225*lcb;

w = c9*c20*CV.*(Lwl/TA).*(0.050776 + 0.93405*(c11.*CV)./(1-CP1)) + ...
    0.27915*c20*sqrt(B/(Lwl*(1-CP1))) + c19*c20; % ! Array


% Thrust deduction factor
t = (0.25014*((B/Lwl)^0.28956)*(((sqrt(B*T))/Dp)^0.2624))/((1-CP+0.0225*lcb)^0.01762) + 0.0015*Cstern;
t = t.*ones(1,length(V));

% Hull efficiency
etaH = (1-t)./(1-w);

%% Froude number limitations
RT(Fn > 0.45) = 0;
w(Fn > 0.45) = 0;
t(Fn > 0.45) = 0;
etaH(Fn > 0.45) = 0;


end
```

Hollenbach

```
function [RT_mean,etaH,t,w] = hollenbach(V,Lwl,Lpp,Los,Lfn,B,TA,TF,S,CB,Dp,...
rho,g,nu,ship_type,sub_type,AVT,teu)
%-------------------------------------------------------------------------%
% hollenbach.m - Calculate calm water resistance with Hollenbach (mean)
%
% Other m-files required: main.m
% Subfunctions: air_resistance.m
%
% Inputs:
% V          -       Ship speed
% Lwl        -       Length in waterline
% Lpp        -       Length between perpendiculars
% Los        -       Length over surface
% Lfn        -       Computational Froude length
% B          -       Breadth (moulded)
% T          -       Draught
% TA         -       Molded draught aft perpendicular
% TA         -       Molded draught fore perpendicular
% S          -       Wetted surface area
% CB         -       Block coefficient
% Dp         -       Propeller diameter
% rho        -       Seawater density
% g          -       Constant of gravity
% nu         -       Viscosity
%
% Outputs:
% RT_mean    -      Total calm water resistance with k, dF and CA (mean)
```

```
% etaH      -      Hull efficiency
% t         -      Thrust deduction factor
% w         -      Wake fraction
%
% Author: Tone Dale
% Department of Marine technology, NTNU
% email address: tonedale@stud.ntnu.no
% April 2020; Last revision: 16-May-2020:
%-------------------------------------------------------------------------%

% Script based on Skipshydro Hollenbach script for mean resistance (credit)

NRud  = 0;        % Number of rudders
NBrac = 0;        % Number of brackets
NBoss = 0;        % Number of bosses
NThr  = 0;        % Number of side thrusters

T = (TA+TF)/2;
N = length(V);


% 'Mean' resistance coefficients
a = [-0.3382 0.8086 -6.0258 -3.5632 9.4405 0.0146 0 0 0 0];
b = [-0.57424 13.3893 90.5960; 4.6614 -39.721 -351.483; -1.14215...
    -12.3296 459.254];
d = [0.854 -1.228 0.497];
e = [2.1701 -0.1602];


% Correction for ships with CB<0.6 by Hollenbach 1998 (Birk 2019)
if CB < 0.49
    b(1) = -0.87674;
elseif (CB >= 0.49) & (CB < 0.6)
    b(1) = -0.57424-25*(0.6-CB)^2;
else
    b(1) = -0.57424;
end



CRstandard = zeros(1,N); % Pre-allocation

% Form factor by MARINTEK, eq. 2.54 in Skipsydro comp
Q = (CB/Lwl)*sqrt(B*(TA+TF));
k = 0.6*Q + 75*Q^3;


% Calculate ship resistance

Fn = V./sqrt(g*Lfn); % Froude number according to Hollenbach
Fnkrit = d*[1 CB CB^2]';
c1 = Fn./Fnkrit;

% Other resistance components
Re = V*Lpp./nu;                                 % Reynold's number for ship
CF = 0.075./(log10(Re)-2).^2;                % Friction coefficient for ship
Rnm = (6*sqrt(6/Lpp)*10^6/1.1395).*V;          % Reynold's number for model
CFm = 0.075./(log10(Rnm)-2).^2;              % ITTC friction line for model
dCF = (110.31.*((150*V).^0.21) - 403.33).*(CF.^2);    % MARINTEK roughness
dCF(dCF<0) = 0;    % Only positive values

% CA from Vienna Model Basin p.637 Birk
if Lpp <= 175
    CA = (0.35-0.002*Lpp)/1000;
else
    CA = 0;
end

% Axial calm water air resistance CAA
CAA = air_resistance(ship_type,sub_type,AVT,S,teu);
```

```
% Residual resistance component
CRFnkrit = max(1.0,(Fn./Fnkrit).^c1);
kL = e(1)*Lpp^(e(2));

    for i = 1:N
        CRstandard(i) = [1 CB CB^2]*(b*[1 Fn(i) Fn(i)^2]')/10;
    end

    CR_hollenbach = CRstandard.*CRFnkrit*kL*prod([T/B B/Lpp Los/Lwl...
        Lwl/Lpp (1+(TA-TF)/Lpp) Dp/TA (1+NRud) (1+NBrac) (1+NBoss)...
        (1+NThr)].^a);

    % When accounting for form factor
    CR_mean = CR_hollenbach.*B*T/S - k.*CFm;
    CT_mean = (1+k).*(CF + dCF) + CR_mean + CA + CAA;
    RT_mean  = CT_mean.*0.5*rho*S.*V.^2;


% Power prediction
 % According to Birk, Hollenbach uses a fixed value of t = 0.19 for single
 % screw ships and 0.15 for twin screw
 % The wake fraction is computed by the model hull efficiency (Birk p.641)

  t = 0.19*ones(1,length(V));
  etaH_model = 0.948*CB^0.3977*((RT_mean/RT_mean)^(-0.58))*...
      ((B/T)^0.1727)*(Dp^2/(B*T))^-0.1334;
  w_model = (1 - (1-t)./etaH_model).*ones(1,length(V));
  w = (t+0.04) + (w_model-(t+0.04)).*((CF+CA)/CFm);

  etaH = (1-t)./(1-w);

% Froude number limitation
f_HB = [0.17 0.20 0.60];                        %'Mean' range for Hollenbach
g_HB = [0.642 -0.635 0.150];                    %'Mean' range for Hollenbach


Fn_min = min(f_HB(1),f_HB(1)+f_HB(2)*(f_HB(3)-CB));
Fn_max = g_HB(1) + g_HB(2)*CB + g_HB(3)*CB^2;

RT_mean(Fn < Fn_min) = 0;
RT_mean(Fn > Fn_max) = 0;

w(Fn < Fn_min) = 0;
w(Fn > Fn_max) = 0;

etaH(Fn < Fn_min) = 0;
etaH(Fn > Fn_max) = 0;

end
```

STAWAVE-1

```
function Rwave = STA1(rho,g,Hs,wave_angle,B,Lpp)
%-------------------------------------------------------------------------%
% STA1.m - Calculate added resistance in waves with STAWAVE-1 by MARIN
%
% Other m-files required: main.m
% Subfunctions: none
%
% Inputs:
% rho        -       Sea water density
% g          -       Constant of gravity
% Hs         -       Significant wave height
% wave_angle -       Wave angle relative to ship heading direction
% B          -       Breadth
% Lwl        -       Length in waterline
% Lpp        -       Length between perpendiculars
% L_bwl      -       Waterline length to 95% of maximum breadth
%
```

```
% Outputs:
% Rwave      -      Added resistance in waves
%
% Author: Tone Dale
% Department of Marine technology, NTNU
% email address: tonedale@stud.ntnu.no
% April 2020; Last revision: 01-May-2020:
%-------------------------------------------------------------------------%
angle = abs(wave_angle); % Wave angle defined for [0,+-180]

L_bwl = 0.18*Lpp; % Comparison ship for Case 1


Rwave= (1/16)*rho*g*Hs.^2*B*sqrt(B/L_bwl);

% Restrictions for wave height and wave direction:
Rwave(Hs > 2.25*sqrt(Lpp/100)) = 0;
Rwave(angle > 45) = 0;

end
```

STAWAVE-2

```
function [R_AWL,STA2_req] = STA2(rho,g,Hs,H,B,Lwl,Lpp,Twave,V,...
    CB,T,wave_angle)
%-------------------------------------------------------------------------%
% STA2.m - Calculate added resistance in waves with STAWAVE-2 by MARIN
%
% Other m-files required: main.m
% Subfunctions: none
%
% Inputs:
% rho        -       Sea water density
% g          -       Constant of gravity
% Hs         -       Significant wave height
% H          -       Mean wave height
% B          -       Breadth
% Lwl        -       Length in waterline
% Lpp        -       Length between perpendiculars
% Twave      -       Mean wave period
% V          -       Ship actual speed
% CB         -       Block coefficient
% T          -       Draught
% U          -       Wind speed relative to ship
% wave_angle -       Wave angle relative to ship heading direction
%
% Outputs:
% R_AWL      -      Added resistance in waves based on PM wave spectrum
% STA2_req   -      Logical value, 1 if requirement is fulfilled, else 0
%
% Author: Tone Dale
% Department of Marine technology, NTNU
% email address: tonedale@stud.ntnu.no
% April 2020; Last revision: 04-May-2020:
%-------------------------------------------------------------------------%

% U is U_true

% Parameters for each timestep
Fn = V./sqrt(g*Lwl);
Z = H/2; % Wave amplitude
T1 = Twave;
R_AWL = zeros(1,length(V));


% Wave sprectrum is required. As recommended by MARIN when only Hs and
% Twave is known, the spectrum is approximated by a theoretical shape.
% Applying the ISSC (modified PM) formula
```

```
% Seastate description, constant parameters
omega = 2*pi*(0.01:0.005:0.5); % Circular frequency of regular waves
dw = (max(omega)-min(omega))/length(omega);
k = (omega.^2)./g;  % Deep water dispersion relation
kyy = 0.25;  % Radius of gyration in lateral direction according to ITTC

%% Loop over timesteps and compute R_AWL with respective Spectrum S(w)
for i = 1:length(Fn)

W = ((sqrt(Lpp/g)*(kyy)^(1/3))./(1.17.*Fn(i)^-0.143)).*omega;

a1 = 60.3*CB^1.34.*ones(1,length(omega));

b1 = -8.5*ones(1,length(omega));
b1(W < 1) = 11;

d1 = -566*(Lpp/B)^(-2.66)*ones(1,length(omega));
d1(W < 1) = 14;

raw = (W.^b1).*exp((b1./d1).*(1-W.^d1)).*a1.*Fn(i)^(1.5).*exp(-3.5.*Fn(i));

R_AWML = 4*rho*g*Z(i)^2*((B^2)/Lpp).*raw;


I1 = besseli(1,1.5*k*T); % modified Bessel function of the first kind

K1 = besselk(1,1.5*k*T); % modified Bessel function of the second kind

f1 = 0.692.*(V(i)/sqrt(T*g)).^0.769 + 1.81*CB^6.95;

alpha = ((pi^2*I1.^2)./(pi^2*I1.^2 + K1.^2)).*f1;

R_AWRL = 0.5*rho*g*Z(i).^2*B.*alpha;

Rwave = R_AWML + R_AWRL;

% ISSC Spectrum
S = (173*((Hs(i)^2)/(T1(i)^4)))*omega.^(-5).*exp((-692./(T1(i).^4)).*...
    omega.^(-4));


Aj_squared = 2.*S.*dw;
Fj = (Rwave/(Z(i)^2)).*Aj_squared;
R_AWL(i) = sum(Fj);

end



%% Restrictions
R_AWL(Fn > 0.30) = 0;
R_AWL(Fn < 0.1) = 0;

angle = abs(wave_angle); % Wave angle defined for [0,+-180]
R_AWL(angle > 45) = 0;

if  (Lpp > 75) & (Lpp/B >= 4.0) & (Lpp/B < 9.0) & (B/T >= 2.2) & ...
        (B/T < 5.5) & (CB >= 0.5) & (CB < 0.9)
    STA2_req = 1;
else
    STA2_req = 0;
    disp('STAWAVE-2 requirement not fulfilled')
end % if

end
```

STAJIP-wind

```
function RAA = STAJIP_wind(ship_type,sub_type,AVT,rho_air,U,U_angle,V)
```

```
%-------------------------------------------------------------------------%
% STAJIP_wind.m - Calculate added resistance in wind by MARIN
%
% Other m-files required: main.m
% Subfunctions: none
%
% Inputs:
% ship_type  -       Ship type
% sub_type   -       Sub ship type
% AVT        -       Transverse projected area of superstructure
% rho_air    -       Air density
% U          -       Relative wind speed
% U_angle    -       Relative wind direction
% V          -       Ship speed over ground
%
% Outputs:
% RAA      -      Added resistance in wind by STAJIP
%
% Author: Tone Dale
% Department of Marine technology, NTNU
% email address: tonedale@stud.ntnu.no
% April 2020; Last revision: 01-May-2020:
%-------------------------------------------------------------------------%
% Here V = Vsog
Urel = U;

%% Drag coefficients read off STA-JIP plots in ISO 15016
% Tanker, laden, conventional bow (Assuming: oil, bulk dry, other bulk)
Cx_tanker = [-0.75 -0.77 -0.72 -0.64 -0.51 -0.39 -0.28 -0.20 -0.12 0.03...
    0.09 0.19 0.34 0.5 0.61 0.74 0.86 0.93 0.98];

% Containership, design condition, with containers
Cx_container = [-0.68 -0.73 -0.74 -0.68 -0.49 -0.32 -0.26 -0.21 -0.22...
    -0.27 -0.14 0.1 0.36 0.60 0.77 0.89 0.89 0.80 0.66];

% Passenger/Cruise
Cx_passenger = [-0.70 -0.72 -0.73 -0.70 -0.48 -0.24 -0.26 -0.1 0.09 0.05...
    -0.05 0.09 0.22 0.38 0.57 0.72 0.80 0.71 0.66];

% General cargo
Cx_cargo = [-0.6 -0.89 -1.0 -1.0 -0.89 -0.84 -0.65 -0.43 -0.28 -0.1 0.09...
    0.49 0.83 1.11 1.39 1.49 1.33 0.91 0.81];

% Large LNG carrier. Average of prismatic and spherical for following sea
Cx_LNG = [-1.01 -0.99 -0.92 -0.81 -0.67 -0.49 -0.30 -0.15 -0.04 0.03 0.10...
    0.22 0.42 0.65 0.78 0.88 0.95 0.96 0.94];

if contains(ship_type,{'bulk dry', 'oil', 'other bulk'})
    CDA_direction = -Cx_tanker;
elseif contains(ship_type,'container')
    CDA_direction = -Cx_container;
elseif contains(ship_type,'passenger')
    CDA_direction = -Cx_passenger;
elseif contains(ship_type,'cargo')
    CDA_direction = -Cx_cargo;
elseif contains(sub_type,'LNG')
    CDA_direction = -Cx_LNG;
else
    CDA_direction = 0;
    disp('STA-JIP wind method not applicable');
end

%% Assign correct CAA value based on actual wind direction in each timestep
x = [0 10:10:180];
U_range = U_angle; % Transform 0 to 360 degrees to between 0 and 180
U_range(U_range>180) = abs(U_range(U_range>180)-360);

CDA = interp1(x,CDA_direction,U_range);

RAA = 0.5*rho_air*CDA*AVT.*Urel.^2 - 0.5*rho_air*CDA_direction(1)*AVT*V.^2;
```

```
end
```

Blendermann wind

```
function RAA = blendermann_wind(ship_type,sub_type,AVT,rho_air,U,U_angle,V)
%------------------------------------------------------------------------%
% blendermann_wind.m - Compute wind resistance accoring to Blendermann
%
% Other m-files required: main.m
% Subfunctions: none
%
% Inputs:
% AVT       -       Area of ship and cargo above waterline (transverse)
% ship_type -       Ship type
% sub_type  -       Sub types defined for tankers/bulk vessels
% U         -       Relative wind speed
% U_angle   -       Relative wind direction
% V         -       Ship speed over ground
%
% Outputs:
% RAA       -      Wind resistance
%
% Author: Tone Dale
% Department of Marine technology, NTNU
% email address: tonedale@stud.ntnu.no
% April 2020; Last revision: 15-July-2020:
%------------------------------------------------------------------------%



% Here V = Vsog
Urel = U;

%% Drag coefficients read off Blendermann diagrams from Brix 1993

% Car carrier
Cx_carcarrier = [-0.55 -0.65 -0.65 -0.60 -0.40 -0.10 0.18 0.15 0 -0.20...
    -0.30 -0.25 -0.12 0.20 0.50 0.70 0.80 0.74 0.60];

% Containership
Cx_container = [-0.55 -0.47 -0.46 -0.52 -0.52 -0.44 -0.34 -0.26 -0.11...
    -0.03 0.08 0.22 0.44 0.58 0.60 0.63 0.58 0.54 0.40];

% Tanker, loaded
Cx_tanker = [-0.90 -0.87 -0.95 -0.95 -0.85 -0.72 -0.51 -0.29 -0.03 0.10...
    0.26 0.32 0.42 0.51 0.57 0.62 0.61 0.60 0.55];

% General cargo
Cx_cargo = [-0.65 -0.67 -0.77 -0.77 -0.70 -0.52 -0.37 -0.21 -0.05 0.15...
    0.22 0.29 0.29 0.37 0.47 0.57 0.65 0.59 0.60];

% Passenger
Cx_passenger = [-0.40 -0.37 -0.35 -0.27 -0.08 0.09 0.04 0 -0.01 -0.03...
    -0.08 -0.08 -0.16 -0.18 -0.06 0.21 0.33 0.38 0.37];

% Offshore Supply ship
Cx_offshore_supply = [-0.55 -0.55 -0.51 -0.50 -0.43 -0.33 -0.25 -0.17...
    -0.12 -0.10 -0.07 0.07 0.37 0.59 0.71 0.79 0.75 0.81 0.81];

% Deep sea drilling ship
Cx_drilling = [-1.05 -1.22 -1.39 -1.38 -1.27 -1.08 -0.78 -0.56 -0.34...
    -0.15 -0.04 0.23 0.67 1.01 1.23 1.37 1.34 1.25 1.25];

% Ro-ro/Lo-lo
Cx_roro = [-0.66 -0.66 -0.74 -0.71 -0.67 -0.55 -0.40 -0.25 -0.14 -0.09...
    -0.15 -0.05 0 0.26 0.52 0.81 0.88 0.79 0.70];

% Research vessel
```

```
Cx_research = [-0.55 -0.59 -0.64 -0.59 -0.54 -0.47 -0.40 -0.29 -0.21...
    -0.18 -0.15 -0.06 0.10 0.39 0.62 0.82 0.83 0.71 0.60];


if contains(ship_type,'car carrier')
    CDA_direction = -Cx_carcarrier;
elseif contains(ship_type,{'bulk dry', 'oil', 'other bulk'})
    CDA_direction = -Cx_tanker;
elseif contains(ship_type,'container')
    CDA_direction = -Cx_container;
elseif contains(ship_type,'passenger')
    CDA_direction = -Cx_passenger;
elseif contains(ship_type,'cargo')
    CDA_direction = -Cx_cargo;
elseif contains(ship_type, 'offshore supply')
    CDA_direction = -Cx_offshore_supply;
elseif contains(ship_type,'deep sea drilling')
    CDA_direction = -Cx_drilling;
elseif contains(sub_type,'ro-ro')
    CDA_direction = -Cx_roro;
elseif contains(sub_type,'research')
    CDA_direction = -Cx_research;
else
    CDA_direction = 0;
    disp('Blendermann wind method not applicable');
end

%% Assign correct CAA value based on actual wind direction in each timestep
x = [0 10:10:180];
U_range = U_angle; % Transfort 0 to 360 degrees to between 0 and 180
U_range(U_range>180) = abs(U_range(U_range>180)-360);

CDA = interp1(x,CDA_direction,U_range);

RAA = 0.5*rho_air*CDA*AVT.*Urel.^2 - 0.5*rho_air*CDA_direction(1)*AVT*V.^2;


end
```

Townsin & Kwon

```
function Radded = kwon(CB,Lwl,V,H,wave_angle,U,U_angle,g,voldisp,ship_type,RT)
%-------------------------------------------------------------------------%
% kwon.m - Calculate speed reduction due to added resistance in wind and
% waves with the Townsin and Kwon method
%
% Other m-files required: main.m
% Subfunctions: beaufort.m
%
% Inputs:
% CB          -       Block coefficient
% Lwl         -       Length in waterline
% V           -       Ship speed
% Hs          -       Significant wave height
% wave_angle -        Wave angle relative to ship heading direction
% Twave       -       Mean wave period
% U           -       Wind speed in ship heading direction
% U_angle     -       Wind speed direction relative to ship heading dir.
% g           -       Constant of gravity
% voldisp     -       Volume displacement
% ship type   -       Ship type
% RT          -       Calm water resistance
%
% Outputs:
% Radded      -      Added resistance in wind and waves
%
% Author: Tone Dale
% Department of Marine technology, NTNU
% email address: tonedale@stud.ntnu.no
```

```
% April 2020; Last revision: 21-June-2020:
%------------------------------------------------------------------------%
% U is U_true

Fn = V./sqrt(g*Lwl);

% Rounding CB to nearest value defined by Kwon
CB =  (round(100*CB/5)*5)/100;

% Speed reduction CU due to block coefficient
CU = zeros(1,length(Fn));

if CB == 0.55
    CU = 1.7 - 1.4*Fn - 7.4*Fn.^2;
elseif CB == 0.60
    CU = 2.2 - 2.5*Fn - 9.7*Fn.^2;
elseif CB == 0.65
    CU = 2.6 - 3.7*Fn - 11.6*Fn.^2;
elseif CB == 0.70
    CU = 3.1 - 5.3*Fn - 12.4*Fn.^2;
elseif CB == 0.75
    CU = 2.4 - 10.6*Fn - 9.5*Fn.^2;
elseif CB == 0.80
    CU = 2.6 - 13.1*Fn - 15.1*Fn.^2;
elseif CB == 0.85
    CU = 3.1 - 18.7*Fn + 28*Fn.^2;
end % if

% Direction reduction coefficient Cbeta due to weather direction
% wave_angle [0,+-180] and U_angle [0,360] relative to the bow
[BN_wave,BN_wind] = beaufort(H,U);

% Applying BN according to wind definition scale
BN = BN_wind;
angle = U_angle;

% For angle defined by waves, use absolute value instead:
Cbeta = zeros(1,length(Fn));
head_sea = ((angle >= 0) & (angle < 30)) | ((angle >= 330) & (angle < 360));
bow_sea = ((angle >= 30) & (angle < 60)) | ((angle >= 300) & (angle < 330));
beam_sea = ((angle >= 60) & (angle < 150)) | ((angle >= 210) & (angle < 300));
following_sea = ((angle >= 150) & (angle < 210));

Cbeta(head_sea)= 1;
Cbeta(bow_sea)= 0.5*(1.7-0.03*(BN(bow_sea)-4).^2);
Cbeta(beam_sea)= 0.5*(0.9-0.06*(BN(beam_sea)-6).^2);
Cbeta(following_sea)= 0.5*(0.4-0.03*(BN(following_sea)-8).^2);

% Form coefficient - Sea-web data is generally for loaded condition

if contains(ship_type,'container')
    Cform = 0.7*BN + (BN.^6.5)/(22*voldisp^(2/3));
else
    Cform = 0.5*BN + (BN.^6.5)/(2.7*voldisp^(2/3));
end

x = (CU.*Cbeta.*Cform)./100;

Radded = x.*RT;

% Restricted to Froude number range below 0.3
Radded(Fn>0.3) = 0;

end
```

Wageningen B-series

```
function [etaD] = wageningen(V,RT,etaH,t,w,Dp,rho)
%------------------------------------------------------------------------%
```

```
% wageningen.m - Calculate open water efficiency by Wageningen B-series,
% Approximated method by Breslin and Andersen (Kristensen 2017)
%
% Other m-files required: main.m
% Subfunctions: none
%
% Inputs:
% V          -       Ship speed
% RT         -       Total calm water resistance
% etaH       -       Hull efficiency
% t          -       Thrust deduction factor
% w          -       Wake fraction
% Dp         -       Propeller diameter
% rho        -       Seawater density
%
% Outputs:
% etaD       -       Propulsive efficiency
%
% Author: Tone Dale
% Department of Marine technology, NTNU
% email address: tonedale@stud.ntnu.no
% April 2020; Last revision: 21-April-2020:
%-------------------------------------------------------------------------%


VA = (1-w).*V;
CTh = (8/pi)*RT./((1-t).*rho.*(VA.*Dp).^2);

eta0_ideal = 2./(1+sqrt(CTh+1));
eta0 = eta0_ideal.*(max(0.69,0.81-0.014.*CTh));

% Relative rotative efficiency etaR = 1.0 assumed
etaR = 1.0;

% Shaft efficiency etaS = 0.98 for direct drive and 0.97-0.96 gearbox
% (Kristensen 2017)
etaS = 0.98;

% Final propulsive efficiency
etaD = eta0.*etaH*etaR*etaS;

end
```

Beauforts scale

```
function [BN_wave,BN_wind] = beaufort(H,U)
%-------------------------------------------------------------------------%
% beafort.m - Assign beauforts number to weather condition
%
% Other m-files required: none
% Subfunctions: none
%
% Inputs:
% H          -       Significant wave height
% U          -       True wind speed
%
% Outputs:
% BN_wind    -      Beauforts number from wind scale
% BN_wave    -      Beauforts number from wave scale
%
% Author: Tone Dale
% Department of Marine technology, NTNU
% email address: tonedale@stud.ntnu.no
% April 2020; Last revision: 15-July-2020:
%-------------------------------------------------------------------------%

% Wave BN from Henschke 1956 (Kwon 2008)
BN = zeros(1,length(H));
BN(H<0) = nan;
```

```
BN((H >= 0) & (H < 0.5)) = 1;
BN((H >= 0.5) & (H < 0.65)) = 2;
BN((H >= 0.65) & (H < 0.75)) = 3;
BN((H >= 0.75) & (H < 1.25)) = 4;
BN((H >= 1.25) & (H < 2.0)) = 5;
BN((H >= 2.0) & (H < 3.5)) = 6;
BN((H >= 3.5) & (H < 6.0)) = 7;
BN((H >= 6.0) & (H < 8.0)) = 8;
BN(H >= 8.0) = nan;

BN_wave = BN;
BN = zeros(1,length(U));

% Wind Beaufort Scale according to ISO 15016
BN((U >= 0) & (U < 0.3)) = 0;
BN((U >= 0.3) & (U < 1.6)) = 1;
BN((U >= 1.6) & (U < 3.4)) = 2;
BN((U >= 3.4) & (U < 5.5)) = 3;
BN((U >= 5.5) & (U < 8.0)) = 4;
BN((U >= 8.0) & (U < 10.8)) = 5;
BN((U >= 10.8) & (U < 13.9)) = 6;
BN((U >= 13.9) & (U < 17.2)) = 7;
BN((U >= 17.2) & (U < 20.7)) = 8;
BN(U >= 20.7) = nan;

BN_wind = BN;


end
```

Air resistance

```
function CAA = air_resistance(ship_type,sub_type,AVT,S,teu)
%-------------------------------------------------------------------------%
% air_resistance.m - Calculate air resistance
%
% Other m-files required: none
% Subfunctions: none
%
% Inputs:
% S          -       Wetted surface area
% AVT        -       Area of ship and cargo above waterline (transverse)
% teu        -       No of containers (in twenty-foot equivalent units)
% ship_type -       Ship type
% sub_type   -       Sub types defined for tankers/bulk vessels
%
% Outputs:
% CAA         -      Axial calm water air resistance
%
% Author: Tone Dale
% Department of Marine technology, NTNU
% email address: tonedale@stud.ntnu.no
% April 2020; Last revision: 15-July-2020:
%-------------------------------------------------------------------------%

% Check ship type and assign CAA

    % Containers (Kristensen, 2017)
    if contains(ship_type,'container')
        CAA = (max(0.09,0.28*teu^-0.126))*10^-3;
        % Bulk/Tankers (Kristensen, 2017)
    elseif contains(sub_type,'small')
        CAA = 0.07*10^-3;
    elseif contains(sub_type,'handysize')
        CAA = 0.07*10^-3;
    elseif contains(sub_type,'handymax')
        CAA = 0.07*10^-3;
    elseif contains(sub_type,'panamax')
        CAA = 0.05*10^-3;
```

```
    elseif contains(sub_type,'aframax')
        CAA = 0.05*10^-3;
    elseif contains(sub_type,'suezmax')
        CAA = 0.05*10^-3;
    elseif contains(sub_type,'vlcc')
        CAA = 0.04*10^-3;
        % Remaining drag coefficient values set to 0.8 based on Blendermann
        %  and Birk 2019 p. 620
    else
        CAA = 0.8*AVT/(800*S);
    end


end
```

Global variables

```
%--------------------------------------------------------------------------%
% Variables.m - Global variable definitions
% Note! Local variables are defined and described locally in functions
%
% Other m-files required: none
% Subfunctions: none
%
% Author: Tone Dale
% Department of Marine technology, NTNU
% email address: tonedale@stud.ntnu.no
% April 2020; Last revision: 16-April-2020
%--------------------------------------------------------------------------%
%
%------------------------------ Constants ---------------------------------%
%
% rho       -       Sea water density
% nu        -       Sea water kinematic viscosity
% g         -       Constant of gravity
%
%------------------------- Hull characteristics -------------------------%
%
% Lwl       -       Length of waterline
% Lpp       -       Length between perpendiculars
% Los       -       Length of surface
% Loa       -       Length over all
% B         -       Ship breadth (moulded, not extreme)
% T         -       Ship draught (maximum druaght summer load line)
% TA        -       Molded draught aft perpendicular
% TF        -       Molded draught fore perpendicular
% voldisp   -       Volume displacement
% S         -       Wetted surface area
% SB        -       Wetted base/transom area
% Sapp      -       Wetted surface area of appendages
% AVT       -       Area of ship and cargo above waterline (transverse)
% AVL       -       Area of ship and cargo above waterline (longitudinal)
% ABT       -       Transverse cross section area of bulb (H-M)
% CB        -       Block coefficient
% CM        -       Midship section coefficient
% CP        -       Prismatic coefficient
% Cstern    -       Shape parameter in Holtrop-Mennen
% LCB       -       Longitudinal centre of buoyancy (H-M)
% V         -       Actual speed
% Vd        -       Design speed
% dwt       -       Dead weight
% ldt       -       Lightship weight
% teu       -       No of containers (in twenty-foot equivalent units)
%
%---------------------- Propeller characteristics ---------------------%
%
% Dp        -       Propeller diameter
% AEA0      -       Propeller expanded ratio
% n         -       Propeller rpm
```

```
%
%----------------------------- Resistance --------------------------------%
%
% CT        -       Total calm water resistance coefficient
% CR        -       Residuary resistance coefficients
% k         -       Form factor
% CF        -       Frictional resistance coefficients
% dCF       -       Hull roughness coefficient
% CDB       -       Base drag coefficient
% CAA       -       Air resistance coefficient
% Capp      -       Appendage resistance coefficient
% CA        -       Correlation allowance
% Fn        -       Froude number
% Re        -       Reynolds number
% RT        -       Total calm water resistance
% Rwind     -       Added resistance due to wind
% Rwave     -       Added resistance due to waves
% R_AWML    -       Resistance due to induced wave motions
% R_AWRL    -       Resistance due to wave reflection
% Rtot      -       Total resistance (RT+Radded)
% h         -       Water depth
% Hs        -       Significant wave height
% ZA        -       Wave amplitude
% Vw        -       Reduced speed corrected for added resistance
%
%----------------------------- Propulsion --------------------------------%
%
% etaD      -       Propulsive efficiency in ideal conditions
% etatot    -       Propulsive efficiency in trial conditions
% eta0      -       Open water (propeller efficiency)
% etaH      -       Hull efficiency
% etaR      -       Relative rotative efficiency
% etaS      -       Shaft efficiency
% PD        -       Deliwered power at the propeller
% t         -       Thrust deduction factor
% w         -       Wake fraction
% VA        -       Speed of inflow to the propeller
% T         -       Torque
% PS        -       Calm water power requirement
% Ptot      -       Total power requirement
% zetaP     -       Slope of linear curve in the load variation test
% ME_n      -       Main engine rpm
% ME_cyl    -       Main engine no. of cylinders
% SM        -       Sea margin
%
%----------------------------- Ship types --------------------------------%
% general_cargo
% bulk_dry
% oil
% passenger
% offshore_supply
% container
% chemical
% ro_ro
% other_offshore
% liquefied_gas
% other_bulk
% refrigerated_cargo
% other_cargo
% other_liquids
```